Intraflagellar transport in the developing and mature vertebrate retina

D i s s e r t a t i o n

zur Erlangung des Grades

"Doktor der Naturwissenschaften"

am Fachbereich Biologie

der Johannes Gutenberg-Universität

in Mainz

von Tina Sedmak

geboren in Ljubljana (Slowenien)

Mainz, März 2011

Dedicated to my family…

"Posvečam mojim domačim…"

I.   Explanatory notes

The present doctoral thesis is a cumulative thesis composed of three main publications: Sedmak et al., 2009 (Publication I), Sedmak and Wolfrum, 2010 (Publication II) and Sedmak and Wolfrum, submitted (Publication III). Publication I is a review article focusing on the visualization of ciliary vesicles based on pre-embedding immunolelectron microscopy published in December 2009 in *Methods of Cell Biology*. This immunoelectron microscopy method enabled us to visualize and locate the intraflagellar transport (IFT) proteins associated with vesicular structures. Publication II demonstrates the distribution of IFT molecules in ciliary and non-ciliary cells of the retina, published in April 2010 in *Journal of Cell Biology*. Publication III deals with the participation of IFT proteins in the ciliogenesis of photoreceptor cells; this manuscript has been submitted recently. In publication III, the main focus is the localization of IFT molecules in different stages of photoreceptor cell ciliogenesis. Results of Publication III demonstrate the involvement of specialized structures in the early ciliogenesis of photoreceptor cells. The results of Publication I, II and III are summarized in section "Summarized Results". All further publications, to which I contributed data and which were published during my doctoral thesis, are marked with asterisks (*). A detailed overview of the contributions made to each publication of the present cumulative thesis is added in the appendix.

II. Acknowledgments

Thank you!

Index of contents

Index of figures

1. General introduction
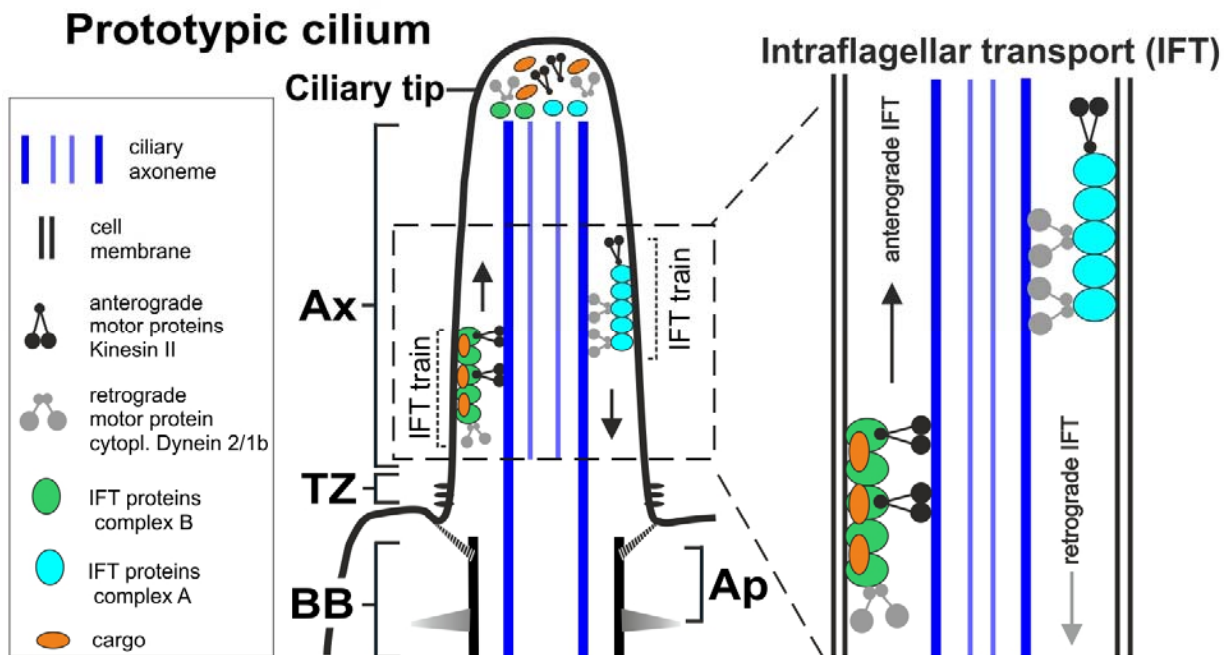
1.1 Cilia and intraflagellar transport (IFT)

Cilia are highly conserved polarized antenna-like organelles emerging from the surface of nearly all eukaryotic cells. Currently cilia are one of the major forms of research in molecular cell biology. Structurally, cilia are organized into three sub-compartments: a basal body (mother centriole) from which the cilia are initially assembled, a transition zone which is important for docking of proteins into the ciliary shaft and a ciliary axoneme. The axoneme is the structural core of the cilium (Fig. 1; Fliegauf et al., 2007). Based on their axonemal microtubule array and their motile attributes cilia are divided into four subtypes: motile cilia 9×2+2 cilia (e.g. motile tracheal cilia), motile 9×2+0 cilia (e.g. monocilia at the embryonic node), immotile 9×2+2 cilia (e.g. kinocilia in the inner ear) and immotile 9×2+0 cilia (e.g. photoreceptor connecting cilium) (reviewed in Fliegauf et al., 2007; Roepman and Wolfrum, 2007). Cilia have many functions ranging from organizing centers for signaling and development, locomotion and sensory function.

Cilia originate from the mature mother centriole, which also forms the basal body. The basal body acts as a nucleating center for the nine microtubule doublets, anchoring the connecting cilium and the axoneme. In his pioneering studies on ciliogenesis Sorokin (1962, 1968) described the two principal pathways of ciliogenesis, now known as the extra- and intracellular pathways of ciliogenesis (Molla-Herman et al., 2010; Ghossoub et al., 2011). In the extracellular pathway of ciliogenesis, the mother centriole docks directly to the plasma membrane, from where the ciliary shaft is formed and is growing towards the extracellular environment. In contrast, in intracellular ciliogenesis, the mother centriole docks to the membrane of the intracellular primary ciliary vesicle and here the cilium is assembled within the ciliary vesicle. After docking and fusion of the elongated intracellular ciliary vesicle with the plasma membrane, the ciliary shaft is released into the extracellular space.

The assembly and maintenance of the cilia, requires the intraflagellar transport (IFT), an evolutionary conserved protein transport mechanism mediated by molecular motors and IFT particles (Rosenbaum and Witman, 2002; Pedersen and Rosenbaum, 2008). IFT was first described in the flagellum of the biflagellate algae *Chlamydomonas* (Kozminski et al., 1993). In a complex with microtubule-based motor proteins like kinesin-II family members and cytoplasmic dynein2/1b (DYNC2H1) IFT enables the bidirectional transport of ciliary cargo molecules along the axoneme (Pazour et al., 1998, 1999; Signor et al., 1999). To date, 19 IFT particles proteins has been identified, divided in two complexes A and B (Cole et al., 1998;

Cole, 2003; Krock et al., 2009). Anterograde IFT is supposed to be coupled to the IFT complex B proteins, whereas the IFT protein complex A thought to be involved in the retrograde trafficking (Evans et al., 2006). Defects in IFT lead to the impair assembly of cilia and flagella (Rosenbaum and Witman, 2002). Analysis of photoreceptor development in mice carrying a mutation in the gene coding for IFT88 (Tg737orpk) indicates that IFT88 is required for normal development and maintenance of photoreceptor outer segments (Pazour et al., 2002a; Baker et al., 2004). In siRNA experiments in which centriolar IFT20 is reduced, the primary cilia are lacking (Jurczyk et al., 2004; Follit et al., 2006, 2008). In addition to their role in ciliary transport, and IFT proteins were proposed to play additional roles in the transport processes in non-ciliary retinal cells and in the formation of the immune synapse (Publication I; Finetti et al., 2009; Baldari and Rosenbaum, 2010). Therefore, the question arises whether IFT proteins are also present in non-ciliary structures during photoreceptor cell ciliogenesis.

Several proteins have been identified as IFT cargo molecules. Membrane proteins of the photoreceptor outer segment like rhodopsin and guanylyl cyclase 1 are described as IFT cargo (Insinna and Besharse, 2008; Bhowmick et al., 2009; Keady et al., 2011). Further, as IFT cargoes, the proteins involved in the trafficking of ciliary membrane proteins such as polycystins 1 and 2 (Pazour et al., 2002b; Bae et al., 2006; Follit et al., 2006; Hoffmeister et al., 2011), the TRPV channel (Qin et al., 2005) and the olfactory cyclic nucleotide gated channel (Jenkins et al., 2006) are proposed.

Fig. 1: Scheme of the prototypic cilium showing the mechanism of intraflagellar transport (IFT). Prototypic cilium is composed of the basal body (BB), transition zone (TZ) and ciliary axoneme (Ax). Distal and subdistal appendages (Ap) are anchoring the BB to the ciliary membrane and to the microtubules in the cytoplasm. IFT trains composed of IFT proteins (complex A (*green*) and complex B (*blue*)) transport cargoes (*orange*) by molecular motors (*grey* and *black* motors). Mechanism of IFT: by anterograde heterotrimeric Kinesin-II (*black*) IFT trains are transported from the ciliary base to the ciliary tip. Retrograde transport of IFT trains from distal tip back to the base is mediated by cytoplasmic dynein 2/1b (*grey*). Anterograde IFT is supposed to be coupled to the IFT complex B proteins (*blue*), whereas the IFT proteins complex A (*green*) may be involved in the retrograde trafficking. Figure is modified after Pedersen and Rosenbaum, 2008.

## 1.2 Ciliary transport in retinal photoreceptor cells

The vertebrate retina is organized in defined layers of five major classes of neurons (rod and cone photoreceptors, horizontal, bipolar, amacrine and ganglion cells). The outmost outer layer of the retina is the retinal pigment epithelium with melanosomes. In melanosomes the pigment melanin functions as a light filter and therewith supports the photoreception (reviewed in Wässle, 2004; Swaroop et al., 2010). The microvilli of the retinal pigment epithelium cells tightly enclose and phagocytize the neighboring outer segments of rod photoreceptor cells (Young, 1976). The photoreceptors - rods and cones - transduce light into an electrical signal. Rods are specialized for dim light conditions, whereas cones respond to bright light and are necessary for color vision.

Photoreceptor cells are highly polarized with specialized sub-compartments: the light sensitive outer segment, the biosynthetically active inner segment, the connecting cilium which connects both segments, the cell body with the nucleus, and the special ribbon synapse at the distal end of the axon. The outer segments of photoreceptor cells are developmentally derived from primary cilia (Besharse and Horst, 1990). The photoreceptor connecting cilium corresponds to the transition zone of the prototypic cilium, whereas the axoneme, basal body and adjacent centriole are consistent with these structures in the photoreceptor cells and in the prototypic cilium (Fig. 2; Publication I). Since there is no protein synthesis in the outer segment (Roepman and Wolfrum, 2007) all outer segment components are continually synthesized in the organelles of the inner segment and transported through the slender connecting cilium to their destinations in the outer segment. Transport vesicles carrying rhodopsin in their membranes bud from the Golgi apparatus (Deretic, 2006) and are unidirectionally transported by cytoplasmic dynein along microtubules (Tai et al., 1999; Sung and Tai, 2000) to a specialized periciliary region of the apical inner segment, near the connecting cilium (Papermaster, 2002; Maerker et al., 2008). Here, the vesicles dock and fuse with the target membrane and therewith probably enable subsequent movement of the membrane cargo into the membrane domain of the connecting cilium (Fig. 2; Roepman and Wolfrum, 2007). For the ciliary delivery two and/or parallel alternative processes have been suggested: (1) there is evidence for F-actin-based ciliary transport of rhodopsin by myosin VIIa (Liu et al., 1999; Wolfrum and Schmitt, 2000) and (2) based on mutational analyses the involvement of the IFT system including kinesin-II as transport motor along microtubules, the currently hypothesized (Marszalek et al., 2000; Pazour et al., 2002a; Insinna et al., 2009*).

Recently, the work by Insinna and co-workers, (2009*) implicated both kinesin-II and KIF17 in the assembly of the photoreceptor outer segment (Insinna et al., 2009*). In

secondary retinal neurons it has been demonstrated that KIF17 regulates the dendritic transport of glutamate receptor subunits to the postsynaptic membrane (Qin and Pourcho, 2001; Kayadjanian, et al., 2007). Since KIF17 and IFT coexist at the post-synaptic dendritic terminals of retinal secondary neurons, KIF17 might be a possible post-synaptic motor candidate for IFT to the dendritic tip (Publication II), which is in correspondence with Insinna et al., 2009*.

In the retina the cell bodies of the photoreceptor cells form the outer nuclear layer. The outer plexiform layer contains the axon terminals of photoreceptor cells which synapse with the processes of secondary retinal neurons: bipolar and horizontal cells. The cell bodies of the amacrine, bipolar and horizontal cells form the inner nuclear layer. In the inner plexiform layer bipolar and horizontal cells form synapses with the amacrine and ganglion cells. The dendrites of the ganglion cells collect the signals of bipolar and amacrine cells and their axons transmit these signals further to the visual centers of the brain.
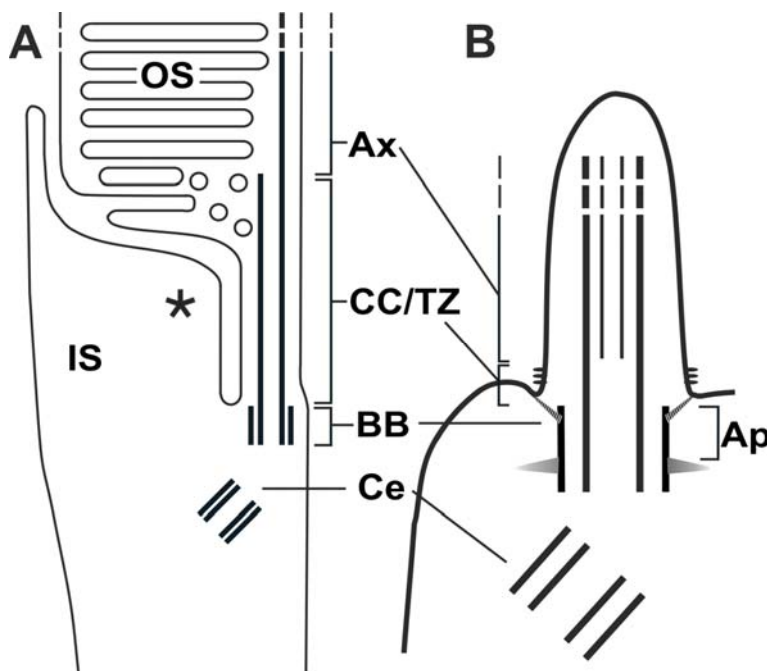
Fig. 2: Schemes of the photoreceptor cell ciliary region compared with the prototypic cilium. (A) Scheme of rod photoreceptor cell: a light-sensitive outer segment (OS) is linked by the connecting cilium (CC) to an inner segment (IS), where biosynthetic active cell organelles are located. Photoreceptor ciliary region consists of the CC with the basal body (BB) at the base and adjacent centriole (Ce). *Arrows* in **A** indicate routes of ciliary cargo transport: post-Golgi vesicles originating from the Golgi apparatus (GA) and translocate along microtubules through the inner segment (IS) to the ciliary base where they dock and fuse with the periciliary membrane. *Asterisk* indicates the region of the periciliary targeting complex in the apical extension of the photoreceptor IS. The axoneme (Ax) is extending apical from the CC. **(A, B)** Photoreceptor OS resembles a highly modified primary cilium and the CC is homologue to the transition zone (TZ) of prototypic cilia. Ap: distal and subdistal appendages.

11

1.3 Ciliogenesis in the photoreceptor cells

Photoreceptor cell development is known to be asynchronous (Tokuyasu and Yamada, 1959; Greiner et al., 1981; Nir et al., 1984; Chatin, 1992; Sung and Chuang, 2010), offering a useful system to study primary cilia assembly.

After exit from final mitosis, functional maturation of a committed photoreceptor precursor (rod or cone) can take weeks to months depending on the species (Swaroop et al., 2010). Early in development every photoreceptor cell has a centrosome near the nuclear region, which contains a mother and a daughter centriole (Greiner et al., 1981). Furthermore, ciliogenesis is tightly coupled to the cell cycle in which the primary cilium is formed in the G1 phase (Pedersen and Rosenbaum, 2008). According to Sorokin´s pioneer work on the ciliogenesis of primary cilia (Sorokin, 1962, 1968) and the recently defined intra- and extracellular pathways of ciliogenesis (Molla-Herman et al., 2010; Ghossoub et al., 2011). In the extracellular pathway of ciliogenesis the mother centriole docks to the apical plasma membrane forming the ciliary shaft and cilium elongates in the extracellular environment. In the intracellular pathway of ciliogenesis the distal part mother centriole becomes associated with the intracellular primary ciliary vesicle and further the ciliary shaft is assembled within this ciliary vesicle, which at the certain length fuses with the plasma membrane into the extracellular space. Although there are indications for the extracellular pathway recent reviews on photoreceptor ciliogenesis pointed out that photoreceptor cells occur via an intracellular pathway (Ghossoub et al., 2011). In order to investigate ciliogenesis of the photoreceptor cells in detail, in this study the electron microscopy analyses unravel the developing mouse retina (Publication III).

1.4 Aims of the thesis

In the previous studies of Pazour et al. (2000, 2002a),; reviewed Pedersen el al. (2008) and in Pedersen and Rosenbaum (2008), IFT proteins have been analyzed in different ciliary cells as in *Chlamydomonas*, *C. elegans* and diverse mouse tissues, like e.g. retina, kidney and testis. The study of Pazour et al. (2002a) demonstrated individual IFT molecules at the ciliary region of the photoreceptor cells in the mature retina. Although in their experiments additional labeling of IFT proteins was demonstrated in the outer plexiform layer, this localization has not been further discussed. To determine the precise subcellular and subciliary distribution of individual IFT proteins (IFT20, IFT52, IFT57, IFT88 and IFT140) in the mature mouse retina using indirect immunofluorescence and immunoelectron microscopy (Publication I, II) in the present doctoral thesis the subcellular localization was analyzed. The improved protocol of the pre-embedding immunoelectron labeling is described in detail together with the first results indicating an additional role of IFT proteins in the association with ciliary cargo vesicles (Publication I). Since the ciliogenesis of the photoreceptor cells in combination with precise spatial localization of individual IFT proteins had not been elucidated so far, analysis of photoreceptor ciliogenesis in developing mouse retina was performed (Publication III).

In the present doctoral thesis following aims were set:

a) **Identification of transport vesicles directed to the primary cilium of photoreceptor cells by immunoelectron microscopy.**

b) **Analysis of the subcellular localization of individual IFT proteins in the mature retina.**

c) **Validation of the photoreceptor cell ciliogenesis in developing mouse retina and participation of individual IFT proteins in the ciliogenesis of photoreceptor cells.**

Add a) Identification of transport vesicles directed to the primary cilium of photoreceptor cells by immunoelectron microscopy

Immunoelectron microscopy (e.g. methods of post- and pre-embedding labeling) enables the analyses of protein localization in subcellular compartments. The fixation of target tissue masks epitopes and limits the detection of proteins. In the post-embedding labeling the antibody incubation occurs on ultrathin sections of fixed tissue (retina) embedded in LR-White. Due to the limitations of fixation it was necessary to establish a less invasive and more sensitive method than post-embedding labeling. For this reason pre-embedding labeling, a method with mild pre-fixation which preserves the tissue and the antigenicity of epitopes was

established in the lab. This improvement and modification of previous pre-embedding protocols provided the basis for all immunoelectron microcopy analyses applied in this doctoral thesis (Publication I, II, III). Establishing and adapting of the high-resolution immunoelectron microscopy pre-embedding method was an important prerequisite of this thesis and therewith providing the significant groundwork. It enabled us to specify spatial localization of IFT proteins in the retina. Correlative a high-resolution immunofluorescence and a pre-embedding immunoelectron microscopy we acquired the visualization of IFT proteins in differential parts of the connecting cilium. In contrast to post-embedding immunoelectron microscopy method, only the pre-embedding labeling enabled us the visualization of transport vesicles associated with IFT proteins (Publication I, II, III).

Add b) Analysis of the subcellular localization of individual IFT proteins in the mature retina

Since the mutations in genes encoding IFT proteins prevent ciliary assembly in all organisms investigated (Cole et al., 1998; Murcia et al., 2000; Pazour et al., 2002a; Tsujikawa and Malicki 2004; Krock and Perkins, 2008; Omori et al., 2008) there is no doubt that IFT is essential for the ciliary development and their maintenance. Since little is known about the subcellular localization of individual IFT proteins in the mature mouse retina applying the methods of immunofluorescence and immunoelectron microscopy using antibodies against individual IFT proteins this was elucidated in the present work (Publication II).

Add c) Validation of the photoreceptor cell ciliogenesis in developing mouse retina and participation of individual IFT proteins in the ciliogenesis of photoreceptor cells

To examine photoreceptor cell ciliogenesis in postnatal day 0 (PN 0), PN3 and PN7, mouse retinas were analyzed using immunofluorescence and electron microscopy. Since the ciliogenesis of photoreceptors is not synchronized, it was important to first define different stages of photoreceptor ciliogenesis. After defining the stages of photoreceptors ciliogenesis the pre-embedding labeling method was applied to the postnatal retina in order to study the distribution of individual IFT molecules in defined stages of photoreceptor cell ciliogenesis (Publication III).

2. Publications

2.1 Publication I

Sedmak T, Sehn E, Wolfrum U (2009) Immunoelectron microscopy of vesicle transport to the primary cilium of photoreceptor cells. In: R.D. Sloboda (ed) Primary cilia. Methods in Cell Biology. Vol. 94 Academic Press Elsivier Inc, pp 259-272

CHAPTER 13

Immunoelectron Microscopy of Vesicle Transport to the Primary Cilium of Photoreceptor Cells

Tina Sedmak, Elisabeth Sehn, *and* **Uwe Wolfrum**

Department of Cell and Matrix Biology, Institute of Zoology, Johannes Gutenberg University, Mainz
D-55099, Germany

Abstract

Cilia are organelles of high structural complexity. Since the biosynthetic machinery is absent from cilia all their molecular components must be synthesized in organelles of the cytoplasm and subsequently transported to the cilium. Ciliary cargos are thought to be translocated in the membrane of transport vesicles or association with these vesicles to the base of the cilium where the vesicles fuse with the periciliary target membrane for further delivery of their cargo into the ciliary compartment by the intraflagellar transport (IFT). Here we describe a modified preembedding labeling method as an alternative technique to conventional postembedding methods eligible for analyses of ciliary cargo vesicles and the distribution of ciliary molecules in subciliary compartments for immunoelectron microscopy. The preembedding labeling method preserves the antigenicity of ciliary antigens and its application reveals differential localization of individual IFT proteins in vertebrate photoreceptor cilia. Since membrane vesicles are conserved, the preembedding protocol additionally allows the identification of ciliary cargo vesicles by immunolabeling of individual IFT proteins and ciliary targeting molecules in ciliary photoreceptor cells. These results do not only confirm the central function of IFT molecules in ciliary transport, but further strengthen their role in transport processes in the cytoplasm. Furthermore, evidence for different alternative transport routes of cargo vesicles directed to different target membranes is gathered.

I. Introduction and Rationale

Cilia are polarized complex organelles that appear early in the evolution of the eukaryotic cell. Although, initially the main attention of the ciliary function was turned on cell and fluid propulsion, in recent years it has become clear that sensory reception is one of the major functions of cilia (Gerdes *et al.*, 2009; Pazour and Bloodgood, 2008). From this it is likely that all cilia perform sensory functions. In particular, primary cilia of mammals serve as multimodal antennae for signals from their extracellular environment (Pazour and Witman, 2003). Therefore, it is not a big surprise that major sensory receptor cells, like insect sensilla or mammalian olfactory cells, adapted cilia for sensory perception. The most drastic evolutionary modifications of cilia structure and function occurred in vertebrate photoreceptor cells (Pazour and Bloodgood, 2008; Roepman and Wolfrum, 2007) (Fig. 1).

In vertebrates, two types of ciliated photoreceptor cells, cones and rods, are arranged in the innermost layer of the neuronal retina of the eye. They are adapted to photopic vision allowing color perception and scotopic vision at low-light conditions, respectively. Cone and rod photoreceptor cells are highly polarized sensory neurons consisting of morphologically and functionally distinct cellular compartments (Fig. 1A). From their cell body an axon projects to the synaptic terminus, where ribbon synapses connect the photoreceptor cells with the second retinal neurons (tom Dieck and Brandstätter, 2006). At the other cell pole, a short dendrite named the inner segment terminates in a
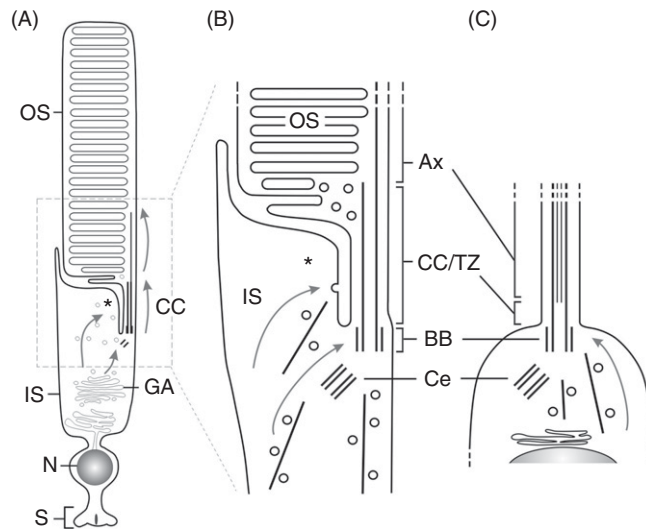
Fig. 1   Schemes of a ciliated photoreceptor cell compared with a prototypic cilium. (A) Scheme of a rod photoreceptor cell: a light-sensitive outer segment (OS) is bridged by the connecting cilium (CC) to an inner segment (IS) where all biosynthetic active cell organelles are located. (B) Schemes of the ciliary region of a rod cell and (C) of a prototypic cilium. *Arrows* in A–C indicate routs of ciliary cargo transport: post-Golgi vesicles bud from the Golgi apparatus (GA), translocate along microtubules through the inner segment (IS) to the ciliary base where they dock and fuse with the periciliary membrane. *Asterisk* indicates the region of the periciliary-targeting complex in the apical extension of the photoreceptor IS. Subsequently, membrane components translocate in the ciliary membrane to the ciliary compartment, the OS or the cilium/flagellum, respectively. Note that the photoreceptor OS resembles a highly modified primary cilium and the CC is homologue to the transition zone (TZ) of other cilia. Ax: axoneme; BB: basal body; Ce: cilia adjacent centriole.

light-sensitive outer segment which resembles a modified sensory cilium (Besharse and Horst, 1990; Pazour and Bloodgood, 2008; Roepman and Wolfrum, 2007). This outer segment is characterized by specialized flattened disk-like membranes where all components of the visual transduction cascade are arranged (Burns and Arshavsky, 2005). The visual signal transduction cascade in vertebrates is one of the best-studied examples of a G-protein transduction cascade. Photoexcitation leads to photoisomerization of the visual pigment rhodopsin which catalyzes GDP/GTP exchange at the visual heterotrimeric G-protein transducin, which in turn activates a phosphodiesterase, catalyzing cGMP hydrolysis in the cytoplasm which leads to the closure of cGMP-gated channels in the plasma membrane, finally resulting in photoreceptor cell hyperpolarization.

In addition to their sensory features, the photoreceptor cell outer segments are similar to other sensory cilia developmentally derived from primary cilia (Insinna and Besharse, 2008; Pazour and Bloodgood, 2008). As in other primary ciliary membranes, the phototransductive membranes of the outer segment are continually renewed throughout lifetime of the cell. Newly synthesized membranes are added at the base of the outer segment, whereas aged disks at the outer segment apex are

phagocytosed by cells of the retinal pigment epithelium (Young, 1976). As it is the case in other cilia, there is no synthesis of biomolecules found in the outer segments and all outer segment components are continually synthesized in the endoplasmic reticulum (ER) organelle of the inner segment and transported through the slender connecting cilium to their destinations in the outer segment (Roepman and Wolfrum, 2007). The visual pigment rhodopsin is the most abundant protein of the outer segment ($\sim$85% of total outer segment protein) (Corless *et al.*, 1976), and an enormous number of rhodopsin molecules (10^7) per day are newly synthesized by photoreceptor cell (Besharse and Horst, 1990). These molecules have to traffic from the synthesizing organelles of the inner segment, through the connecting cilium, to their destination in the outer segment. Transport vesicles bearing rhodopsin in their membranes bud from the Golgi apparatus (Deretic, 2006) and are unidirectionally transported by cytoplasmic dynein along microtubules (Sung and Tai, 2000; Tai *et al.*, 1999) to a specific periciliary specialization (e.g., the periciliary ridge complex in amphibians or the membrane adhesion complex between the collar-like extension of the inner segment and the connecting cilium in rodents and mammals) at the base of the connecting cilium (Maerker *et al.*, 2008; Papermaster, 2002). Here at this specialization the vesicles dock and fuse with the target membranes of the apical inner segment and the membrane cargo is thought to move subsequently into the membrane domain of the connecting cilium (Roepman and Wolfrum, 2007). For the ciliary delivery two alternative processes have been suggested: (1) there is evidence for F-actin-based ciliary transport of rhodopsin by myosin VIIa (Liu *et al.* 1999; Wolfrum and Schmitt, 2000) and (2) based on mutational analyses the involvement of the intraflagellar transport (IFT) system including kinesin-II as transport motor along microtubules was favored (Insinna *et al.*, 2009; Marszalek *et al.*, 2000; Pazour *et al.*, 2002).

Although accumulating evidence indicates that vesicular transport of ciliary proteins from the *trans*-Golgi network is critical for proper development and maintenance of nonsensory cilia (Follit *et al.*, 2006), this process is much better understood in the sensory cilia of photoreceptor cells. This, as well as their clear morphological and functional compartmentalization, defines vertebrate photoreceptor cells as an excellent cellular system for study of the transport of cargo vesicles directed to cilia. In the present chapter we will focus on the visualization of vesicles containing ciliary cargo in photoreceptor cells by immunoelectron microscopy. We provide methodological instructions for a preembedding labeling procedure of vertebrate retina suitable for immunodetection of antigens in well-preserved transport vesicles.

II. Materials

A. Reagents and Solutions

Buffered solutions: Sorensen phosphate buffer (PB) 0.2 M (pH 7.4), 0.2 M $Na_2HPO_4 \cdot 2H_2O$ titrated with 0.2 M KH_2PO_4; phosphate-buffered saline (PBS), 137 mM NaCl, 3 mM KCl, 8 mM $Na_2HPO_4 \cdot 2H_2O$, 4 mM KH_2PO_4 (Ca^{2+} and Mg^{2+} free), pH 7.4; 0.05 M Tris-HCl buffer, pH 7.6; cacodylate buffer (CB), 0.2 M cacodylic acid$\cdot 3H_2O$ sodium salt, pH 7.4.

Fixatives: (1) Prefixation: 4% paraformaldehyde (PFA) in 0.1 M PB; PFA stock solution is freshly prepared just before use. PFA powder (extra pure Merck, Darmstadt, Germany) is dissolved in H_2O_{bidest} by constant stirring on a heating plate at 70°C (hood), droplets of 1 N NaOH are added until the solution clears. (2) Interim fixation: 2.5% glutaraldehyde (GA) (EM-grade 25% aqueous stock solution, Sigma-Aldrich, Deisenhofen, Germany) in 0.1 M CB. (3) Postfixation: 0.5% OsO_4 (stock).

Sucrose solutions 10, 20, and 30% in 0.1 M PB; 2% agar (Appichem, Darmstadt, Germany) solution in PBS.

Blocking solution: 10% normal goat serum (NGS) (Sigma-Aldrich), 1% bovine serum albumin (BSA) (Sigma-Aldrich) in PBS.

Antibody dilution solution: 3% NGS and 1% BSA in PBS. For 24-well plate at least 750 µl solution per well is necessary.

Antibodies: first antibodies: anti-IFT20, anti-IFT52, anti-IFT57 (Pazour *et al*., 2002), and anti-MAGI-2 (Santa Cruz Inc., Santa Cruz, CA, USA); anti-mouse and anti-rabbit IgG biotin-conjugated second antibodies (Vector Laboratories Inc., Burlingame, CA, USA).

VECTASTAIN® ABC kit (Vector Laboratories Inc.): avidin (reagent A), biotinylated-horseradish-peroxidase (HRP) (reagent B).

1% 3,3′-diaminobenzidine tetrahydrochloride (DAB) (Sigma-Aldrich) in 0.05 M Tris-HCl used to prepare 0.05% DAB solution (hood).

Silver enhancement: solution A: 3% hexamethylenetetramine ($C_6H_{12}N_4$) in H_2O_{bidest}; solution B: 5% silver nitrate (Ag NO_3) in H_2O_{bidest}; solution C: 2.5% borax (disodium tetraborate) ($Na_2B_4O_7 \cdot 10H_2O$) in H_2O_{bidest}; solution D: 0.05% tetrachlorogold (III) acid trihydrate ($AuCl_4 \cdot 3H_2O$) in H_2O_{bidest}; solution E: 2.5% sodium thiosulfate (Na_2SO_3) in H_2O_{bidest}.

Dehydration: graded series of 30–99.8% undenaturated ethanol; propylene oxide.

Embedding resin: Araldite® (ARALDITE CY212) and Araldite® hardener (ARALDITE HY 964) are mixed without air bubbles before accelerator (2,4,6,-Tris dimethylaminomethylphenol) is added (all compounds from Serva, Heidelberg, Germany).

B. Special Equipments and Tools

Dissection instruments, injection needle (ϕ 0.6 mm), copper block (size of object slide), super frost® object slides (Menzel, Braunschweig, Germany), superglue (UHU®), razor blades, a fine (size # 0) smooth art paint brush, toothpicks, 24-well plates, small homemade container with a nylon net (mesh size 80 µm^2) at the bottom, ACLAR® embedding film (Ted Pella Inc., Redding, CA, USA) plastic container with cover, copper grids (75 square mesh, diameter 3.05 mm) filmed with formvar support films, binocular, light microscope, vibratome, and ultramicrotome.

C. Animals

Present protocol is adapted to eyes of following vertebrates: *Xenopus laevis*, C57BL/6J mice, Wistar rats, domestic pig, and the Rhesus monkey, *Macaca mulatta*. Mice, rats, and

Xenopi are sustained on a 12-h light–dark cycle, with food and water *ad libitum* at local animal house. Pig eyes are obtained from the local slaughter house. *Macaca* eyes are provided from German Primate Center, Göttingen, Germany. All experiments conform with the statement by the Association for Research in Vision and Ophthalmology and by the local administration concerning the care and use of animals in research.

III. Methods and Procedures

A. Tissue Dissection and Prefixation (Day 1)

Although the present preembedding labeling protocol is described for retinas from eyes of diverse vertebrates (mouse, rat, pig, Rhesus monkey, and frog) it can be applied to other tissues. Eye balls are removed from sacrificed animals, dissected, and placed in fresh 4% PFA prefixative for 50 min at room temperature (RT). For better fixative penetration the cornea and the lens of the eyes are perforated with a needle (ϕ 0.6 mm). After 30 min prefixation sections along the *ora serrata* are performed so that the lens and the vitreous body can be removed. The remaining eye ball is placed into fresh prefixative for further 20 min. For removing the prefixative specimens are washed in 0.1 M PB for 4×15 min under constant rocking on ice. For cryoprotection the eye cups are infiltrated with 10% sucrose in 0.1 M PB for 2 h on ice. Subsequently, retinas are isolated from eye cups and placed in 20% sucrose (1–2 h; rocking on ice) followed by overnight incubation in 30% sucrose at 4°C.

B. Cracking, Embedding, and Vibratome Sectioning (Day 2)

To enable the penetration of antibodies into the tissue, plasma membranes are "cracked" by at least 3–4 freezing and thawing cycles. For this, sucrose-covered retinas are dissected in 3–4 pieces, which are spread on a super frost® slide and frozen on a copper block precooled by liquid nitrogen. Subsequently, frozen samples are melted on the heating plate (37°C). After cracking, specimens are rinsed with PBS (4×15 min, rocking on ice) and embedded in warm 2% agar in PBS (<50°C) in silicon-embedding molds. Soiled agar blocks are placed in ice-cold PBS and can be stored for a few days in PBS at 4°C.

Specimens are cut with a vibratome (Leica VT 1000 S). For this the specimen chamber is filled with ice-cold PBS. Agar blocks are fixed with superglue at the vibratome specimen holder, trimmed, and sectioned. 50-μm-thick sections are grabbed with a fine smooth art paint brush and transferred into a homemade container with a nylon net bottom located in a 24-well plate filled with ice-cold PBS.

C. Antibody Incubation (Day 2–7)

After washing in cold PBS for 15 min (rocking on ice), nonspecific binding of the first antibodies is prevented by floating sections in blocking solution for 2 h, on a shaker

at RT. Subsequently, floating sections are incubated with first antibodies for 4 days on a shaker at 4°C. To prevent evaporation of the solution the 24-well plate is sealed with parafilm. After washing with PBS (4×15 min), sections are incubated with biotin-conjugated second antibodies for 2 h on a shaker at RT. Unbound second antibodies are washed away with PBS (4×15 min).

D. DAB Staining (Day 7)

The antibody staining is visualized using the VECTASTAIN® ABC kit according to manufacture instructions. VECTASTAIN® ABC kit provides the avidin-biotin-horseradish-peroxidase (HRP) complex (ABC) (Hsu *et al.*, 1981), which binds the biotin-conjugated second antibodies. PBS-washed sections are incubated with the premixed ABC of the VECTASTAIN® kit for 1.5 h in the dark.

After washes in PBS and then in 0.05 M Tris-HCl buffer, pH 7.6 (both 2×15 min, in the dark) the immune complex is visualized by a DAB reaction. For this, sections are preincubated with freshly prepared 0.05% DAB solution for 10 min at RT followed by incubation with 0.05% DAB solution containing 0.01% H_2O_2 until the sections change to brown (~5 min) indicating that DAB has been oxidized, converted into an insoluble brown polymer (Graham and Karnovsky, 1966). This reaction is stopped by the exchange of the DAB solution to 0.05 M Tris-HCl buffer, pH 7.6, and subsequent frequent washes in this Tris-HCl buffer for at least 30 min. After buffer change to 0.1 M CB (2×15 min) specimens are fixed in 2.5% GA in 0.1 M CB for 1 h at 4°C stabilizing the DAB staining as well as the cellular ultrastructure of the specimen. This interim fixation is stopped by washing with 0.1 M CB 15 min, before storing the samples in fresh 0.1 M CB overnight at 4°C.

Comment: For controls, first or second antibodies are omitted. Additional controls are preformed to analyze the endogenous peroxidase activity. For suppressing endogenous peroxidase activity sections are incubated with 3% H_2O_2 for 10 min before incubating with blocking solution.

E. Silver Enhancement of DAB Product (Day 8)

Silver enhancement is utilized to visualize the DAB product amplifying the staining for subsequent electron microscopic analyses (modified protocol from Leranth and Pickel, 1989). For this, sections are washed in H_2O_{bidest} (4×15 min, on a shaker at RT) to remove all available phosphates to prevent false labeling. For silver enhancement of the DAB product the three solutions A–C are mixed in a ratio of 5:0.25:0.5 and left on the specimens for 15 min at 60°C. After washing in H_2O_{bidest} (at least 3×3 min) sections are incubated with solution D for 4 min at RT and washed in H_2O_{bidest} again as above, before incubated with solution E for 4 min at RT. During H_2O_{bidest} washes (3×3 min) samples are transferred into smaller volume reaction tubes and H_2O_{bidest} is exchanged in two steps to 0.1 M CB.
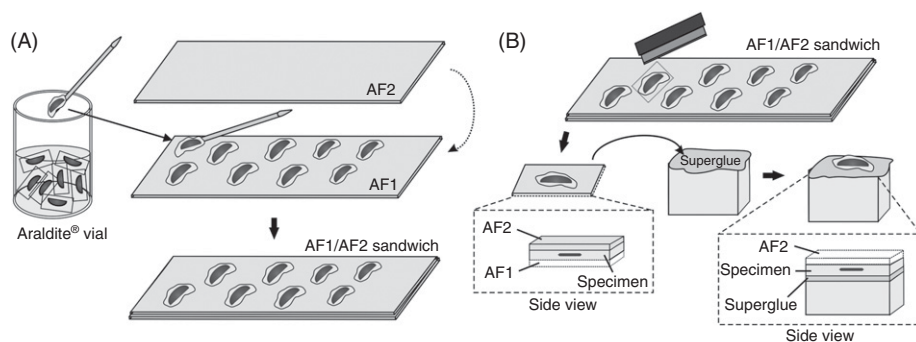
Fig. 2 Mounting and flat-embedding of vibratome sections. (A) Vibratome sections are transferred from the Araldite® containing glass vial using a toothpick to an ACLAR® film (AF1) and covered with a second ACLAR® film (AF2). (B) Selected sections are excised from the AF1/AF2 sandwich and the ACLAR® films are separated using a razor blade. The ACLAR® film containing the Araldite® flat-embedded sections are mounted with superglue onto an Araldite® block. Subsequently, ACLAR® film is removed and after trimming specimen blocks are read for ultrathin sectioning.

F. Postfixation, Flat–Embedding, and Polymerization (Day 8–12)

Postfixation of the samples is carried out in 0.5% OsO_4 in 0.1 M CB for 15 min at 4° C. After washing in ice-cold 0.1 M CB for 3×10 min, samples were dehydrated in a graded series of undenaturated ethanol (30–90%) (each dehydration step 10 min, 96 and 99.8% ethanol 2×10 min). Because Araldite® does not mingle with ethanol, propylene oxide is used as an intermedium for 2×5 min in small glass vials under the hood. Subsequently, samples are incubated in a 1:1 mixture of propylene oxide and Araldite® resin overnight. During this the propylene oxide is allowed to evaporate from the mixture and thereby, Araldite® resin slowly concentrates in the specimens. On day 9, each sample is transferred with a toothpick into a new glass vial containing pure Araldite® and placed again under the hood overnight before the sections are transferred with a toothpick on ACLAR® film and covered with a second ACLAR® film (Fig. 2A). Subsequently, sandwiches of Araldite® flat-embedded samples are polymerized for 48 h at 60°C (day 11, day 12).

G. Ultrathin Sections, Transmission Electron Microscopy Analyses, and Image Processing (Day 13)

Sections are selected by criteria "gross-morphology" changes of the retina sections by light microscopy. Selected sections are excised and the two ACLAR® films of the sandwich are separated by using a razor blade (Fig. 2B). The ACLAR® film containing the Araldite®-embedded section is fixed with superglue onto an Araldite® block oriented with the section "sunny side" down (Fig. 2B). After the glue is congealed the second ACLAR® film is detached and the specimen block is ultrathin sectioned (<60 nm) with an ultramicrotome Reichert Ultracut S. Ultrathin sections are collected

on formvar-coated copper grids and are observed without or with heavy metal counterstaining (2% ethanolic uranyl acetate in 50% ethanol; 2% aqueous lead citrate) in a Technai 12 BioTwin transmission electron microscope (FEI, Eindhoven, the Netherlands). Images are obtained with a CCD camera (SIS MegaView3, Surface Imaging Systems, Herzogenrath, Germany) and processed with Adobe Photoshop CS (Adobe Systems, San Jose, CA, USA).

IV. Results and Discussion

Cilia are characteristic organelles of eukaryotes showing high structural complexity and diversity (600 to $>$ 1200 polypeptides) (Pedersen and Rosenbaum, 2008; Roepman and Wolfrum, 2007). Since neither ribosomes nor membrane vesicles are present in cilia all their components must be synthesized in the cytoplasm of the cell body and subsequently delivered into the cilium. In the case of ciliary membrane proteins, electron microscopic analyses have indicated that proteins are synthesized on the rough ER and after passage through the Golgi apparatus they are incorporated in the membrane of post-Golgi vesicles and transported to the base of the cilium (Bouck, 1971; Papermaster, 2002; Sorokin, 1962). Here the vesicles dock and fuse with the periciliary membrane for the further delivery into the ciliary compartment. Furthermore, there is evidence that compounds of the axoneme of cilia and flagella, synthesized in the cytoplasm, associate with post-Golgi vesicles for their transport to the cilium (Rosenbaum and Witman, 2002). In either case, transport vesicles and their cargo get associated with the intraflagellar transport (IFT) machinery at the base of the cilium prior to the further transport into the cilium. IFT protein complexes are thought to be assembled at the base of cilia and flagella. They are universal components of anterograde and retrograde microtubule-based transport processes in cilia required for the assembly and maintenance of cilia (Pedersen and Rosenbaum, 2008). In the present analysis of vesicular trafficking to the ciliary compartment we utilize the association of specific individual IFT proteins and of other molecules of ciliary-targeting machinery with transport vesicles for the visualization of ciliary cargo vesicles by immunoelectron microscopy. Fixation and embedding procedures always compromise between good morphology preservation and retention of antigenicity (Oliver and Jamur, 1999). Because fixations for postembedding procedures do not preserve membranes in general this constitutes an unacceptable condition for the analysis of cargo vesicles (Takamiya *et al*., 1980), and because postembedding labeling of ciliary antigens on plastic sections failed or was so far of poor quality (Luby-Phelps *et al.*, 2008; T. Sedmak and U. Wolfrum, unpublished) we developed an alternative preembedding immunolabeling strategy to overcome these problems. For this purpose we modified previous preembedding protocols (Brandstätter *et al*., 1996).

A. Expression and Subcellular Localization of Individual IFT in Photoreceptor Cells

Immunohistochemical analyses of cryosections through the retina of diverse vertebrate species by indirect immunofluorescence confirmed previous data obtained for the
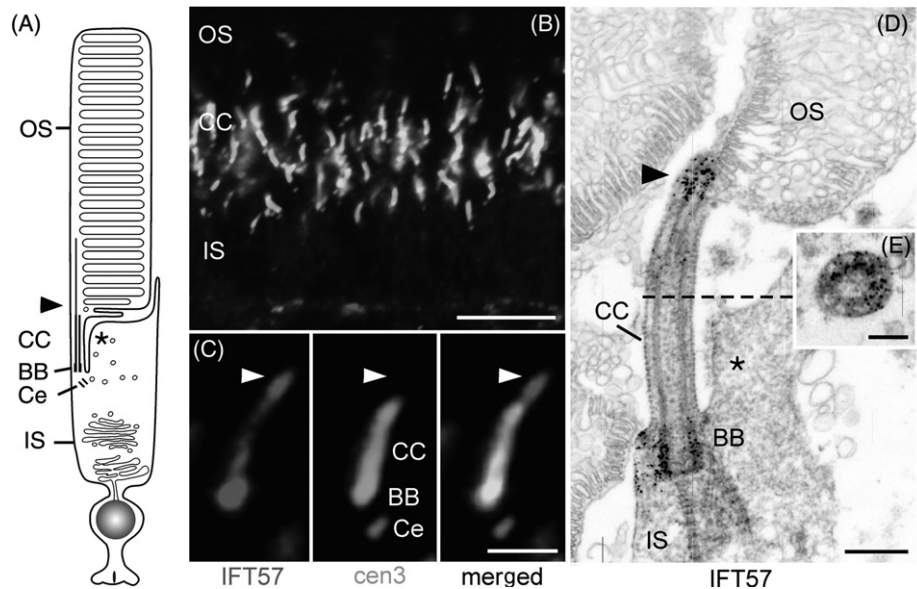
Fig. 3 Localization of IFT57 in the photoreceptor cilium. (A) Scheme of a rod photoreceptor cell. (B, C) Double immunofluorescence staining of IFT57 (red) and centrin3 (cen3) (green) in a cryosection through photoreceptor cell layer of a mouse retina. IFT57 partly colocalizes with centrin 3, a molecular marker for the ciliary apparatus (Trojan *et al.*, 2008). (C) High-magnification images of a single photoreceptor cilium from (B). IFT57 colocalizes with centrin 3 at the basal body (BB) and in the connecting cilium (CC), but not at the cilium adjacent centriole (Ce). In the absence of centrin 3, IFT57 is concentrated at the base of the outer segment (OS) (*arrow head*). (D) Preembedding immunoelectron microscopy labeling of IFT57 in a longitudinal section through part of a mouse rod cells. IFT57 is concentrated at the base of the OS (*arrow head*), sparsely decorated in the CC, and labeled in the periciliary region of the BB, but is absent from the periciliary apical extension of the IS (*asterisk*). (E) IFT57 labeling in a cross-section through the CC. Scale bars: B, 5 µm; C, 0.6 µm; D, 0.2 µm; E, 0.1 µm. (See Plate no. 17 in the Color Plate Section.)

ciliary localization of individual IFT proteins in the photoreceptor cell of the vertebrate retina (Luby-Phelps *et al.*, 2008; Pazour *et al.*, 2002) (Fig. 3B and C). However, our detailed analysis of the subciliary distribution of individual IFT polypeptides by high-resolution immunofluorescence microscopy combined with molecular markers of ciliary subcompartments determined a differential localization of individual IFT molecules in photoreceptor cells; a presence or an absence of the individual IFTs: at the cilia-adjacent centriole, at the basal body, in the periciliary membrane adhesion complex of the inner segment extension, in the connecting cilium, and in the axoneme (for details see Sedmak *et al.*, in preparation). Use of the preembedding methodology described above enabled us to demonstrate the subciliary localization of individual IFT proteins for the first time by the ultrastructural resolution of electron microscopy, exemplarily shown for IFT57 in Fig. 3D and E. In conclusion, our results further support the differential localization of individual IFT molecules in the subciliary compartment indicating slightly diverse but overlapping cellular functions.

B. Identification of Ciliary Cargo Vesicles in the Cytoplasm on Their Track to the Cilium

In addition to the subciliary analyses our preembedding method enabled us to stain the molecules associated with membrane vesicles present in the inner segment of photoreceptor cells. Using antibodies to label ciliary molecules and molecules involved in ciliary targeting (Maerker et al., 2008; Bauß et al., in preparation) we identified a set of inner segment vesicles as ciliary cargo vesicles independent of their cargo by immunoelectron microscopy (Fig. 4). Applying our preembedding protocol we detected individual IFT molecules, namely IFT20, IFT52, and IFT57, as well as molecules of the periciliary-targeting complex at the surface of vesicles present in the cytoplasm of the apical inner segment of photoreceptor cells (Figs. 4A/A′–C/C′). In
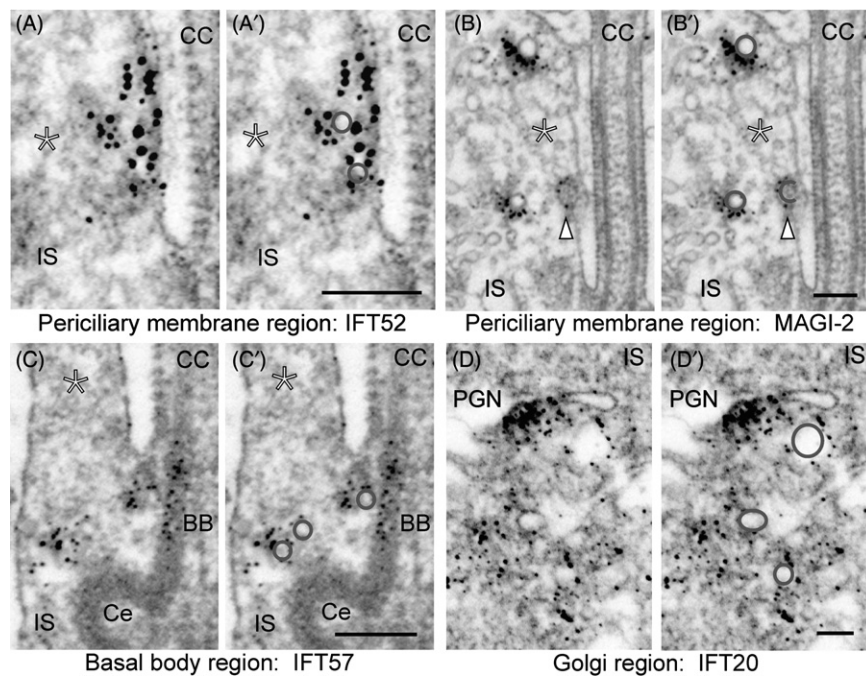
Fig. 4   Ciliary cargo vesicles identified by preembedding immunolabeling of individual IFT molecules and MAGI-2 in mouse photoreceptor cells. (A/A′, B/B′) Electron micrographs of longitudinal sections of the connecting cilium (CC) and the periciliary apical extension of the inner segment (IS) (*asterisk*) labeled with antibodies to IFT52 (A/A′) and to MAGI-2 (membrane associated guanylate kinase, WW and PDZ domain containing 2) protein (B/B′), a novel component of the periciliary targeting complex of the apical inner segment (Bauß et al., in preparation; Maerker et al., 2008). (A–B′) IFT52 and MAGI-2 are decorated at vesicles (circles in A′, B′) present at the docking zone of cargo vesicles. (C/C′) Immunoelectron microscopy labeling of IFT57 at cargo vesicles at the base of the photoreceptor cilium—in the region of the basal body (BB) and the adjacent centriole (Ce). *Arrowhead* indicates vesicle exocytosis in the periciliary targeting membrane. (D) Immunoelectron microscopy labeling of IFT20 in a cross-section through post-Golgi network (PGN) in the photoreceptor IS. IFT20 is associated with the membrane stacks of the PGN and present at budded post-Golgi vesicles. Scale bars: 0.2 μm. (See Plate no. 18 in the Color Plate Section.)

addition, these molecules were localized at vesicles during the processes of docking, fusion, and exocytosis (Fig. 4B/B′). IFT20 was further found to be associated with the membrane stacks of the post-Golgi network and with post-Golgi vesicles containing ciliary cargo (Fig. 4D/D′). Latter observation supported recent data (Follit *et al.*, 2006, 2008).

All in all, ciliary cargo vesicles were identified in all steps of the inner segment transport track traversed by the vesicles on their destination to the ciliary compartment, the photoreceptor outer segment (see detailed description above). These results confirm the data of previous studies on the visualization of cytoplasm or synaptic vesicles applying slightly different preembedding labeling techniques (Brandstätter *et al.*, 1996; Chuang et al., 2001; Melo *et al.*, 2009; Tanner *et al.*, 1996; van den Pol, 1986). Application of the protocol on retinas of different vertebrate species and preliminary data indicate that the present preembedding procedure described here is transferable to other cilia containing tissues and cells.

The present preembedding labeling method has certain advantages in comparison to conventional postembedding procedures: the rather mild prefixation is comparable to treatments used for immunohistochemical and cytochemical methods and preserves the antigenity of ciliary molecules much better than the processing in postembedding protocols. Although the preembedding protocol includes the rather crude cracking step, membranes are archived in an acceptable condition necessary for successful identification of cargo vesicles in the cytoplasm.

Acknowledgments

References

Besharse, J.C., and Horst, C.J. (1990). The photoreceptor connecting cilium—a model for the transition zone. *In* "Ciliary and Flagellar Membranes" (R.A. Bloodgood, ed.), pp. 389–417. Plenum, New York.

Bauß, K., Maerker, T., Sehn, E., Kersten, F., Kremer, H., and Wolfrum, U. Cargo vesicle association and direct binding MAGI-2 to the of USH1G protein SANS. (in preperation).

Bouck, G.B. (1971). The structure, origin, isolation, and composition of the tubular mastigonemes of the Ochromas flagellum. *J. Cell Biol*. **50**, 362–384.

Brandstätter, J.H., Lohrke, S., Morgans, C.W., and Wassle, H. (1996). Distributions of two homologous synaptic vesicle proteins, synaptoporin and synaptophysin, in the mammalian retina. *J. Comp. Neurol*. **370**, 1–10.

Burns, M.E., and Arshavsky, V.Y. (2005). Beyond counting photons: Trials and trends in vertebrate visual transduction. *Neuron* **48**, 387–401.

Chuang, J.Z., Milner, T.A., and Sung, C.H. (2001). Subunit heterogeneity of cytoplasmic dynein: Differential expression of 14 kDa dynein light chains in rat hippocampus. *J. Neurosci*. **21**, 5501–5512.

Corless, J.M., Cobbs, W.H., III, Costello, M.J., and Robertson, J.D. (1976). On the asymmetry of frog retinal rod outer segment disk membranes. *Exp. Eye Res*. **23**, 295–324.

Deretic, D. (2006). A role for rhodopsin in a signal transduction cascade that regulates membrane trafficking and photoreceptor polarity. *Vision Res*. **46**, 4427–4433.

Follit, J.A., San Agustin, J.T., Xu, F., Jonassen, J.A., Samtani, R., Lo, C.W., and Pazour, G.J. (2008). The Golgin GMAP210/TRIP11 anchors IFT20 to the Golgi complex. *PLoS. Genet.* **4**, e1000315.

Follit, J.A., Tuft, R.A., Fogarty, K.E., and Pazour, G.J. (2006). The intraflagellar transport protein IFT20 is associated with the Golgi complex and is required for cilia assembly. *Mol. Biol. Cell* **17**, 3781–3792.

Gerdes, J.M., Davis, E.E., and Katsanis, N. (2009). The vertebrate primary cilium in development, homeostasis, and disease. *Cell* **137**, 32–45.

Graham, R.C., Jr. and Karnovsky, M.J. (1966). The early stages of absorption of injected horseradish peroxidase in the proximal tubules of mouse kidney: Ultrastructural cytochemistry by a new technique. *J. Histochem. Cytochem.* **14**, 291–302.

Hsu, S.M., Raine, L., and Fanger, H. (1981). Use of avidin-biotin-peroxidase complex (ABC) in immunoperoxidase techniques: A comparison between ABC and unlabeled antibody PAP procedures. *J. Histochem. Cytochem.* **29**, 577–580.

Insinna, C., and Besharse, J.C. (2008). Intraflagellar transport and the sensory outer segment of vertebrate photoreceptors. *Dev. Dyn.* **237**, 1982–1992.

Insinna, C., Humby, M., Sedmak, T., Wolfrum, U., and Besharse, J.C. (2009). Different roles for KIF17 and kinesin II in photoreceptor development and maintenance. *Dev. Dyn.* **238**, 2211–2222.

Leranth, C., and Pickel, V.M. (1989). Electron microscopic preembedding double immunostaining methods. *In* "Neuroanatomical Tract-Tracing Methods" (L. Heimer and L. Zaborszky, eds.), pp. 129–172. Plenum Press, New York.

Liu, X., Udovichenko, I.P., Brown, S.D., Steel, K.P., and Williams, D.S. (1999). Myosin VIIa participates in opsin transport through the photoreceptor cilium. *J. Neurosci.* **19**, 6267–6274.

Luby-Phelps, K., Fogerty, J., Baker, S.A., Pazour, G.J., and Besharse, J.C. (2008). Spatial distribution of intraflagellar transport proteins in vertebrate photoreceptors. *Vision Res.* **48**, 413–423.

Maerker, T., van Wijk, E., Overlack, N., Kersten, F.F., McGee, J., Goldmann, T., Sehn, E., Roepman, R., Walsh, E.J., Kremer, H., and Wolfrum, U. (2008). A novel Usher protein network at the periciliary reloading point between molecular transport machineries in vertebrate photoreceptor cells. *Hum. Mol. Genet.* **17**, 71–86.

Marszalek, J.R., Liu, X., Roberts, E.A., Chui, D., Marth, J.D., Williams, D.S., and Goldstein, L.S.B. (2000). Genetic evidence for selective transport of opsin and arrestin by kinesin-II in mammalian photoreceptors. *Cell* **102**, 175–187.

Melo, R.C., Spencer, L.A., Perez, S.A., Neves, J.S., Bafford, S.P., Morgan, E.S., Dvorak, A.M., and Weller, P.F. (2009). Vesicle-mediated secretion of human eosinophil granule-derived major basic protein. *Lab. Invest.* **89**, 769–781.

Oliver, C., and Jamur, M.C. (1999). Fixation and Embedding. *In* "Methods in Molecular Biology" (L.C. Lavois, ed.), pp. 319–326, Humana Press Inc., Totowa, NJ.

Papermaster, D.S. (2002). The birth and death of photoreceptors: The Friedenwald Lecture. *Invest. Ophthalmol. Vis. Sci.* **43**, 1300–1309.

Pazour, G.J., Baker, S.A., Deane, J.A., Cole, D.G., Dickert, B.L., Rosenbaum, J.L., Witman, G.B., and Besharse, J.C. (2002). The intraflagellar transport protein, IFT88, is essential for vertebrate photoreceptor assembly and maintenance. *J. Cell Biol.* **157**, 103–113.

Pazour, G.J., and Bloodgood, R.A. (2008). Targeting proteins to the ciliary membrane. *Curr. Top. Dev. Biol.* **85**, 115–149.

Pazour, G.J., and Witman, G.B. (2003). The vertebrate primary cilium is a sensory organelle. *Curr. Opin. Cell Biol.* **15**, 105–110.

Pedersen, L.B., and Rosenbaum, J.L. (2008). Intraflagellar transport (IFT) role in ciliary assembly, resorption and signalling. *Curr. Top. Dev. Biol.* **85**, 23–61.

Roepman, R., and Wolfrum, U. (2007). Protein networks and complexes in photoreceptor cilia. *In* "Subcellular Proteomics—From Cell Deconstruction to System Reconstruction" (M. Faupel and E. Bertrand, ed.), pp. 209–235. Springer, Dordrecht.

Rosenbaum, J.L., and Witman, G.B. (2002). Intraflagellar transport. *Nat. Rev. Mol. Cell Biol.* **3**, 813–825.

Sedmak, T., and Wolfrum, U. Differential ciliary and non-ciliary localization of intraflagellar transport molecules in the mammalian retina. (in preparation).

Sorokin, S. (1962). Centrioles and the formation of rudimentary cilia by fibroblasts and smooth muscle cells. *J. Cell Biol*. **15**, 363–377.

Sung, C.H., and Tai, A.W. (2000). Rhodopsin trafficking and its role in retinal dystrophies. *Int. Rev. Cytol*. **195**, 215–267.

Tai, A.W., Chuang, J.Z., Bode, C., Wolfrum, U., and Sung, C.H. (1999). Rhodopsin's carboxy-terminal cytoplasmic tail acts as a membrane receptor for cytoplasmic dynein by binding to the dynein light chain Tctex-1. *Cell* **97**, 877–887.

Takamiya, H., Batsford, S., and Vogt, A. (1980). An approach to postembedding staining of protein (immunoglobulin) antigen embedded in plastic: Prerequisites and limitations. *J. Histochem. Cytochem*. **28**, 1041–1049.

Tanner, V.A., Ploug, T., and Tao-Cheng, J.H. (1996). Subcellular localization of SV2 and other secretory vesicle components in PC12 cells by an efficient method of preembedding EM immunocytochemistry for cell cultures. *J. Histochem. Cytochem*. **44**, 1481–1488.

tom Dieck, S., and Brandstätter, J.H. (2006). Ribbon synapses of the retina. *Cell Tissue Res*. **326**, 339–346.

Trojan, P., Krauss, N., Choe, H.W., Giessl, A., Pulvermuller, A., and Wolfrum, U. (2008). Centrins in retinal photoreceptor cells: Regulators in the connecting cilium. *Prog. Retin. Eye Res*. **27**, 237–259.

van den Pol, A.N. (1986). Tyrosine hydroxylase immunoreactive neurons throughout the hypothalamus receive glutamate decarboxylase immunoreactive synapses: A double pre-embedding immunocytochemical study with particulate silver and HRP. *J. Neurosci*. **6**, 877–891.

Wolfrum, U., and Schmitt, A. (2000). Rhodopsin transport in the membrane of the connecting cilium of mammalian photoreceptor cells. *Cell Motil. Cytoskeleton* **46**, 95–107.

Young, R.W. (1976). Visual cells and the concept of renewal. *Invest. Ophthalmol. Vis. Sci*. **15**, 700–725.

2.2 Publication II

Sedmak T, Wolfrum U (2010) Intraflagellar transport molecules in ciliary and nonciliary cells of the retina. J. Cell Biol. 189: 171-186

Intraflagellar transport molecules in ciliary and nonciliary cells of the retina

Tina Sedmak and Uwe Wolfrum

Department of Cell and Matrix Biology, Institute of Zoology, Johannes Gutenberg University Mainz, D-55099 Mainz, Germany

The assembly and maintenance of cilia require intraflagellar transport (IFT), a process mediated by molecular motors and IFT particles. Although IFT is a focus of current intense research, the spatial distribution of individual IFT proteins remains elusive. In this study, we analyzed the subcellular localization of IFT proteins in retinal cells by high resolution immunofluorescence and immunoelectron microscopy. We report that IFT proteins are differentially localized in subcompartments of photoreceptor cilia and in defined periciliary target domains for cytoplasmic transport, where they are associated with transport vesicles. IFT20 is not in the IFT core complex in photoreceptor cilia but accompanies Golgi-based sorting and vesicle trafficking of ciliary cargo. Moreover, we identify a nonciliary IFT system containing a subset of IFT proteins in dendrites of retinal neurons. Collectively, we provide evidence to implicate the differential composition of IFT systems in cells with and without primary cilia, thereby supporting new functions for IFT beyond its well-established role in cilia.

Introduction

Intraflagellar transport (IFT) was first described in the flagella of *Chlamydomonas* (Kozminski et al., 1993) and has since been proven to be a conserved process in a variety of motile and non-motile cilia in eukaryotic organisms (Sloboda, 2005). IFT comprises the bidirectional transport of IFT particles containing ciliary or flagellar cargo along the outer doublet microtubules of the axoneme (Rosenbaum and Witman, 2002). These processes ensure the assembly and the molecular turnover of ciliary components (Qin et al., 2004) but also take part in signaling processes generated in the cilium (Wang et al., 2006). Genetic evidence indicates that kinesin-II family members serve as anterograde transport motors in IFT (Kozminski et al., 1995; Cole et al., 1998; Snow et al., 2004), whereas the cytoplasmic dynein 2/1b mediates IFT in the retrograde direction (Pazour et al., 1998, 1999; Signor et al., 1999a). Biochemical analyses revealed that IFT particles are composed of IFT proteins organized into two complexes, A and B (Cole et al., 1998; Cole, 2003). The sequences of IFT proteins are highly conserved between species, and mutations in these genes disturb ciliary assembly in all organisms tested (Cole et al., 1998; Murcia et al., 2000; Pazour et al., 2002; Tsujikawa and Malicki, 2004;

Krock and Perkins, 2008; Omori et al., 2008). Nevertheless, the specific functions of the individual IFT proteins in IFT as well as their subcellular and subcompartmental localization in cilia remain to be elucidated (Sloboda, 2005). Interestingly, there is growing evidence for a role of IFT proteins in processes not associated with cilia (Pazour et al., 2002; Follit et al., 2006; Jékely and Arendt, 2006; Finetti et al., 2009; Baldari and Rosenbaum, 2010).

Over the last decade, IFT has been studied intensively in sensory cilia, including photoreceptor cell outer segments (OSs) in the vertebrate retina (e.g., Beech et al., 1996; Pazour et al., 2002; Baker et al., 2003; Insinna et al., 2008, 2009; Krock and Perkins, 2008; Luby-Phelps et al., 2008). Vertebrate photoreceptors are highly polarized sensory neurons consisting of morphologically and functionally distinct cellular compartments. A short axon projects from the cell body of the photoreceptor to form synaptic contact with secondary retinal neurons (bipolar and horizontal cells), and at the opposite pole, a short dendrite is differentiated into the inner segment (IS) and the light-sensitive OS (Fig. 1; Besharse and Horst, 1990; Roepman and Wolfrum, 2007). The OS is similar to other sensory cilia (Insinna and Besharse, 2008) but, in addition, contains specialized

Correspondence to Uwe Wolfrum: wolfrum@uni-mainz.de

Abbreviations used in this paper: BB, basal body; CC, connecting cilium; GA, Golgi apparatus; IFT, intraflagellar transport; INL, inner nuclear layer; IS, inner segment; ONL, outer nuclear layer; OPL, outer plexiform layer; OS, outer segment; RPE, retinal pigment epithelium.

Supplemental Material can be found at:
http://jcb.rupress.org/content/suppl/2010/04/05/jcb.200911095.DC1.html

The Rockefeller University Press $30.00
J. Cell Biol. Vol. 189 No. 1 171–186
www.jcb.org/cgi/doi/10.1083/jcb.200911095

JCB 171
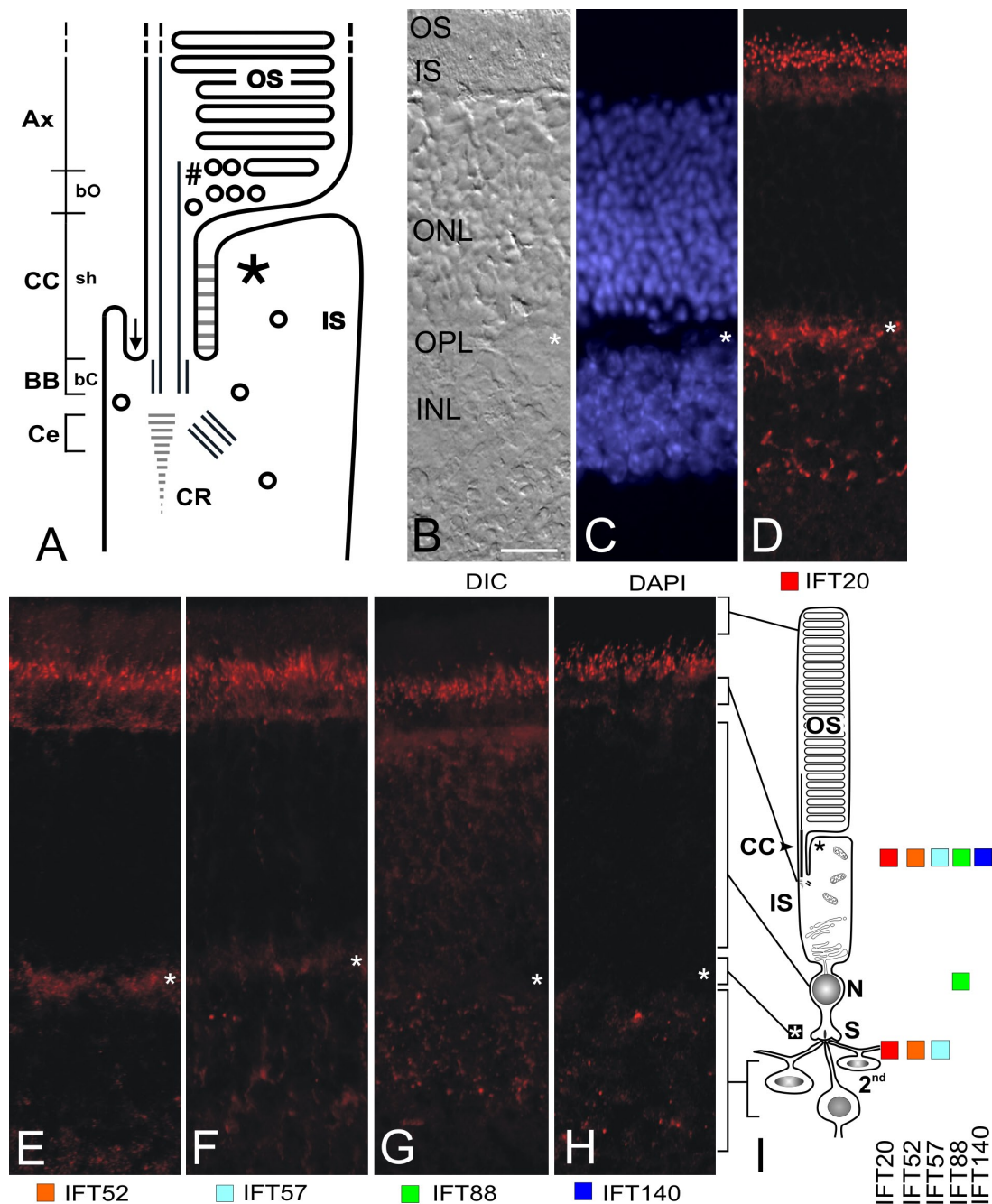
Figure 1. **Localization of IFT proteins in the retina.** (A) Schema of the ciliary apparatus of a rod photoreceptor cell: the photosensitive OS linked by the CC to the IS. The CC is composed of a basal part (bC), which represents the region of the BB, and the CC shaft (sh). The shaft continues into the base of the OS (bO; number sign). Microtubules of the axoneme (Ax) extend into the OS. A centriole (Ce) is adjacent to the BB and the ciliary rootlet (CR). A black asterisk indicates the apical periciliary extension of the IS. The arrow points into the groove between the IS and CC. (B–D) Longitudinal cryosection through a mouse retina. Differential interference contrast (DIC) image (B), DAPI staining (C), and indirect immunofluorescence of anti-IFT20 (D) are shown. (E–H) Immunofluorescence of longitudinal cryosections through mouse retinas stained for IFT52 (E), -57 (F), -88 (G), and -140 (H). (I) Schema of a rod cell and connection to secondary retinal neurons (2nd) illustrating the differential localization of IFT proteins. Photoreceptor cell bodies harboring nuclei (N) are located in the ONL. Synapses (S) to secondary neurons in the OPL (white asterisks) are shown. Bar, 10 μm.

flattened disk-like membranes, where all components of the visual transduction cascade are arranged (Yau and Hardie, 2009). These phototransductive membranes are continually renewed throughout lifetime; newly synthesized membranes are added at the base of the OS, whereas aged disks at the apex are phagocytosed by cells of the retinal pigment epithelium (RPE; Young, 1976). This high membrane turnover implies an efficient and massive vectorial transport of all OS components from the site of their biogenesis in the photoreceptor IS to the base of the OS, the site of disk neogenesis. On its route to the OS, cargo has to be reloaded from IS transport carriers to ciliary transport systems in a specialized compartment of the apical IS (Papermaster, 2002; Roepman and Wolfrum, 2007; Maerker et al., 2008). In addition to the unidirectional constitutive translocations of OS

molecules, light-dependent bidirectional movement of molecules across the connecting cilium (CC) contributes to the long range light adaptation of rod photoreceptor cells (Calvert et al., 2006). Structural and molecular characteristics qualify the CC as the equivalent of the transition zone localized between the basal body (BB) and the axoneme in proteotypic cilia (Fig. 1 A; Besharse and Horst, 1990; Roepman and Wolfrum, 2007; Insinna and Besharse, 2008). Some microtubules of the CC extend throughout almost the entire length of the OS, where they mediate protein trafficking within the OS (Liu et al., 2002; Reidel et al., 2008).

IFT has been proposed as an essential transport mechanism in photoreceptor cells (Rosenbaum et al., 1999), and its critical importance has been demonstrated subsequently (Pazour et al., 2002; Tsujikawa and Malicki, 2004; Krock and Perkins, 2008). As in other ciliated and flagellated cells, the mode of the IFT operation and the assignment of specific functions to individual IFT proteins are still lacking in photoreceptor cells (Baker et al., 2004; Hou et al., 2007; Bhowmick et al., 2009). A systematic analysis of the subcellular distribution of IFT proteins in photoreceptor cells will provide important insights into the roles of IFT proteins unique for specialized photoreceptor cilia but also into more general processes associated with IFT proteins common to all cilia and flagella. So far, studies on the distribution of IFT proteins in photoreceptor cells were limited to a few immunofluorescence analyses (Pazour et al., 2002; Tsujikawa and Malicki, 2004; Krock and Perkins, 2008) and to a preliminary electron microscopic study on IFT88 (Luby-Phelps et al., 2008), which collectively provided only limited insight into the spatial distribution of IFT proteins.

In this study, we used a combination of high resolution immunofluorescence and immunoelectron microscopy for the analyses of the spatial distribution of IFT proteins in retinal neurons. Our data reveal that IFT proteins are differentially localized in subciliary compartments but also present in nonciliary compartments of photoreceptor cells. Furthermore, the localization of IFT proteins in dendritic processes of nonciliated neurons indicates that IFT protein complexes operate in nonciliated cells and may participate in intracellular vesicle trafficking in eukaryotic cells in general.

Results

Although substantial biochemical and genetic efforts have been undertaken and genetic evidence indicates important roles of each IFT particle protein in the development and maintenance of cilia, the functions of the individual IFT molecules remained largely elusive (Sloboda, 2005). This is partly because of the insufficient knowledge concerning the subcellular localization of the IFT proteins. In this study, we have systematically analyzed the expression and subcellular localization of four different IFT complex B proteins, IFT20, -52, -57, and -88, as well as the complex A protein IFT140 in the mouse retina.

Expression of IFT proteins in the mammalian retina

IFT protein expression was accessed by Western blots using previously characterized affinity-purified polyclonal antibodies

raised to murine IFT proteins (Pazour et al., 2002; Baker et al., 2003; Follit et al., 2006). These experiments verified the expression of all five IFT proteins in the murine retina (Fig. S1, A and B). The antibodies to four IFT proteins each recognized a single band of expected size in retinal protein extracts, which implied that these antibodies are monospecific. Only anti-IFT52 detected a second band with a slightly lower molecular weight in retinal extracts, which was not observed in analyses of testis samples (Fig. S1, A and C). This band might be caused by a splice variant of IFT52, which is expressed in the retina but is absent in testis.

The retina is composed of well-defined layers consisting of specific cell types or even at subcellular compartments of retinal cells (Fig. 1). This spatial organization makes it relatively easy to determine the subcellular localization of proteins in retinal sections, even under light microscopy. To determine the subcellular distribution of IFT proteins in the retina, cryosections of mouse eye were analyzed by indirect immunofluorescence. As expected from previous studies (Pazour et al., 2002; Krock and Perkins, 2008), all IFT molecules were most abundant in the photoreceptor layer of the retina (Fig. 1). Weak immunoreactivity for IFT88 was also found in the outer nuclear layer (ONL), where the perikarya of the photoreceptor cells are located (Fig. 1 G), and for all IFT molecules in the inner nuclear layer (INL), where the perikarya of the secondary retinal neurons are found (Fig. 1, D–H). Immunostaining for IFT20, -52, and -57 was also observed in the outer plexiform layer (OPL), which contains the presynaptic terminals of photoreceptor cells connected to the postsynaptic terminals of the dendritic processes in secondary retinal neurons, namely bipolar and horizontal cells (Fig. 1, D–F). In addition, IFT20 was expressed in the cells of the RPE and in the ganglion cell layer (Fig. S2 A). The localization of these five IFT proteins in the mouse retina (Fig. 1 I) was identical to that found by indirect immunofluorescence in human and bovine retinas (Fig. S3). To exclude epitope masking by fixation (Follit et al., 2006), we also performed immunocytochemistry on methanol-fixed cryosections and observed no changes in immunostaining (Fig. S4).

Differential subciliary localization of IFT proteins in the photoreceptor cilium

To elucidate the subciliary localization of IFT proteins in the photoreceptor cell layer of the mouse retina, cryosections were analyzed by double labeling with antibodies against IFT proteins and markers of subciliary compartments. Double labeling with anti–centrin-3, a marker for the CC, the BB, and the adjacent centriole (Trojan et al., 2008), and with antibodies to IFT proteins allowed us to determine the spatial localization of IFT proteins in the photoreceptor ciliary apparatus (Fig. 2).

High resolution immunofluorescence imaging of double labeled specimens revealed different subciliary localization of the IFT proteins, as shown in Fig. 2. Double labeling experiments revealed that IFT52, -57, -88, and -140 were concentrated on the tip of the CC in the OS base (Fig. 2, B′–E′). IFT88 and -140 were also detected in the axoneme, which extended further into the distal part of the OS of photoreceptors (Fig. 2, D′ and E′). Latter axonemal localization of these IFT proteins was confirmed
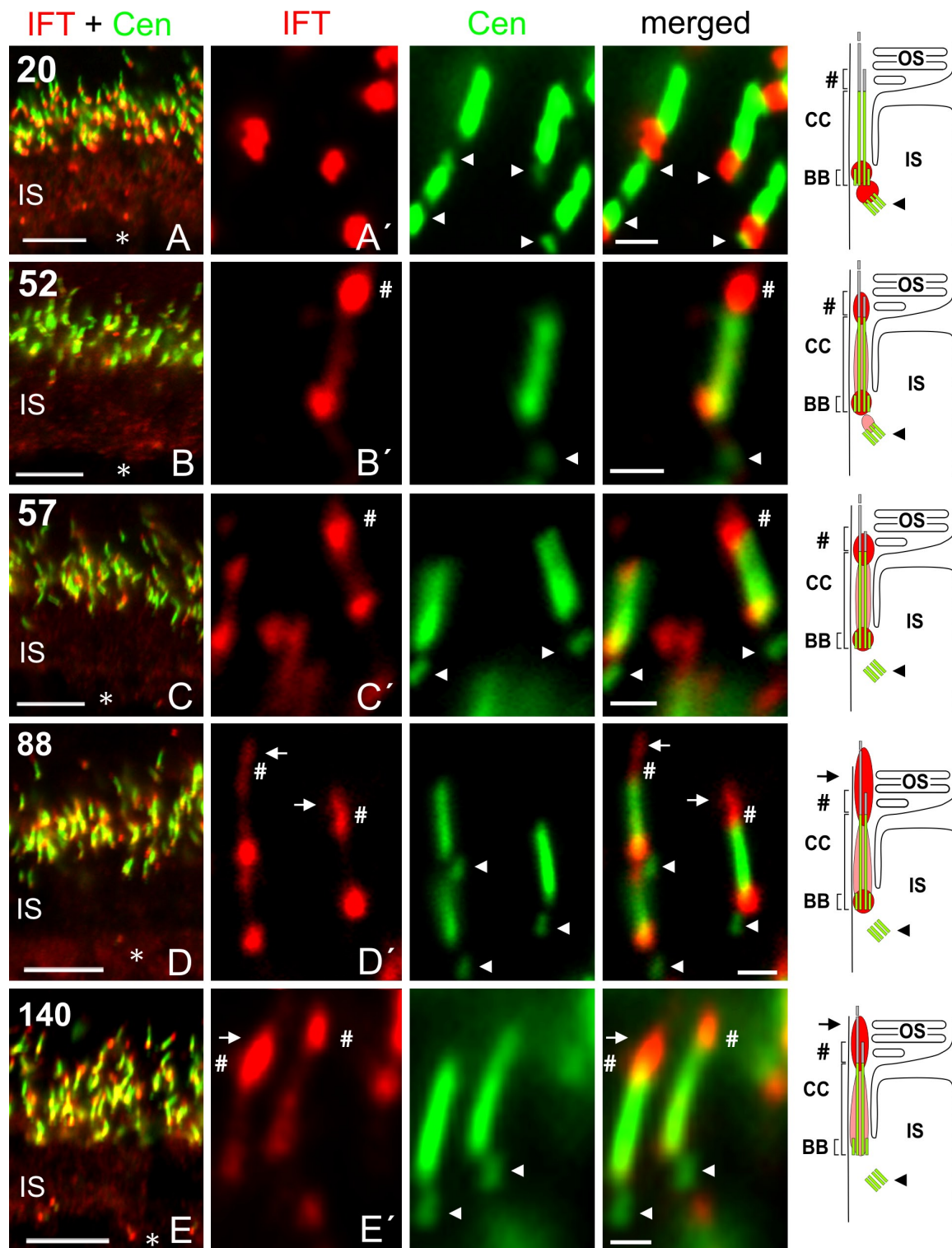
Figure 2. **Differential localization of IFT proteins in photoreceptor cell cilia.** (A–E) Merged images of indirect immunofluorescence double labeling with antibodies to IFT proteins and the ciliary marker anti–centrin-3 (Cen) in cryosections through mouse retinas. (A′–E′) High magnification images of double immunofluorescences in ciliary parts of photoreceptor cells and schemes illustrating subciliary localizations of IFT proteins in relation to centrin-3 located in the CC, its ciliary shaft, its BB, and at the adjacent centriole (arrowheads). IFT20 is present in the basal part of the CC and at the centriole, where IFT52 is also found. IFT52, -57, -88, and -140 are located in the CC, concentrated in its basal part and the OS base (number signs); IFT88 and -140 staining further extends into the axoneme (arrows) of the OS. Asterisks indicate nuclei. Bars: (A–E) 5 µm; (A′–C′ and E′) 0.5 µm; (D′) 1 µm.

by double labeling with an antibody to RP1, a molecular marker for the photoreceptor axoneme (Fig. S2 C; Liu et al., 2002). Weaker staining of IFT52, -57, -88, and -140 was present along

the shaft of the CC (Fig. 2, B′–E′). Strong immunoreactivity for IFT52, -57, and -88 was also observed in the basal part of the CC, whereas the anti-IFT140 immunofluorescence was less

intense in this area (Fig. 2, B′–E′). In contrast to the other IFT proteins analyzed, IFT20 was only detected in the basal part of the CC and at the distal region of the adjacent centriole (Fig. 2 A′). We also detected weak immunofluorescence of IFT52 at the centriole (Fig. 2 B′).

To pinpoint the subcellular localization of the IFT molecules in photoreceptor cells more precisely, we performed immunoelectron microscopy, accessing our recently introduced preembedding labeling technique (Maerker et al., 2008; Sedmak et al., 2009). Our electron microscopy data confirmed the subciliary localization of the IFT proteins in photoreceptor cells, as demonstrated by immunofluorescence. Furthermore, they provided deeper insights into the spatial distribution of IFT proteins in retinal cells. Exploiting the high resolution of the electron microscope, we observed IFT52, -57, -88, and -140 labeling in the OS base and in the basal part of the photoreceptor CC (Fig. 3, A and E; Fig. 4, A and D; and Fig. 5, A and D). In addition, IFT57, -88, and -140 were routinely detected alongside the microtubule doublets in the shaft of the CC (Fig. 3, D and G; and Fig. 4, A and D), whereas IFT52 was concentrated in patches associated with the ciliary membrane and microtubule doublets (Fig. 5 A). The IFT88 and -140 staining extended along the axoneme further into the photoreceptor OS (Figs. 3 E and 4 A). The intense labeling of IFT88 at the axoneme of the OS (Fig. 3 H) is consistent with recently published data on GFP-tagged IFT88 in transgenic frogs (Luby-Phelps et al., 2008). At the base of the CC, IFT52, -57, -88, and -140 were consistently associated with the BB (Fig. 3, A, E, and I; Fig. 4, A and C; and Fig. 5 D). In addition, IFT57, -88, and -140 were regularly concentrated beneath the periciliary groove (Fig. 3, A, E, and I; and Fig. 4 A), in the region where the IFT particle assembly has been suggested in *Chlamydomonas* (Deane et al., 2001). Furthermore, clusters of immunolabeling by antibodies to IFT57, -88, and -140 were routinely observed at vesicle-like structures in the periphery of the basal bodies and of the adjacent centriole in the cytoplasm of the photoreceptor IS (Fig. 3, A, C, and I; and Fig. 4 C). To emphasize vesicles and vesicle-like structures hardly recognizable in the low contrast images of the present immunoelectron microscopy analysis, we provide images at higher magnification of selected regions with and without colorized vesicles (Fig. 3, C, C′, I, and I′; and Fig. 4, C and C′). These results are consistent with the idea that IFT proteins are associated with IFT protein complexes and vesicles in the region surrounding the BB–centriole complex of the photoreceptor cell (Luby-Phelps et al., 2008).

Immunoelectron microscopy further revealed that the immunofluorescence labeling of IFT20 in the basal part of the CC represents the BB of the photoreceptor CC (Fig. 6 A). Similar to the other IFT proteins investigated, the immunoelectron microscopy staining of IFT20 and -52 also appeared in clusters in the cytoplasm at the periphery of the BB and the adjacent centriole of the CC (Fig. 6 A). In contrast to the group of IFT57, -88, and -140, IFT20 and -52 were absent from the ciliary groove (Figs. 5 and 6 A). However, substantial immunoelectron microscopic labeling of IFT20 and -52 was found in the cytoplasm of the periciliary collar-like extension of the photoreceptor IS (Fig. 5, A and C; and Fig. 6, A and C). In this periciliary specialization,
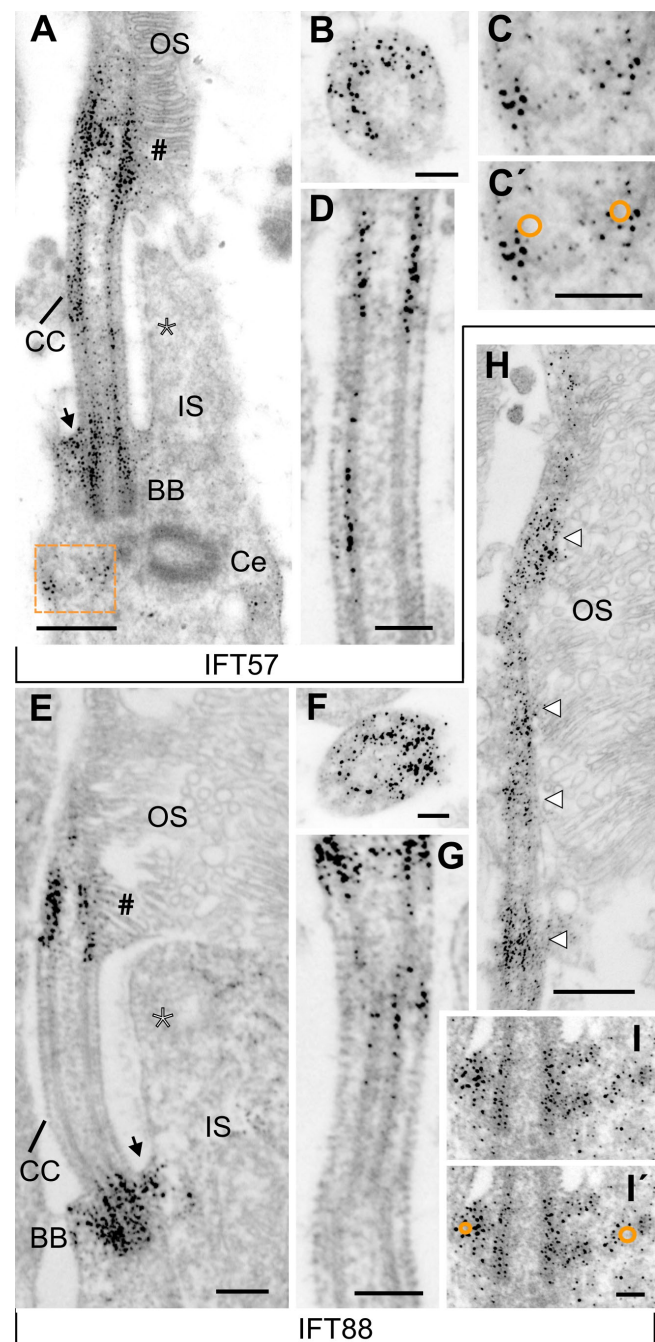
Figure 3. **Immunoelectron microscopic localization of IFT57 and -88 in mouse photoreceptor cells.** (A–I) Electron micrographs of anti-IFT57 (A–D) and -IFT88 (E–I) immunolabeling in sections through parts of mouse photoreceptor cells. (A and E) Longitudinal section through the photoreceptor ciliary apparatus. Cross section (B and F) and longitudinal section (D and G) through the shaft of the CC. (H) Longitudinal section through the axoneme (arrowheads) extending into the OS. IFT57 is concentrated at the OS base (number signs) and in the BB region of the CC but also along microtubules in the CC shaft. In the IS, IFT57 is located below the ciliary groove (arrow) but neither at the centriole (Ce) nor in the periciliary extension of the apical IS (asterisk; A–D). IFT88 is concentrated at the OS base (number signs) and in the BB of the CC, whereas the CC shaft is sparsely stained. In the IS, IFT88 is located below the ciliary groove (arrow) but not in the periciliary apical IS extension (asterisk). (C) Higher magnification image of A (orange rectangle); IFT57 association with vesicle-like structures is highlighted by orange circles in C′. (I) Higher magnification of IFT88 association with vesicle-like structures in the periphery of the BB in the IS, highlighted by orange circles in I′. Bars: (A and H) 0.4 µm; (B, F, I, and I′) 0.1 µm; (C–D, and G) 0.2 µm; (E) 0.25 µm.

Figure 4. **Immunoelectron microscopic localization of IFT140 in parts of mouse photoreceptor cells.** (A and D) Electron micrographs of anti-IFT140 immunolabeling in longitudinal sections through photoreceptor ciliary apparatus. (B) Cross section through the apical CC. Anti-IFT140 labeling is detected mainly in the OS base (number signs) and at the BB. IFT140 is additionally present in the axoneme (arrowheads) projecting into the OS and in the IS below the ciliary groove (arrow) but not at the periciliary apical IS extension (asterisk). (C) In the periphery of the BB, IFT140 is associated with vesicle-like structures, highlighted by orange circles in C'. Bars: (A and C–D) 0.2 µm; (B) 0.1 µm.

Figure 5. **Immunoelectron microscopic localization of IFT52 in mouse photoreceptor cells.** (A–E) Electron micrographs of anti-IFT52 immunolabeling in sections through parts of mouse photoreceptor cells. (A) Longitudinal sections through the ciliary region (images from three different photoreceptor cells). (B) Cross section through the shaft of the CC. IFT52 immunolabeling is present at the OS base (number sign), in a particle-like structure in the shaft of the CC, and in the periciliary apical IS extension (asterisks). (C) Longitudinal section through periciliary apical IS extension (asterisks). IFT52 is labeled at vesicle-like structures, highlighted by orange circles in C'. (D) IFT52 labeling in a longitudinal section through the BB region. IFT52 is decorated at a vesicle-like structure in the periphery of the BB, highlighted by orange circles in D'. (E) Higher magnification IFT52 labeling clustered at a vesicle-like structure in the IS, highlighted by the orange circle in E'. Bars: (A) 0.4 µm; (B) 0.25 µm; (C–E') 0.1 µm.
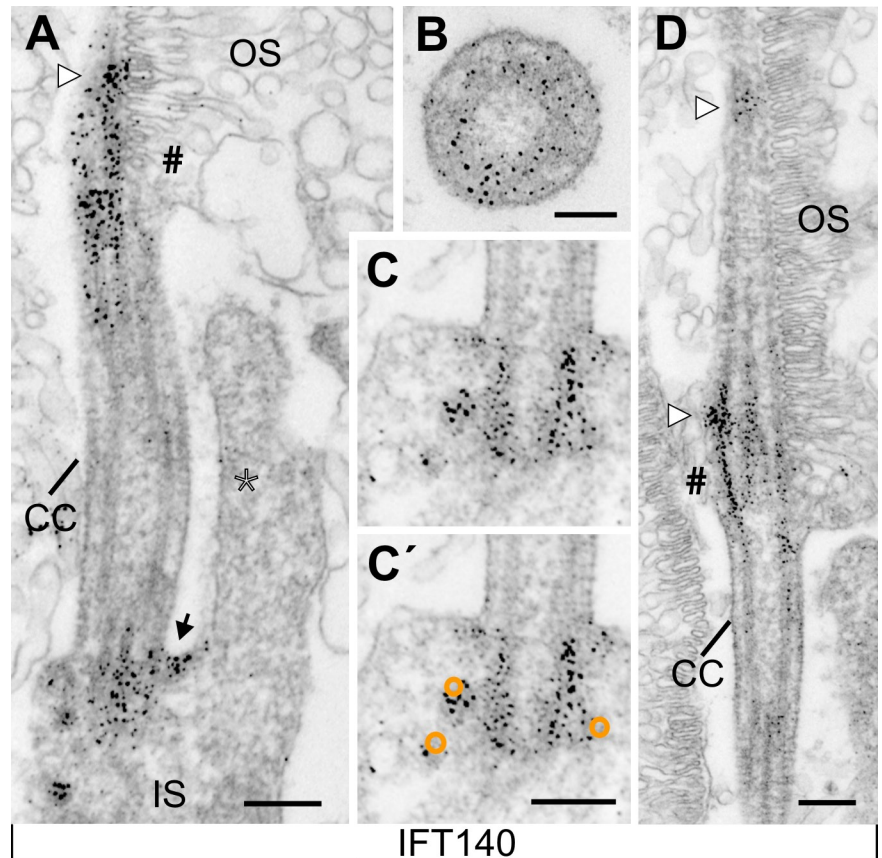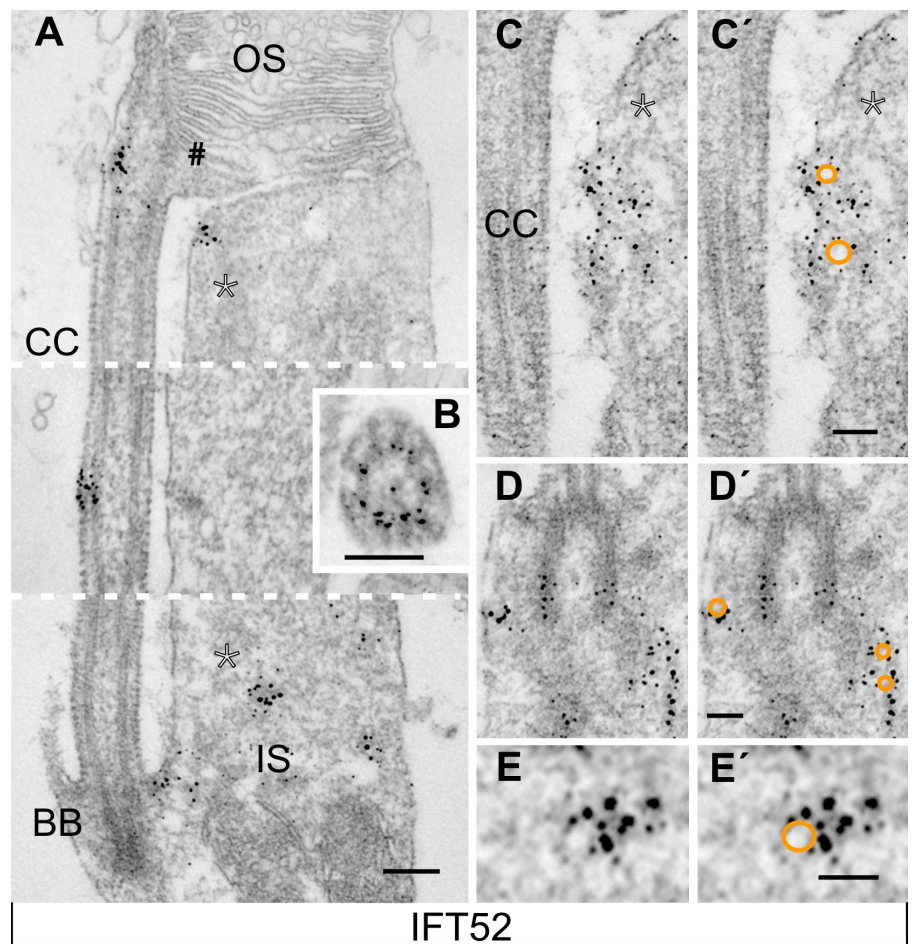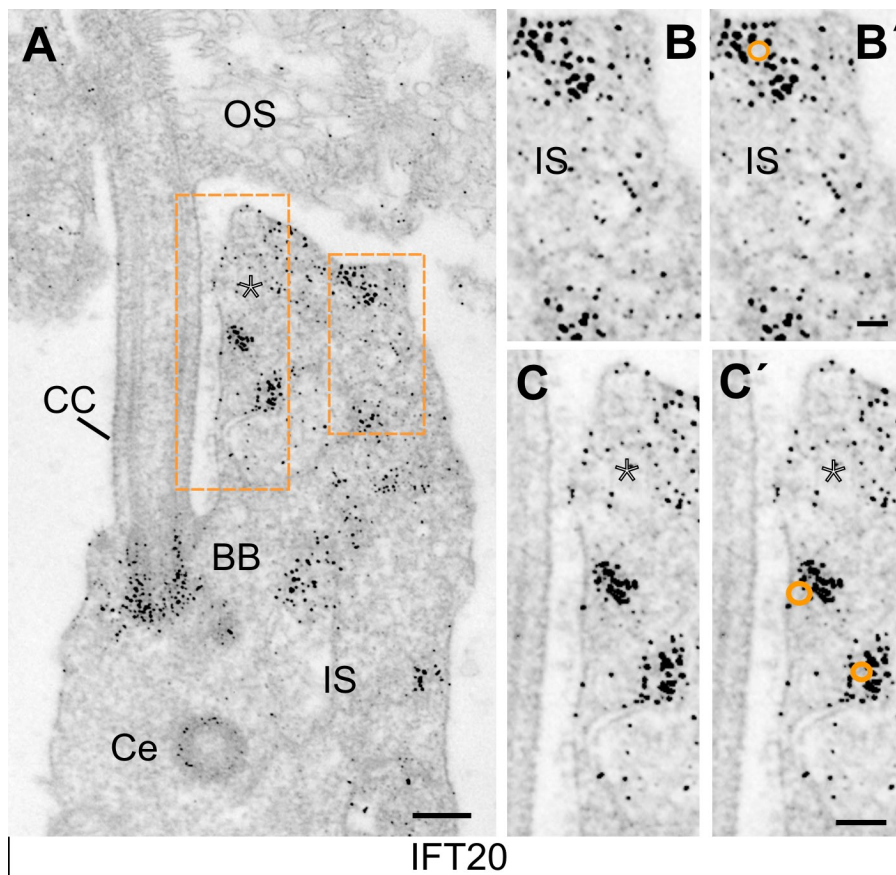
Figure 6. **Immunoelectron microscopic localization of IFT20 in mouse photoreceptor cells.** (A–C) Electron micrographs of anti-IFT20 immunolabeling in longitudinal sections through parts of mouse photoreceptor cells. (A) Anti-IFT20 immunolabeling in the photoreceptor ciliary apparatus. IFT20 is decorated at the BB but not in other parts of the CC or at the OS base. In the IS, IFT20 is located at the apical region of the centriole (Ce) and in the cytoplasm of the periciliary apical IS extension (asterisk). (B and C) Higher magnification of parts of the periciliary IS extension of A (orange rectangles) showing the association of IFT20 with vesicle-like structures, highlighted by orange circles in B′ and C′. Bars: (A) 0.2 µm; (B and B′) 0.05 µm; (C and C′) 0.1 µm.

IFT20 and -52 were concentrated in clusters at vesicle-like structures in the cytoplasm and affiliated with the membrane of the IS facing the membrane of the CC (Fig. 5, A and C; and Fig. 6, B and C). The latter periciliary membrane domain of the apical IS has been recently identified as a target for docking and fusion of cargo vesicles transported through the IS on their destination to the OS (Liu et al., 2007; Maerker et al., 2008), suggesting the involvement of IFT20 and -52 in these processes.

Association of IFT proteins with the Golgi apparatus (GA) and post-Golgi transport vesicles

Inspired by our aforementioned results, we next explored the subcellular distribution of IFT proteins in the Golgi regions of retinal neurons. We performed double labeling with antibodies against IFT20 and the Golgi resident GM130 (Nakamura et al., 1995), which was previously introduced as a reliable Golgi marker in photoreceptor cells (Mazelova et al., 2009). These analyses revealed a partial colocalization of IFT20 with GM130 in the IS of photoreceptor cells (Fig. 7, A and A′) and the cell bodies of the secondary retinal neurons (bipolar and horizontal cells) in the INL (Fig. 7, E–G′). In addition, we found a colocalization of IFT20 with GM130 in ganglion cells and in the non-neuronal cells of the RPE (Fig. S2 A). Immunoelectron microscopy analysis of photoreceptor cells confirmed that IFT20 is associated with the membrane stacks of the GA and vesicle-like structures, which most probably represent post-Golgi transport vesicles (Fig. 7, B–D′; Sung and Tai, 2000; Maerker et al., 2008).

Additionally, immunoelectron microscopy analysis confirmed IFT20 labeling of the GA in secondary retinal neurons (Fig. 7, F–G′). In contrast to IFT20, IFT52, -57, -88, and -140 were not detected in the Golgi of retinal cells.

Localization of IFT proteins in dendritic processes of nonciliated retinal neurons

The present immunofluorescence results as well as a previous study in mammalian retinas have indicated expression of IFT proteins in the OPL of the retina (Pazour et al., 2002), which contains the synapses between the photoreceptor cells and dendritic processes of secondary retinal neurons. Our present immunofluorescence data confirm the presence of IFT20, -52, and -57 but not of IFT88 and -140 in the OPL (Fig. 1 and Fig. S2 B). The precise localization of IFT proteins in the synaptic region was assessed by another series of double labeling experiments in which antibodies to the IFT proteins were colabeled with synaptic markers. Costaining of IFT proteins with antibodies against RIBEYE, a specific marker of the photoreceptor ribbon synapse (tom Dieck et al., 2005), did not show any overlap in the resulting immunofluorescence (Fig. 8, A–C). IFT20, -52, and -57 were localized below the ribbon synapse labeling of RIBEYE, indicating the presence of these IFT proteins in the postsynaptic terminals and dendritic processes of bipolar and horizontal cells. Preembedding immunoelectron microscopy analysis further confirmed postsynaptic localization of IFT proteins (Fig. 8, E–G). IFT20, -52, and -57 were concentrated in the dendritic terminals of bipolar and horizontal
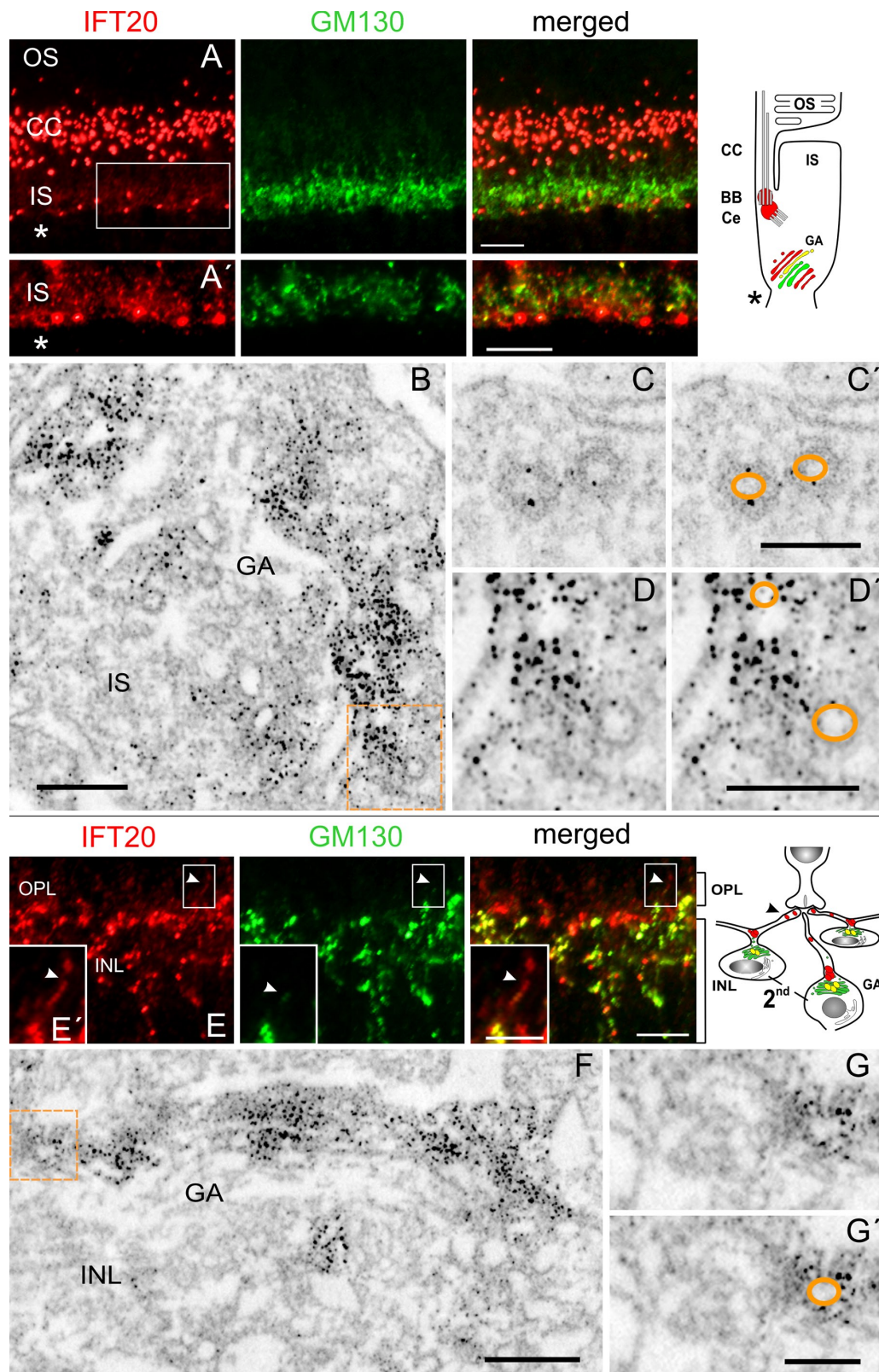
Figure 7. **Subcellular localization of IFT20 at the GA in neurons of the mouse retina.** (A–D) Localization of IFT20 in the GA of photoreceptor cells. (A) Indirect immunofluorescence of a double labeling with anti-IFT20 and anti-GM130, a marker for the GA. (A′) Higher magnification image of the indicated part (white rectangle) in A. Merged images reveal partial colocalization of IFT20 and GM130 in the GA of the IS summarized in the cartoon on the right. Asterisks indicate the apical part of the ONL. (B) Electron micrographs of anti-IFT20 immunolabeling in a cross section through the GA in the IS of a mouse photoreceptor cell. IFT20 is associated with the membrane stacks of the GA. (C and D) Anti-IFT20 labels vesicle-like structures, probably representing post-Golgi vesicles, highlighted by orange circles in C′ and D′. D and D′ are higher magnifications of B (orange rectangle). (E–G) Localization of IFT20 in the GA of secondary retinal neurons (2nd). (E) Indirect immunofluorescence of double labeling with anti-IFT20 and anti-GM130 in the OPL and

cells (Fig. 8, E–G). In addition to these IFT proteins, KIF17 was located in these postsynapses (Fig. 8 H). In no case were the presynaptic terminals of rod and cone photoreceptors stained by antibodies against IFT proteins. Furthermore, IFT20, -52, and -57 were also detected in the cytoplasm of dendritic processes of the retinal secondary neurons (Fig. 9, B–D) where the IFT proteins were clustered at vesicle-like structures (Fig. 9, B′–D′).

Discussion

In this study, we investigated the subcellular spatial distribution of five IFT particle proteins of complex A and B in cells of the mammalian retina. The applied preembedding labeling method for immunoelectron microscopy enabled spatial mapping of IFT proteins to subcellular compartments of cells and subciliary compartments of a primary cilium for the first time. In addition, it allowed the identification of ciliary cargo vesicles associated with the IFT proteins (Sedmak et al., 2009). Our results confirm the central function of IFT molecules in ciliary transport and further strengthen their role in transport processes in the cytoplasm of ciliated cells but also of nonciliated cells.

IFT proteins participate in all modules of the molecular transport destined to photoreceptor cilia

We provide evidence that IFT particle proteins participate in all principle modules of the transport destined to the photoreceptor cilia necessary for ciliogenesis (photoreceptor OS formation) and the maintenance of the light-receptive OS (Fig. 10 A). Localization of IFT20 in the GA and its association with transport vesicles in the cytoplasm of all retinal cell types and of the adjacent RPE support the model of the general nonciliary function of IFT20 as a molecular mediator between the sorting machinery of the GA, the vesicular transport of cilia components, and their delivery to the ciliary base (Follit et al., 2006, 2008). In the GA, IFT20 is thought to be anchored to Golgi membranes by the golgin protein GMAP210, and after vesicle budding, IFT20 marks the ciliary-destined vesicles that translocate from the Golgi to the base of the cilium, where IFT20 binds to other complex B subunits (Follit et al., 2006, 2008; Omori et al., 2008).

In photoreceptor cells, we monitored IFT20-associated vesicles on their track through the IS to the base of the CC. In the defined periciliary compartment, all five IFT proteins studied were abundantly concentrated and associated with cargo vesicles. These findings affirm previous results (Pazour et al., 2002; Luby-Phelps et al., 2008) and thereby support the hypothesis of the assembly and arrangement of IFT complexes at the base of cilia and flagella (Rosenbaum and Witman, 2002; Pedersen and Rosenbaum, 2008). As in other ciliary systems, all IFT molecules were found to be associated with Golgi-derived transport vesicles in photoreceptor cells. Previous experiments showed

that the visual pigment rhodopsin is transported along microtubules by cytoplasmic dynein to the periciliary apical membrane of the IS (Fig. 10 A; Tai et al., 1999). At the ciliary base of photoreceptors, the cargo is transferred from the module of the cytoplasmic IS transport to the module of ciliary delivery, in particular to the ciliary IFT system (Papermaster, 2002; Roepman and Wolfrum, 2007). This transfer of membrane cargo to the specialized periciliary membrane domain is in principle an exocytotic process. The certain involvement of IFT molecules in this process supports the hypothesis that the evolution of eukaryotic cilia and in particular the IFT system is originated from the exocytotic system in ancestral nonciliated cells (Avidor-Reiss et al., 2004; Jékely and Arendt, 2006). Nevertheless, present immunoelectron microscopy data revealed slightly different localizations of IFT proteins in this periciliary region (Fig. 10 A): IFT57, -88, and -140 were found beneath the groove formed by the transition of the ciliary membrane and the plasma membrane. In contrast, IFT20 and -52 were located in the apical extension of the IS. The latter region we recently identified as a periciliary target membrane for ciliary-destined transport vesicles in mammalian photoreceptor cells (Maerker et al., 2008). The differential distribution of IFT protein subsets may depend on the sequential assembly of IFT particles for the delivery into the cilium. However, because there is no overlap between the membrane localization of the two IFT protein subsets, they may be associated with different ciliary cargoes, which are independently delivered to different target zones in the periciliary compartment. In photoreceptor cells, different transport routes through the IS were recently suggested for different OS cargoes (Karan et al., 2008; Bhowmick et al., 2009), making different target zones in the IS plausible.

In addition to their abundant concentration at the ciliary base, IFT proteins were found in the distinct parts of the primary cilium of photoreceptors: in the BB, the CC, the basal OS, and the axoneme (Fig. 1). In the region of the BB, all IFT proteins were present and associated with cargo vesicles. In the CC, IFT52, -57, -88, and -140 were detected alongside the microtubule doublets, but IFT20 was absent. This confirms previous studies and supports the hypothesis that the first set of IFT proteins participates in the molecular cargo trafficking or is transported as cargo (in the case of complex A component IFT140, which is thought to be involved in retrograde IFT) through the CC (Rosenbaum et al., 1999; Baker et al., 2004; Insinna and Besharse, 2008; Insinna et al., 2008, 2009; Krock and Perkins, 2008; Luby-Phelps et al., 2008; Pedersen and Rosenbaum, 2008; Pigino et al., 2009). The faint decoration of the IFT proteins in the shaft of the CC by immunofluorescence and immunoelectron microscopy may reflect the velocity of the IFT particles as they pass through the CC. The concentration of IFT57, -88, and -140 at the base of the OS indicates a certain role of these IFT proteins in the formation of novel photosensitive

---

the INL. (E′) Higher magnification of a dendritic extension (arrowheads) indicated in E (white rectangles). Merged images reveal partial colocalization of IFT20 and GM130 in dendritic extension and in the GA of second retinal neurons outlined in the cartoon on the right. (F) Electron micrograph of anti-IFT20 immunolabeling in a cross section through the GA of second neurons in the INL. IFT20 associates with the membranes stacks of the GA of horizontal and bipolar cells. (G) Higher magnification of F (orange rectangle). IFT20 clusters at vesicle-like structures (post-Golgi vesicles), highlighted by the orange circle in G′. Ce, centriole. Bars: (A, A′, and E) 5 µm; (B) 0.4 µm; (C, C′, G, and G′) 0.1 µm; (D, D′, and F) 0.2 µm; (E′) 2.5 µm.
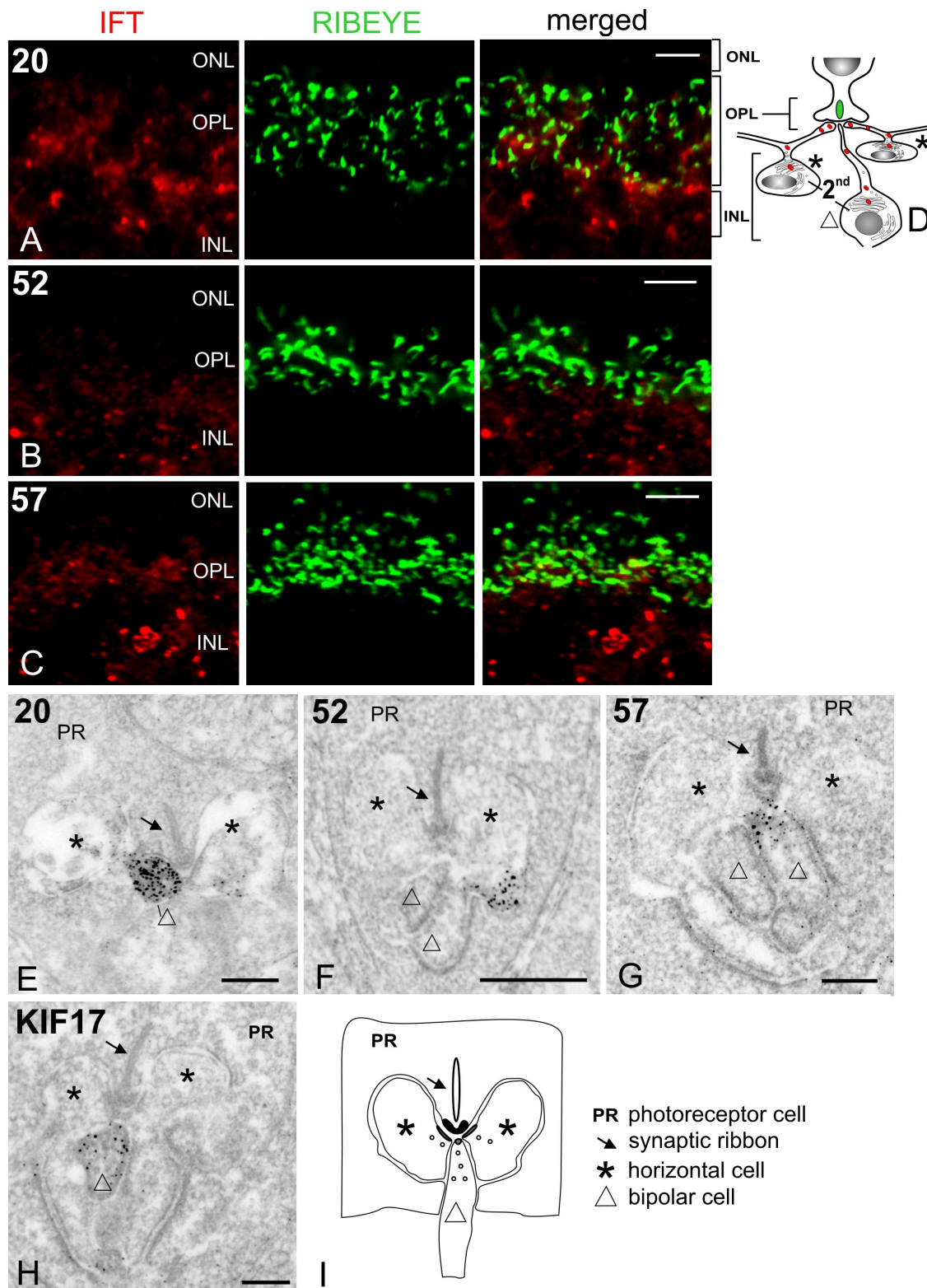
Figure 8. **Postsynaptic localization of IFT20, -52, and -57 and KIF17 in OPL synapses.** (A–C) Indirect immunofluorescence double labeling by antibodies to IFT20, -52, and -57 and RIBEYE, a marker for the presynaptic region of photoreceptor cell ribbon synapses in cryosections through mouse retinas. Merged images reveal no colocalization of RIBEYE and IFT proteins. (D) Cartoon of postsynaptic localization of IFT proteins in secondary retinal neurons (2nd), bipolar cells (triangle), and horizontal cells (asterisks). (E–G) Electron micrographs of immunolabeling of IFT20, -52, and -57 in the OPL synapses between photoreceptor cells (PR) and bipolar cells (triangles) and horizontal cells (asterisks). (H) Electron micrograph of anti-KIF17 immunolabeling in the OPL synapses. (I) Cartoon of the organization of a rod ribbon synapse contact to bipolar cells (triangle) and horizontal cells (asterisks). Arrows indicate synaptic ribbons in photoreceptor cells. IFT proteins and KIF17 are restricted to the postsynaptic terminals of dendritic processes of second retinal neurons. Bars: (A and B) 3 µm; (C) 5 µm; (E–H) 0.2 µm.
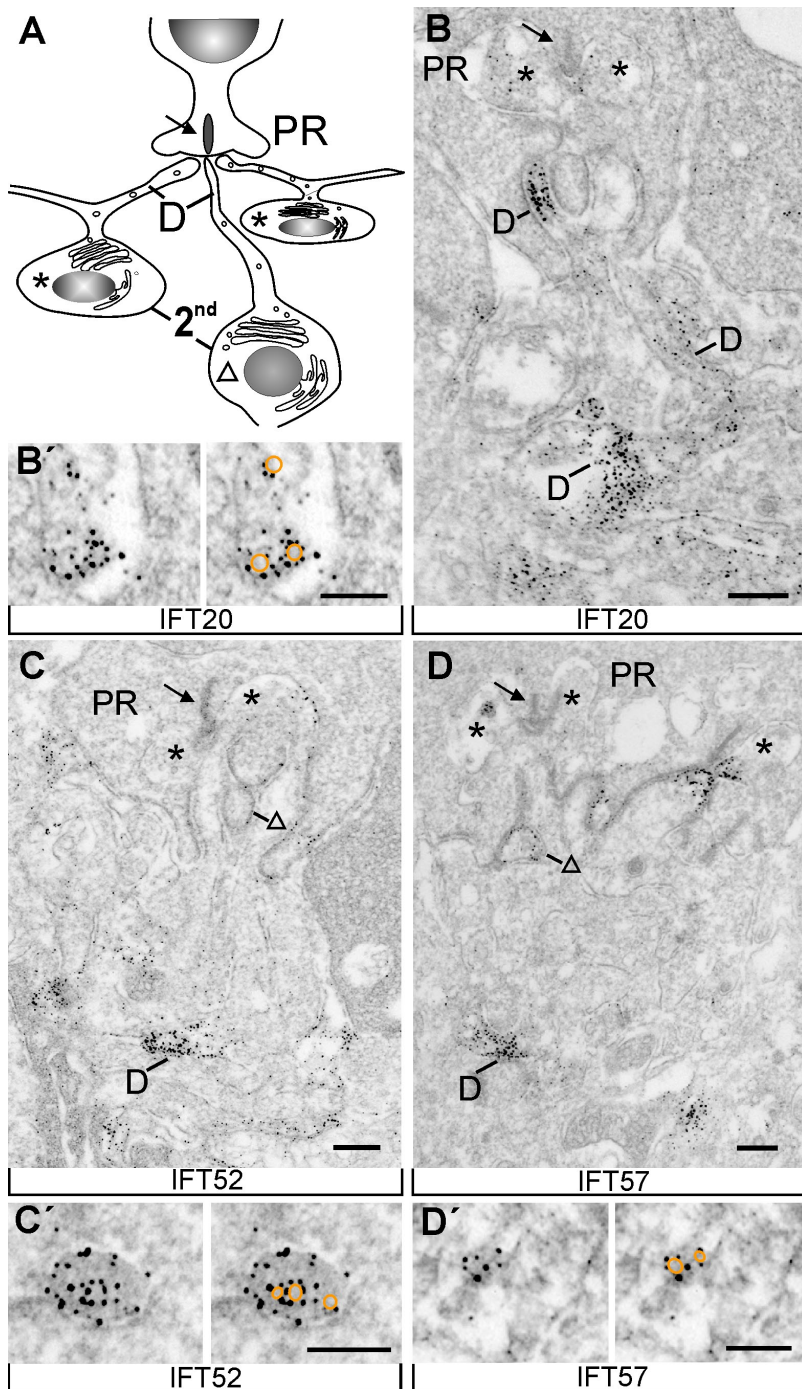
Figure 9. **Localization of IFT20, -52, and -57 in dendritic processes of secondary retinal neurons.** (A) Cartoon of the organization of an OPL synapse connection between a rod photoreceptor cell (PR) and the secondary retinal neurons (2nd), bipolar cells (triangle), and horizontal cells (asterisks). D, dendritic processes. (B–D) Electron micrographs of immunolabeling of IFT20, -52, and -57 in the OPL of mouse retinas. All three IFT proteins are decorated in dendritic processes of second neurons. (B′–D′) High magnification details of B–D indicating the association of IFT20, -52, and -57 with vesicle-like structures highlighted by orange circles. Arrows indicate the synaptic ribbon, and triangles and asterisks highlight bipolar and horizontal cells, respectively. Bars: (B–D) 0.2 µm; (B′–D′) 0.1 µm.

membranous disks. All de novo synthesized disk compounds are shipped through the CC, unloaded from their transport carriers (e.g., kinesin-II–driven IFT particles), and incorporated into the newly formed disks at the OS base. Although the molecular mechanism is currently still under debate, there is evidence that endocytosis of membrane vesicles is involved in the formation of nascent disk membranes at the base of the OS (Usukura and Obata, 1995; Chuang et al., 2007; unpublished data).

In the photoreceptor axoneme, which extends from the CC and projects deep into the OS (Liu et al., 2004; Insinna and Besharse, 2008), only IFT88 and -140 were detected. This suggests that only a subset of IFT proteins participates in IFT

processes associated with the transport of cargo that is not incorporated into the nascent disks at the OS base and translocates along the microtubules of the axoneme in the OS. The axonemal localization and function of IFT88 is in agreement with a correct differentiation of the CC but failure of a proper OS formation in photoreceptor cells of mice carrying the hypomorphic mutation in IFT88 (Tg737[orpk]; Pazour et al., 2002; Baker et al., 2004). Because most components of the photosensitive disks are incorporated into the nascent disks already at base of the OS, only a subset of OS molecules has to be distributed more apically as cargo for the transport machinery of the axoneme (Roepman and Wolfrum, 2007). Such cargoes, distributed

Figure 10. **Models of processes associated with IFT proteins in retinal neurons.** (A) IFT in photoreceptor cells. On its destination to the OS, cytoplasmic dynein 1 (DYNC1) mediates the transport of cargo vesicles along microtubules from the GA on route 1 to the base of the CC (BB region) and on route 2 to the periciliary extension (asterisk) of the IS. In the IS, IFT20 is associated with cargo vesicles on both routes. Route 1 vesicles are directed to the periciliary groove (big arrow) in the periphery of the BB where they associate with IFT57, -88, and -140 and fuse with the periciliary groove membrane. Route 2 vesicles directed to the periciliary IS extension are associated with IFT20 and -52 and fuse with the periciliary target membrane (red). Subsequently, kinesin-II family motors mediate transport of route 1 and 2 cargoes attached to IFT particles containing IFT52, -57, -88, and -140 but not IFT20 through the CC. At the OS base, the majority of IFT proteins dissociate from the cargo, which is incorporated into membranes of de novo organized OS disks. Further apical, IFT particles containing IFT88 and -140 but not IFT20, -52, and -57 are transported along axonemal microtubules. For retrograde transport, IFT particles are picked up by cytoplasmic dynein 2/1b (DYNC2H1). Ax, axoneme. (B) IFT in dendritic process of nonciliated secondary retinal neurons. In the dendritic processes (D) of second retinal neurons, cargo vesicles are transported by KIF17 to the dendritic postsynaptic terminal (post). Dendritic IFT particles contain IFT20, -52, and -57. At the dendritic terminal, IFT particles dissociate from their cargo, which is incorporated into the postsynaptic membrane. PR, photoreceptor cell; pre, presynapse.
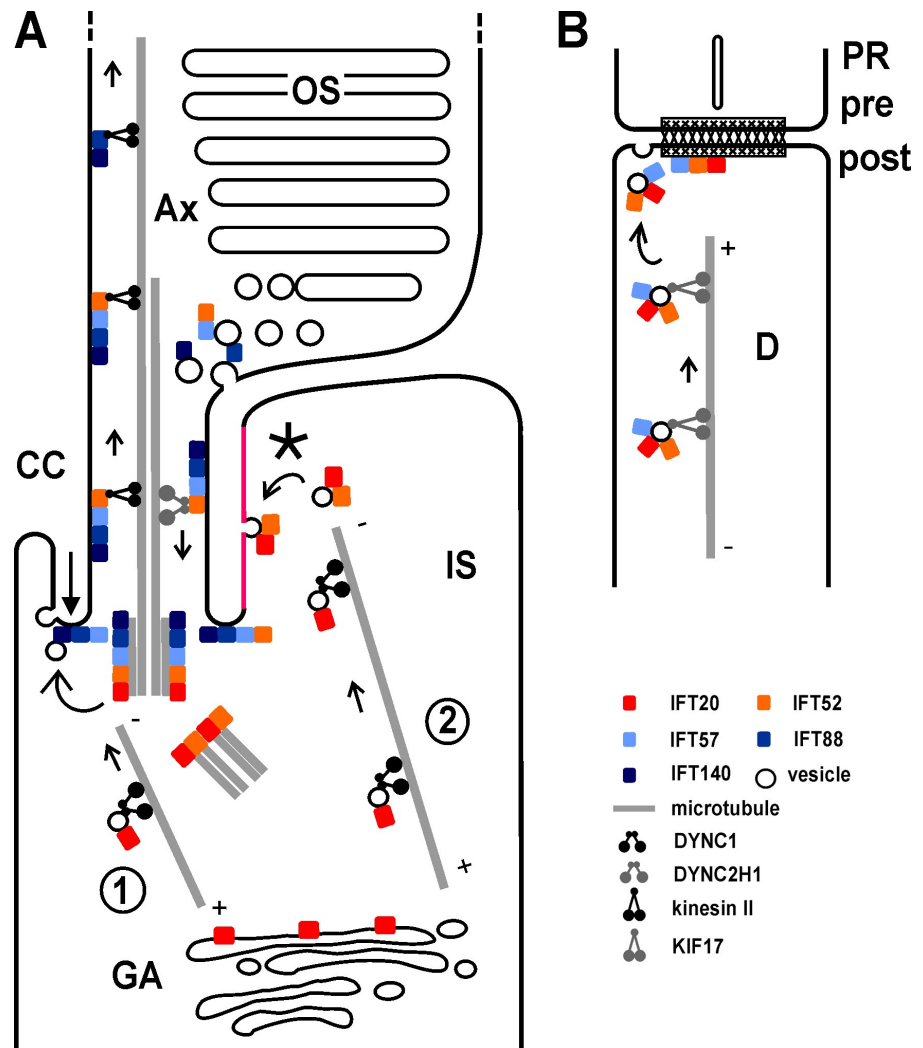
in the OS independently from the disk neogenesis, are, for example, arrestin and the visual G-protein transducin, which light-dependently cycle between the inner and the OS (Calvert et al., 2006). Recent data indicate that these bidirectional movements are dependent on the axonemal microtubule track (Peterson et al., 2005; Reidel et al., 2008; Orisme et al., 2010). The IFT complex B protein IFT88 may contribute to the translocation of both signaling molecules into the OS during photoreceptor adaptation, whereas, in the clearance of transducin and arrestin from the OS, the IFT complex A compound IFT140 may participate. Our findings confirm previous observations in other cilia and flagella, in which sets of IFT components were also found to be sequentially organized or spatially distributed in ciliary subcompartments (Evans et al., 2006; Ou et al., 2007; Lee et al., 2008).

IFT20 is not a component of the IFT core complex B in photoreceptor cilia

In contrast to all other IFT molecules investigated, we did not find IFT20 in the CC of photoreceptor cells. The present subcellular mapping by the sophisticated light and electron microscopy consistently revealed that IFT20 is restricted to the periciliary cytoplasm of the apical IS and the BB but is neither present

in the CC nor in more apical sections of the photoreceptor cilium in all species investigated. This is in contrast to previous studies suggesting a ciliary localization of IFT20 (Pazour et al., 2002; Follit et al., 2006, 2008, 2009). Follit et al. (2006) discuss that the ciliary detection is dependent on the fixation protocol because of epitope masking after fixation, which our control experiments did not confirm. Nevertheless, all published immunofluorescence data on the intrinsic IFT20 ciliary staining are not convincing, and a solid ciliary localization of IFT20 is only found after IFT20 overexpression (Follit et al., 2006, 2008). It is possible that the high sensitivity of the elaborated techniques used in this study is still not sensitive enough for the detection of IFT20 in photoreceptor cilia or that IFT20 epitopes are not accessible for the antibodies because of variations in the composition and position of the IFT molecules in the particles. Nevertheless, we believe that IFT20 is not present in photoreceptor cilia. IFT20's absence from the ciliary IFT complex B is supported by the lack of IFT20 in IFT particle fractions of gradients derived from photoreceptors (Baker et al., 2003) and unpublished data on proteomic dissection of the complex B in cultured mammalian cells. Furthermore, the analysis of complex B composition in *Chlamydomonas* demonstrated that IFT20 is linked to a complex B core by weak and

transient interactions (Lucker et al., 2005), which might play a role in the assembly and rearrangements of IFT protein complexes at the flagellum base (Iomini et al., 2001). In fact, IFT particles containing IFT20 are present in the apical IS and the BB, which is consistent with previously obtained data (Pazour et al., 2002; Follit et al., 2006, 2008) that promote a mediator role of IFT20 between the Golgi system and the cargo delivery to target membranes.

Evidence for a novel IFT system in dendrites of nonciliated retinal neurons

Besides the presence of IFT20 in the GA, IFT systems were recently found in nonciliated cells, associated with exocytosis at the immune synapse required for T cell interaction with antigen-presenting cells (Finetti et al., 2009; Baldari and Rosenbaum, 2010). In the mammalian retina, a weak immunoreactivity for IFT proteins present in the OPL was construed as a localization of IFT proteins in the photoreceptor synaptic terminals (Pazour et al., 2002). The latter finding, together with IFT-associated kinesin-II localization at these synapses (Muresan et al., 1999), raised the possibility of a function of IFT proteins in presynaptic terminals (Pazour et al., 2002). Nevertheless, in this study, we show that IFT20, -52, and -57 proteins are localized not in the presynaptic terminals of photoreceptor cells but in the postsynaptic terminals of the bipolar and horizontal cells. Double immunofluorescence staining with synaptic markers and preembedding labeling of IFT molecules conclusively revealed localization of the three IFT molecules in the postsynaptic dendritic terminals and dendritic shafts of secondary retinal neurons. This spatial distribution and the association of these IFT molecules with cytoplasmic membrane vesicles suggest participation of an IFT system at the vesicular transport to the specialized membrane of the postsynaptic dendritic terminal (Fig. 10 B). It has been demonstrated that the kinesin-II family member KIF17 navigates large protein complexes containing subunits of neurotransmitter receptors to the postsynaptic terminals (Setou et al., 2000; Guillaud et al., 2003). In secondary retinal neurons, KIF17 regulates the dendritic transport of glutamate receptor subunits to the postsynaptic membrane (Qin and Pourcho, 2001; Kayadjanian, et al., 2007). It is notable that the specific targeting of neurotransmitter receptors is critically important for plasticity of the postsynaptic terminal and might be a regulatory point for synaptic plasticity and neuronal morphogenesis. KIF17 has been found as an alternative kinesin motor to kinesin-II in IFT (Signor et al., 1999b). In the vertebrate retina, KIF17 was identified as part of a protein complex containing IFT20 and -57, which is essential for photoreceptor OS development (Insinna et al., 2008, 2009). Our present data indicate that the dendritic processes of secondary retinal neurons contain a nonciliary IFT protein complex that includes IFT20, -52, and -57 and KIF17 but neither IFT88 nor the heterotrimeric kinesin-II (Fig. 10 B). Thus, the nonciliary dendritic IFT complex differs in its composition from the one recently described for the immune synapse (Finetti et al., 2009). We reason that IFT protein complexes are modularly composed and that their defined arrangement may be cell specific and/or dependent on a particular role of

the IFT protein complex in intracellular membrane trafficking to selective target membranes.

In conclusion, a major implication of the present data is that IFT protein complexes contain different IFT proteins in different compartments of photoreceptor primary cilia. In addition, we demonstrate that IFT20 is more a mediator between the cargo sorting in the Golgi, the cytoplasmic cargo trafficking, and the delivery into the cilium than an intrinsic ciliary component. Furthermore, we identified a nonciliary IFT system by mapping IFT proteins to dendrites of retinal neurons. Our data support new perspectives on IFT function beyond its well-established roles in cilia assembly, maintenance, and sensory function of cilia and flagella.

Materials and methods

Animals, tissue dissection, and human tissue
All experiments conformed to the statement by the Association for Research in Vision and Ophthalmology regarding the care and use of animals in research. Mature C57BL/6J mice were maintained on a 12-h light–dark cycle, with food and water ad libitum. After the sacrifice of animals, eyeballs were dissected for further analyses. Bovine eyes were obtained from the local slaughter house. Human eyes (female, age 78, 13 h postmortem) were donated (Department of Ophthalmology, University Medical Center of the Johannes Gutenberg University Mainz). Informed consent was obtained for subjects; procedures adhered to the Declaration of Helsinki and were approved by the local review board. Retina was isolated from eyeball and further processed for immunofluorescence analysis as described in Immunofluorescence microscopy.

Antibodies and fluorescent dyes
Antisera against IFT20, -52, -57, -88, and -140 proteins were raised in rabbit, and affinity-purified antibodies used in this study were previously characterized (Pazour et al., 2002; Baker et al., 2003; Follit et al., 2006) and provided by G.J. Pazour (University of Massachusetts Medical School, Worcester, MA). Monoclonal antibodies to centrin-3 were used as a molecular marker for the ciliary apparatus of photoreceptors (Trojan et al., 2008). Monoclonal mouse antibodies to RIBEYE (CtBP2) and to the Golgi-resident GM130 were purchased from BD and were previously used as a cis and medial Golgi marker in photoreceptor cells by Mazelova et al. (2009). Polyclonal rabbit anti-KIF17 was obtained from Abcam and previously used in Insinna et al. (2009). Anti-RP1 antibody raised in chicken was a gift from E.A. Pierce (University of Pennsylvania School of Medicine, Philadelphia, PA; Liu et al., 2002). Secondary antibodies Alexa Fluor 488 or 568 (Invitrogen), IRDye 680 or 800 (Rockland), donkey anti–rabbit horse conjugated with reddish peroxidase (GE Healthcare), and biotinylated secondary antibodies (Vector Laboratories) were used. Nuclear DNA was stained by 1 µg/µl DAPI (Sigma-Aldrich).

Western blot analyses
For Western blot analyses, isolated mouse retinas and testes were homogenized in buffer containing a protease inhibitor cocktail (Roche). Specimens were extracted in modified radioimmunoprecipitation assay buffer (50 mM Tris-HCl, 150 mM NaCl, 0.1% SDS, 2 mM EDTA, 1% NP-40, 0.5% Na deoxycholate, 1 mM Na vanadate, and 30 mM Na-pyrophosphate, pH 7.4). For denaturing gel electrophoresis, samples were mixed with SDS-PAGE sample buffer (62.5 mM Tris-HCl, 10% glycerol, 2% SDS, 5% mercaptoethanol, 1 mM EDTA, and 0.025 mM bromophenol blue, pH 6.8). Protein extracts from retinas and testes were separated on 12% or 15% polyacrylamide gels, respectively, and transferred onto polyvinylidene difluoride membranes (Millipore). The membrane was blocked with blocking reagent (AppliChem) or nonfat dry milk (AppliChem) for 2 h at room temperature. Immunoreactivity was detected by the appropriate primary and corresponding secondary antibodies using an infrared imaging system (Odyssey; LI-COR Biosciences) for AppliChem-blocked membrane or the chemiluminescence detection system (ECL Plus Western blotting detection system; GE Healthcare) for nonfat dry milk–blocked membrane. In the latter case, ECL-exposed and developed x-ray films were scanned using a Duoscan T2500 (Agfa-Gevaert), and images were processed in Photoshop CS (Adobe Systems).

Immunofluorescence microscopy

Eyes of adult mice were placed in tissue-freezing medium (Leica) enclosed by boiled-liver block and cryofixed in melting isopentane (Wolfrum, 1991). Mouse eyes were sectioned in 10-µm cryosections at −20°C in a cryostat (HM 560 Cryo-Star; MICROM). Cryosections were placed on poly-L-lysine–precoated coverslips. Some cryosections were additionally fixed for 1 min in cold methanol containing 0.05% EGTA and washed with PBS. After incubation with 0.01% Tween 20 in PBS, PBS-washed sections were incubated with blocking solution (0.5% cold-water fish gelatin and 0.1% ovalbumin in PBS), followed by overnight incubation with primary antibodies, and diluted in blocking solution at 4°C. Washed cryosections were incubated with Alexa Fluor–conjugated secondary antibodies in PBS with DAPI. After PBS washes, sections were mounted in Mowiol 4.88 (Hoechst) and analyzed in a microscope (LEITZ DMRB; Leica) through a 63× NA 1.32 HCX Plan-Apochromat and a 100× NA 1.3 Plan-Fluotar oil objective lens. Images were obtained with a charge-coupled device camera (ORCA ER; Hamamatsu Photonics). Image acquisition was always performed at the same gain and exposure settings. Image contrast was adjusted offline with Photoshop CS using different tools, including color correction and pixel resampling.

Immunoelectron microscopy

For immunoelectron microscopy, a recently introduced protocol was applied (Maerker et al., 2008; Sedmak et al., 2009). During fixation of isolated mouse eyes in 4% PFA in Sorensen buffer (0.1 M Na$_2$HPO$_4$·2H$_2$O and 0.1 M KH$_2$PO$_4$, pH 7.4), eyes were perforated, and lenses were removed. Washed retinas were dissected from eye cups and infiltrated with 10 and 20% sucrose in Sorensen buffer, followed by incubation in buffered 30% sucrose overnight. After four cycles of freezing in liquid nitrogen and thawing at 37°C, retinas were washed in PBS and embedded in buffered 2% Agar (Sigma-Aldrich). Agar blocks were sectioned with a Vibratome (VT 1000 S; Leica) in 50-µm slices. Vibratome sections were blocked in 10% normal goat serum and 1% bovine serum albumin in PBS and subsequently incubated with primary antibodies against IFT proteins for 4 d at 4°C. After washing with PBS, the appropriate biotinylated secondary antibodies were applied to the sections. After PBS washes, antibody reactions were visualized by a Vectastain ABC kit (Vector Laboratories) according to the manufacturer's instructions. The Vectastain ABC kit provides the avidin-biotin HRP complex (ABC), which binds the biotin-conjugated secondary antibodies. The immunocomplex was visualized by adding 0.01% hydrogen peroxide to 0.05 M DAB solution. In this reaction, DAB was oxidized, converting DAB into insoluble polymers. Subsequently, stained retinas were fixed in 2.5% glutaraldehyde in 0.1 M cacodylate buffer, pH 7.4, and DAB precipitates were silver enhanced, applying a modified protocol by Leranth and Pickel (1989) followed by postfixation in 0.5% OsO$_4$ in 0.1 M cacodylate buffer on ice. Dehydrated specimens were flat-mounted between two sheaths of ACLAR-films (Ted Pella, Inc.) in Araldite resin. Ultrathin sections were analyzed in a transmission electron microscope (Tecnai 12 BioTwin; FEI) using different magnifications ranging from 11,500 to 26,500. Images were obtained with a charge-coupled device camera (SIS Megaview3; Surface Imaging Systems) acquired by analSIS (Soft Imaging System) and processed with Photoshop CS.

Online supplemental material

Fig. S1 presents Western blot analyses of murine retinas and testes demonstrating the retinal expression and monospecificity of the antibodies to the different IFT proteins used. Fig. S2 shows analyses of the distribution of IFT proteins in subcellular compartments of ocular cells. Fig. S3 shows analyses of the spatial distribution of IFT proteins in retinal cells of nonrodent mammals. Fig. S4 demonstrates no differences in anti-IFT20 indirect immunofluorescence staining in fixed and unfixed mouse retinas. Online supplemental material is available at http://www.jcb.org/cgi/content/full/jcb.200911095/DC1.

References

Avidor-Reiss, T., A.M. Maer, E. Koundakjian, A. Polyanovsky, T. Keil, S. Subramaniam, and C.S. Zuker. 2004. Decoding cilia function: defining specialized genes required for compartmentalized cilia biogenesis. *Cell.* 117:527–539. doi:10.1016/S0092-8674(04)00412-X

Baker, S.A., K. Freeman, K. Luby-Phelps, G.J. Pazour, and J.C. Besharse. 2003. IFT20 links kinesin II with a mammalian intraflagellar transport complex that is conserved in motile flagella and sensory cilia. *J. Biol. Chem.* 278:34211–34218. doi:10.1074/jbc.M300156200

Baker, S.A., G.J. Pazour, G.B. Witman, and J.C. Besharse. 2004. Photoreceptors and intraflagellar transport. In *Photoreceptor cell biology and inherited retinal degenerations*. Recent Advances in Human Biology, vol. 10. D.S. Williams, editor. World Scientific, Singapore. 109–132.

Baldari, C.T., and J. Rosenbaum. 2010. Intraflagellar transport: it's not just for cilia anymore. *Curr. Opin. Cell Biol.* 22:75–80. doi:10.1016/j.ceb.2009.10.010

Beech, P.L., K. Pagh-Roehl, Y. Noda, N. Hirokawa, B. Burnside, and J.L. Rosenbaum. 1996. Localization of kinesin superfamily proteins to the connecting cilium of fish photoreceptors. *J. Cell Sci.* 109:889–897.

Besharse, J.C., and C.J. Horst. 1990. The photoreceptor connecting cilium - a model for the transition zone. *In* Ciliary and Flagellar Membranes. R.A. Bloodgood, editor. Plenum, New York. 389–417.

Bhowmick, R., M. Li, J. Sun, S.A. Baker, C. Insinna, and J.C. Besharse. 2009. Photoreceptor IFT complexes containing chaperones, guanylyl cyclase 1 and rhodopsin. *Traffic.* 10:648–663. doi:10.1111/j.1600-0854.2009.00896.x

Calvert, P.D., K.J. Strissel, W.E. Schiesser, E.N. Pugh Jr., and V.Y. Arshavsky. 2006. Light-driven translocation of signaling proteins in vertebrate photoreceptors. *Trends Cell Biol.* 16:560–568. doi:10.1016/j.tcb.2006.09.001

Chuang, J.Z., Y. Zhao, and C.H. Sung. 2007. SARA-regulated vesicular targeting underlies formation of the light-sensing organelle in mammalian rods. *Cell.* 130:535–547. doi:10.1016/j.cell.2007.06.030

Cole, D.G. 2003. The intraflagellar transport machinery of *Chlamydomonas reinhardtii*. *Traffic.* 4:435–442. doi:10.1034/j.1600-0854.2003.t01-1-00103.x

Cole, D.G., D.R. Diener, A.L. Himelblau, P.L. Beech, J.C. Fuster, and J.L. Rosenbaum. 1998. *Chlamydomonas* kinesin-II–dependent intraflagellar transport (IFT): IFT particles contain proteins required for ciliary assembly in *Caenorhabditis elegans* sensory neurons. *J. Cell Biol.* 141:993–1008. doi:10.1083/jcb.141.4.993

Deane, J.A., D.G. Cole, E.S. Seeley, D.R. Diener, and J.L. Rosenbaum. 2001. Localization of intraflagellar transport protein IFT52 identifies basal body transitional fibers as the docking site for IFT particles. *Curr. Biol.* 11:1586–1590. doi:10.1016/S0960-9822(01)00484-5

Evans, J.E., J.J. Snow, A.L. Gunnarson, G. Ou, H. Stahlberg, K.L. McDonald, and J.M. Scholey. 2006. Functional modulation of IFT kinesins extends the sensory repertoire of ciliated neurons in *Caenorhabditis elegans*. *J. Cell Biol.* 172:663–669. doi:10.1083/jcb.200509115

Finetti, F., S.R. Paccani, M.G. Riparbelli, E. Giacomello, G. Perinetti, G.J. Pazour, J.L. Rosenbaum, and C.T. Baldari. 2009. Intraflagellar transport is required for polarized recycling of the TCR/CD3 complex to the immune synapse. *Nat. Cell Biol.* 11:1332–1339. doi:10.1038/ncb1977

Follit, J.A., R.A. Tuft, K.E. Fogarty, and G.J. Pazour. 2006. The intraflagellar transport protein IFT20 is associated with the Golgi complex and is required for cilia assembly. *Mol. Biol. Cell.* 17:3781–3792. doi:10.1091/mbc.E06-02-0133

Follit, J.A., J.T. San Agustin, F. Xu, J.A. Jonassen, R. Samtani, C.W. Lo, and G.J. Pazour. 2008. The Golgin GMAP210/TRIP11 anchors IFT20 to the Golgi complex. *PLoS Genet.* 4:e1000315. doi:10.1371/journal.pgen.1000315

Follit, J.A., F. Xu, B.T. Keady, and G.J. Pazour. 2009. Characterization of mouse IFT complex B. *Cell Motil. Cytoskeleton.* 66:457–468. doi:10.1002/cm.20346

Guillaud, L., M. Setou, and N. Hirokawa. 2003. KIF17 dynamics and regulation of NR2B trafficking in hippocampal neurons. *J. Neurosci.* 23:131–140.

Hou, Y., H. Qin, J.A. Follit, G.J. Pazour, J.L. Rosenbaum, and G.B. Witman. 2007. Functional analysis of an individual IFT protein: IFT46 is required for transport of outer dynein arms into flagella. *J. Cell Biol.* 176:653–665. doi:10.1083/jcb.200608041

Insinna, C., and J.C. Besharse. 2008. Intraflagellar transport and the sensory outer segment of vertebrate photoreceptors. *Dev. Dyn.* 237:1982–1992. doi:10.1002/dvdy.21554

Insinna, C., N. Pathak, B. Perkins, I. Drummond, and J.C. Besharse. 2008. The homodimeric kinesin, Kif17, is essential for vertebrate photoreceptor sensory outer segment development. *Dev. Biol.* 316:160–170. doi:10.1016/j.ydbio.2008.01.025

Insinna, C., M. Humby, T. Sedmak, U. Wolfrum, and J.C. Besharse. 2009. Different roles for KIF17 and kinesin II in photoreceptor development and maintenance. *Dev. Dyn.* 238:2211–2222. doi:10.1002/dvdy.21956

Iomini, C., V. Babaev-Khaimov, M. Sassaroli, and G. Piperno. 2001. Protein particles in *Chlamydomonas* flagella undergo a transport cycle consisting of four phases. *J. Cell Biol.* 153:13–24. doi:10.1083/jcb.153.1.13

Jékely, G., and D. Arendt. 2006. Evolution of intraflagellar transport from coated vesicles and autogenous origin of the eukaryotic cilium. *Bioessays.* 28:191–198. doi:10.1002/bies.20369

Karan, S., J.M. Frederick, and W. Baehr. 2008. Involvement of guanylate cyclases in transport of photoreceptor peripheral membrane proteins. *Adv. Exp. Med. Biol.* 613:351–359. doi:10.1007/978-0-387-74904-4_41

Kayadjanian, N., H.S. Lee, J. Piña-Crespo, and S.F. Heinemann. 2007. Localization of glutamate receptors to distal dendrites depends on subunit composition and the kinesin motor protein KIF17. *Mol. Cell. Neurosci.* 34:219–230. doi:10.1016/j.mcn.2006.11.001

Kozminski, K.G., K.A. Johnson, P. Forscher, and J.L. Rosenbaum. 1993. A motility in the eukaryotic flagellum unrelated to flagellar beating. *Proc. Natl. Acad. Sci. USA.* 90:5519–5523. doi:10.1073/pnas.90.12.5519

Kozminski, K.G., P.L. Beech, and J.L. Rosenbaum. 1995. The *Chlamydomonas* kinesin-like protein FLA10 is involved in motility associated with the flagellar membrane. *J. Cell Biol.* 131:1517–1527. doi:10.1083/jcb.131.6.1517

Krock, B.L., and B.D. Perkins. 2008. The intraflagellar transport protein IFT57 is required for cilia maintenance and regulates IFT-particle-kinesin-II dissociation in vertebrate photoreceptors. *J. Cell Sci.* 121:1907–1915. doi:10.1242/jcs.029397

Lee, E., E. Sivan-Loukianova, D.F. Eberl, and M.J. Kernan. 2008. An IFT-A protein is required to delimit functionally distinct zones in mechanosensory cilia. *Curr. Biol.* 18:1899–1906. doi:10.1016/j.cub.2008.11.020

Leranth, C., and V.M. Pickel. 1989. Electron microscopic preembedding double immunostaining methods. *In* Neuroanatomical Tract-Tracing Methods 2. L. Heimer and L. Záborszky, editors. Plenum press, New York. 129–172.

Liu, Q., J. Zhou, S.P. Daiger, D.B. Farber, J.R. Heckenlively, J.E. Smith, L.S. Sullivan, J. Zuo, A.H. Milam, and E.A. Pierce. 2002. Identification and subcellular localization of the RP1 protein in human and mouse photoreceptors. *Invest. Ophthalmol. Vis. Sci.* 43:22–32.

Liu, Q., J. Zuo, and E.A. Pierce. 2004. The retinitis pigmentosa 1 protein is a photoreceptor microtubule-associated protein. *J. Neurosci.* 24:6427–6436. doi:10.1523/JNEUROSCI.1335-04.2004

Liu, Q., G. Tan, N. Levenkova, T. Li, E.N. Pugh Jr., J.J. Rux, D.W. Speicher, and E.A. Pierce. 2007. The proteome of the mouse photoreceptor sensory cilium complex. *Mol. Cell. Proteomics.* 6:1299–1317. doi:10.1074/mcp.M700054-MCP200

Luby-Phelps, K., J. Fogerty, S.A. Baker, G.J. Pazour, and J.C. Besharse. 2008. Spatial distribution of intraflagellar transport proteins in vertebrate photoreceptors. *Vision Res.* 48:413–423. doi:10.1016/j.visres.2007.08.022

Lucker, B.F., R.H. Behal, H. Qin, L.C. Siron, W.D. Taggart, J.L. Rosenbaum, and D.G. Cole. 2005. Characterization of the intraflagellar transport complex B core: direct interaction of the IFT81 and IFT74/72 subunits. *J. Biol. Chem.* 280:27688–27696. doi:10.1074/jbc.M505062200

Maerker, T., E. van Wijk, N. Overlack, F.F. Kersten, J. McGee, T. Goldmann, E. Sehn, R. Roepman, E.J. Walsh, H. Kremer, and U. Wolfrum. 2008. A novel Usher protein network at the periciliary reloading point between molecular transport machineries in vertebrate photoreceptor cells. *Hum. Mol. Genet.* 17:71–86. doi:10.1093/hmg/ddm285

Mazelova, J., N. Ransom, L. Astuto-Gribble, M.C. Wilson, and D. Deretic. 2009. Syntaxin 3 and SNAP-25 pairing, regulated by omega-3 docosahexaenoic acid, controls the delivery of rhodopsin for the biogenesis of cilia-derived sensory organelles, the rod outer segments. *J. Cell Sci.* 122:2003–2013. doi:10.1242/jcs.039982

Murcia, N.S., W.G. Richards, B.K. Yoder, M.L. Mucenski, J.R. Dunlap, and R.P. Woychik. 2000. The Oak Ridge Polycystic Kidney (orpk) disease gene is required for left-right axis determination. *Development.* 127:2347–2355.

Muresan, V., A. Lyass, and B.J. Schnapp. 1999. The kinesin motor KIF3A is a component of the presynaptic ribbon in vertebrate photoreceptors. *J. Neurosci.* 19:1027–1037.

Nakamura, N., C. Rabouille, R. Watson, T. Nilsson, N. Hui, P. Slusarewicz, T.E. Kreis, and G. Warren. 1995. Characterization of a cis-Golgi matrix protein, GM130. *J. Cell Biol.* 131:1715–1726. doi:10.1083/jcb.131.6.1715

Omori, Y., C. Zhao, A. Saras, S. Mukhopadhyay, W. Kim, T. Furukawa, P. Sengupta, A. Veraksa, and J. Malicki. 2008. Elipsa is an early determinant of ciliogenesis that links the IFT particle to membrane-associated small GTPase Rab8. *Nat. Cell Biol.* 10:437–444. doi:10.1038/ncb1706

Orisme, W., J. Li, T. Goldmann, S. Bolch, U. Wolfrum, and W.C. Smith. 2010. Light-dependent translocation of arrestin in rod photoreceptors is signaled through a phospholipase C cascade and requires ATP. *Cell. Signal.* 22:447–456. doi:10.1016/j.cellsig.2009.10.016

Ou, G., M. Koga, O.E. Blacque, T. Murayama, Y. Ohshima, J.C. Schafer, C. Li, B.K. Yoder, M.R. Leroux, and J.M. Scholey. 2007. Sensory ciliogenesis in *Caenorhabditis elegans*: assignment of IFT components into distinct modules based on transport and phenotypic profiles. *Mol. Biol. Cell.* 18:1554–1569. doi:10.1091/mbc.E06-09-0805

Papermaster, D.S. 2002. The birth and death of photoreceptors: the Friedenwald Lecture. *Invest. Ophthalmol. Vis. Sci.* 43:1300–1309.

Pazour, G.J., C.G. Wilkerson, and G.B. Witman. 1998. A dynein light chain is essential for the retrograde particle movement of intraflagellar transport (IFT). *J. Cell Biol.* 141:979–992. doi:10.1083/jcb.141.4.979

Pazour, G.J., B.L. Dickert, and G.B. Witman. 1999. The DHC1b (DHC2) isoform of cytoplasmic dynein is required for flagellar assembly. *J. Cell Biol.* 144:473–481. doi:10.1083/jcb.144.3.473

Pazour, G.J., S.A. Baker, J.A. Deane, D.G. Cole, B.L. Dickert, J.L. Rosenbaum, G.B. Witman, and J.C. Besharse. 2002. The intraflagellar transport protein, IFT88, is essential for vertebrate photoreceptor assembly and maintenance. *J. Cell Biol.* 157:103–113. doi:10.1083/jcb.200107108

Pedersen, L.B., and J.L. Rosenbaum. 2008. Intraflagellar transport (IFT) role in ciliary assembly, resorption and signalling. *Curr. Top. Dev. Biol.* 85:23–61. doi:10.1016/S0070-2153(08)00802-8

Peterson, J.J., W. Orisme, J. Fellows, J.H. McDowell, C.L. Shelamer, D.R. Dugger, and W.C. Smith. 2005. A role for cytoskeletal elements in the light-driven translocation of proteins in rod photoreceptors. *Invest. Ophthalmol. Vis. Sci.* 46:3988–3998. doi:10.1167/iovs.05-0567

Pigino, G., S. Geimer, S. Lanzavecchia, E. Paccagnini, F. Cantele, D.R. Diener, J.L. Rosenbaum, and P. Lupetti. 2009. Electron-tomographic analysis of intraflagellar transport particle trains in situ. *J. Cell Biol.* 187:135–148. doi:10.1083/jcb.200905103

Qin, H., D.R. Diener, S. Geimer, D.G. Cole, and J.L. Rosenbaum. 2004. Intraflagellar transport (IFT) cargo: IFT transports flagellar precursors to the tip and turnover products to the cell body. *J. Cell Biol.* 164:255–266. doi:10.1083/jcb.200308132

Qin, P., and R.G. Pourcho. 2001. Immunocytochemical localization of kainate-selective glutamate receptor subunits GluR5, GluR6, and GluR7 in the cat retina. *Brain Res.* 890:211–221. doi:10.1016/S0006-8993(00)03162-0

Reidel, B., T. Goldmann, A. Giessl, and U. Wolfrum. 2008. The translocation of signaling molecules in dark adapting mammalian rod photoreceptor cells is dependent on the cytoskeleton. *Cell Motil. Cytoskeleton.* 65:785–800. doi:10.1002/cm.20300

Roepman, R., and U. Wolfrum. 2007. Protein networks and complexes in photoreceptor cilia. *In* Subcellular Proteomics: From Cell Deconstruction to System Reconstruction. E. Bertrand and M. Faupel, editors. Springer, Dordrecht, Netherlands. 209–235.

Rosenbaum, J.L., and G.B. Witman. 2002. Intraflagellar transport. *Nat. Rev. Mol. Cell Biol.* 3:813–825. doi:10.1038/nrm952

Rosenbaum, J.L., D.G. Cole, and D.R. Diener. 1999. Intraflagellar transport: the eyes have it. *J. Cell Biol.* 144:385–388. doi:10.1083/jcb.144.3.385

Sedmak, T., E. Sehn, and U. Wolfrum. 2009. Immunoelectron microscopy of vesicle transport to the primary cilium of photoreceptor cells. In *Primary cilia*. Methods in Cell Biology, vol. 94, R.D. Sloboda, editor. Academic Press, London. 259–272.

Setou, M., T. Nakagawa, D.H. Seog, and N. Hirokawa. 2000. Kinesin superfamily motor protein KIF17 and mLin-10 in NMDA receptor-containing vesicle transport. *Science.* 288:1796–1802. doi:10.1126/science.288.5472.1796

Signor, D., K.P. Wedaman, J.T. Orozco, N.D. Dwyer, C.I. Bargmann, L.S. Rose, and J.M. Scholey. 1999a. Role of a class DHC1b dynein in retrograde transport of IFT motors and IFT raft particles along cilia, but not dendrites, in chemosensory neurons of living *Caenorhabditis elegans*. *J. Cell Biol.* 147:519–530. doi:10.1083/jcb.147.3.519

Signor, D., K.P. Wedaman, L.S. Rose, and J.M. Scholey. 1999b. Two heteromeric kinesin complexes in chemosensory neurons and sensory cilia of *Caenorhabditis elegans*. *Mol. Biol. Cell.* 10:345–360.

Sloboda, R.D. 2005. Intraflagellar transport and the flagellar tip complex. *J. Cell. Biochem.* 94:266–272. doi:10.1002/jcb.20323

Snow, J.J., G. Ou, A.L. Gunnarson, M.R. Walker, H.M. Zhou, I. Brust-Mascher, and J.M. Scholey. 2004. Two anterograde intraflagellar transport motors cooperate to build sensory cilia on C. elegans neurons. *Nat. Cell Biol.* 6:1109–1113. doi:10.1038/ncb1186

Sung, C.H., and A.W. Tai. 2000. Rhodopsin trafficking and its role in retinal dystrophies. *Int. Rev. Cytol.* 195:215–267. doi:10.1016/S0074-7696(08)62706-0

Tai, A.W., J.Z. Chuang, C. Bode, U. Wolfrum, and C.H. Sung. 1999. Rhodopsin's carboxy-terminal cytoplasmic tail acts as a membrane receptor for cytoplasmic dynein by binding to the dynein light chain Tctex-1. *Cell.* 97:877–887. doi:10.1016/S0092-8674(00)80800-4

tom Dieck, S., W.D. Altrock, M.M. Kessels, B. Qualmann, H. Regus, D. Brauner, A. Fejtová, O. Bracko, E.D. Gundelfinger, and J.H. Brandstätter. 2005.

Molecular dissection of the photoreceptor ribbon synapse: physical interaction of Bassoon and RIBEYE is essential for the assembly of the ribbon complex. *J. Cell Biol.* 168:825–836. doi:10.1083/jcb.200408157

Trojan, P., N. Krauss, H.W. Choe, A. Giessl, A. Pulvermüller, and U. Wolfrum. 2008. Centrins in retinal photoreceptor cells: regulators in the connecting cilium. *Prog. Retin. Eye Res.* 27:237–259. doi:10.1016/j.preteyeres.2008.01.003

Tsujikawa, M., and J. Malicki. 2004. Intraflagellar transport genes are essential for differentiation and survival of vertebrate sensory neurons. *Neuron.* 42:703–716. doi:10.1016/S0896-6273(04)00268-5

Usukura, J., and S. Obata. 1995. Morphogenesis of photoreceptor outer segments in retinal development. *Prog. Retin. Eye Res.* 15:113–125. doi:10.1016/1350-9462(95)00006-2

Wang, Q., J. Pan, and W.J. Snell. 2006. Intraflagellar transport particles participate directly in cilium-generated signaling in *Chlamydomonas*. *Cell.* 125:549–562. doi:10.1016/j.cell.2006.02.044

Wolfrum, U. 1991. Tropomyosin is co-localized with the actin filaments of the scolopale in insect sensilla. *Cell Tissue Res.* 265:11–17. doi:10.1007/BF00318134

Yau, K.W., and R.C. Hardie. 2009. Phototransduction motifs and variations. *Cell.* 139:246–264. doi:10.1016/j.cell.2009.09.029

Young, R.W. 1976. Visual cells and the concept of renewal. *Invest. Ophthalmol. Vis. Sci.* 15:700–725.

Supplemental material

Sedmak and Wolfrum, http://www.jcb.org/cgi/content/full/jcb.200911095/DC1
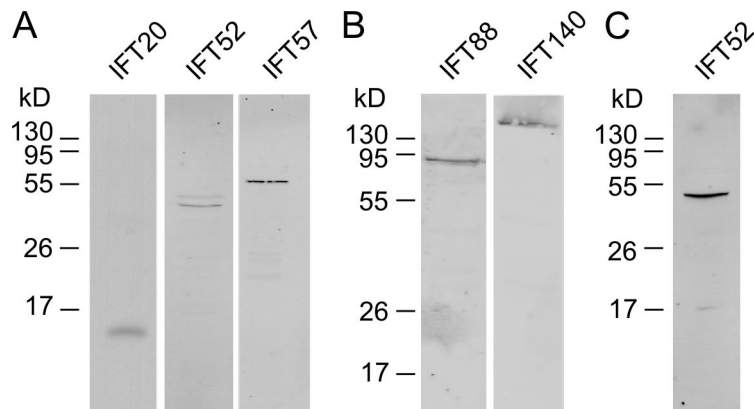
Figure S1.   **IFT protein expression in mouse retina.** (A and B) Western blot analyses of protein extracts of mouse retina with antibodies against murine IFT proteins demonstrate expression of all five IFT proteins. The affinity-purified polyclonal antibodies against IFT20, -57, -88, and -140 recognized single bands of predicted sizes (IFT20, 15 kD; IFT57, 57 kD; IFT88, 90 kD; and IFT140, 140 kD), indicating their monospecificity. Only anti-IFT52 recognized, besides the predicted 52-kD band, an additional single band of lower molecular mass (~50 kD) not detected in testis extracts (C). Retina and testis extracts in A and C were separated on 15% polyacrylamide gels; retina extract in B was separated on a 12% polyacrylamide gel. The immunoreactivity of the first lane was detected by ECL; the second through the sixth lanes were analyzed by an Odyssey infrared imaging system.

THE JOURNAL OF CELL BIOLOGY
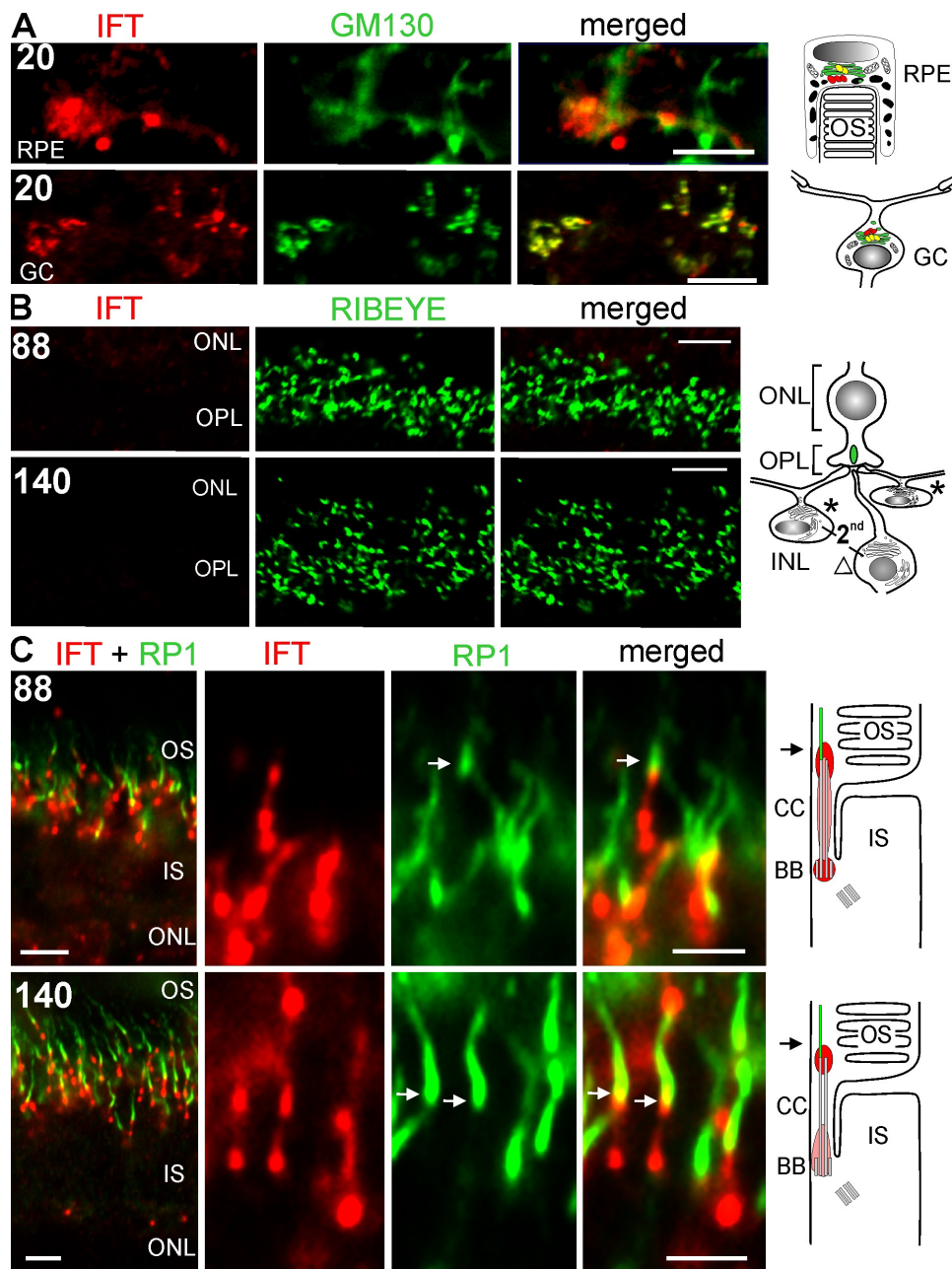
Figure S2. Double labeling of IFT proteins and molecular markers for subcellular compartments. (A) Indirect immunofluorescence double labeling with anti-IFT20 and -GM130 in cells of the RPE and in ganglion cells (GC) of mouse retinas. IFT20 and GM130 are partly colocalized at the GA of the RPE cells and of the ganglion cell outlined in the adjacent cartoons. (B) Indirect immunofluorescence analyses double labeling with antibodies to IFT88 and -140 and anti-RIBEYE, a molecular marker for the presynaptic ribbon of photoreceptor synapses, in the OPL of mouse retinas. Only weak immunofluorescence labeling of anti-IFT88 and -IFT140 were found in the OPL, which was not associated with ribbon synapse stained by the anti-RIBEYE. Asterisks and the triangle indicate horizontal and bipolar cells, respectively. (C) Indirect immunofluorescence double labeling of cryosections through the mouse retina with anti-IFT88 and -IFT140 and antibodies against the axonemal protein retinitis pigmentosa 1 (RP1). Merged images of immunofluorescence double labeling of IFT88 and -140 and the RP1 show partial colocalization of IFT88 and -140 with RP1. Schematic cartoons represent the labeling pattern of IFT88 and -140 and RP1 proteins in the ciliary region of photoreceptor cells. Arrows indicate the axoneme. Bars: (A, B, and C [left]) 5 µm; (C, right) 1.25 µm.
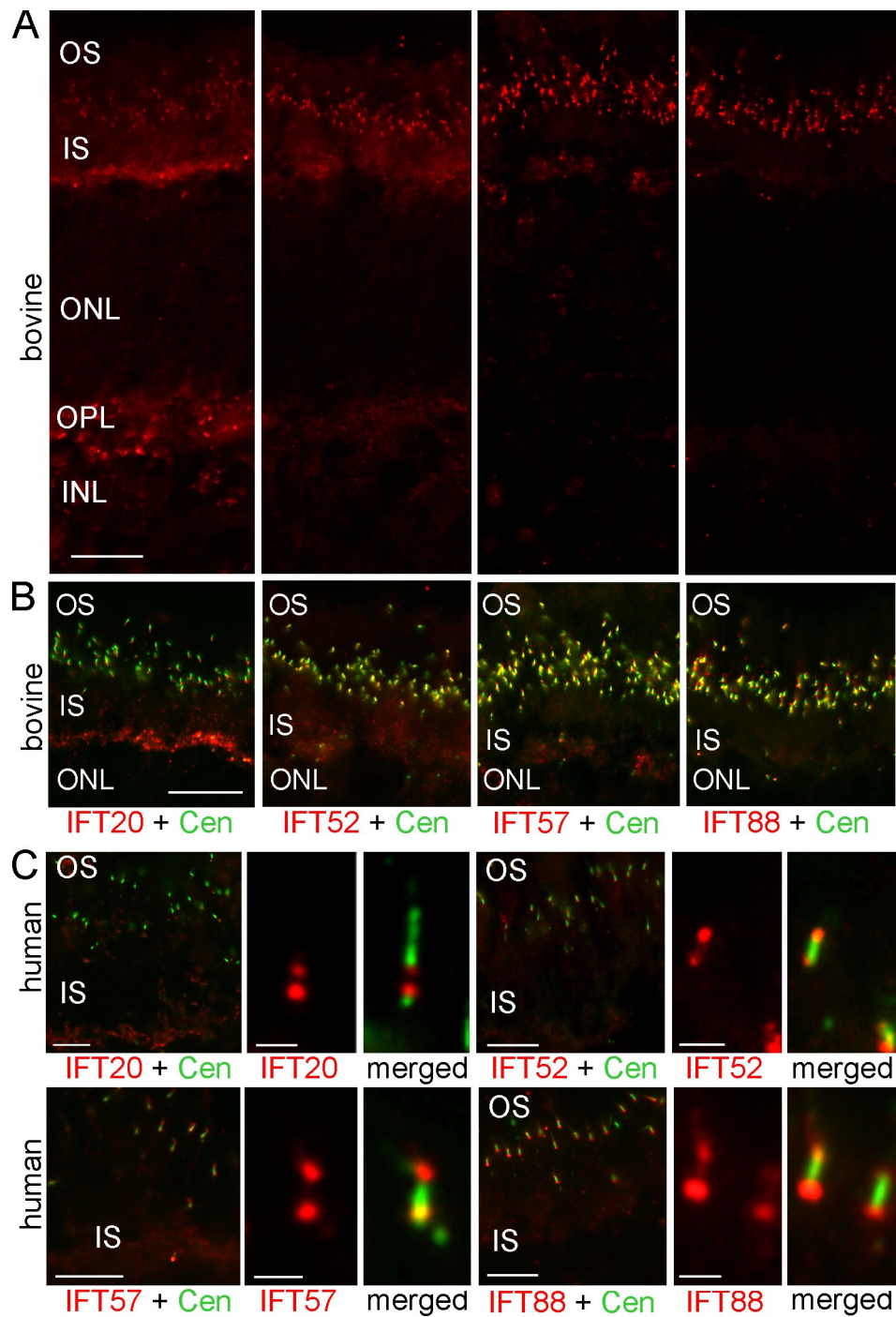
Figure S3.   **Expression of IFT proteins in bovine and human retina.** (A–C) Indirect immunofluorescence analyses of IFT proteins in bovine (A and B) and human (C) retinal cryosections. (B and C) Double labeling with antibodies to IFT20, -52, -57, and -88 and ciliary marker centrin-3 (Cen). All four IFT proteins, IFT20, -52, -57, and -88, partly colocalize with centrin-3. Bars: (A) 10 µm; (B and C [left]) 5 µm; (C, right) 0.5 µm.
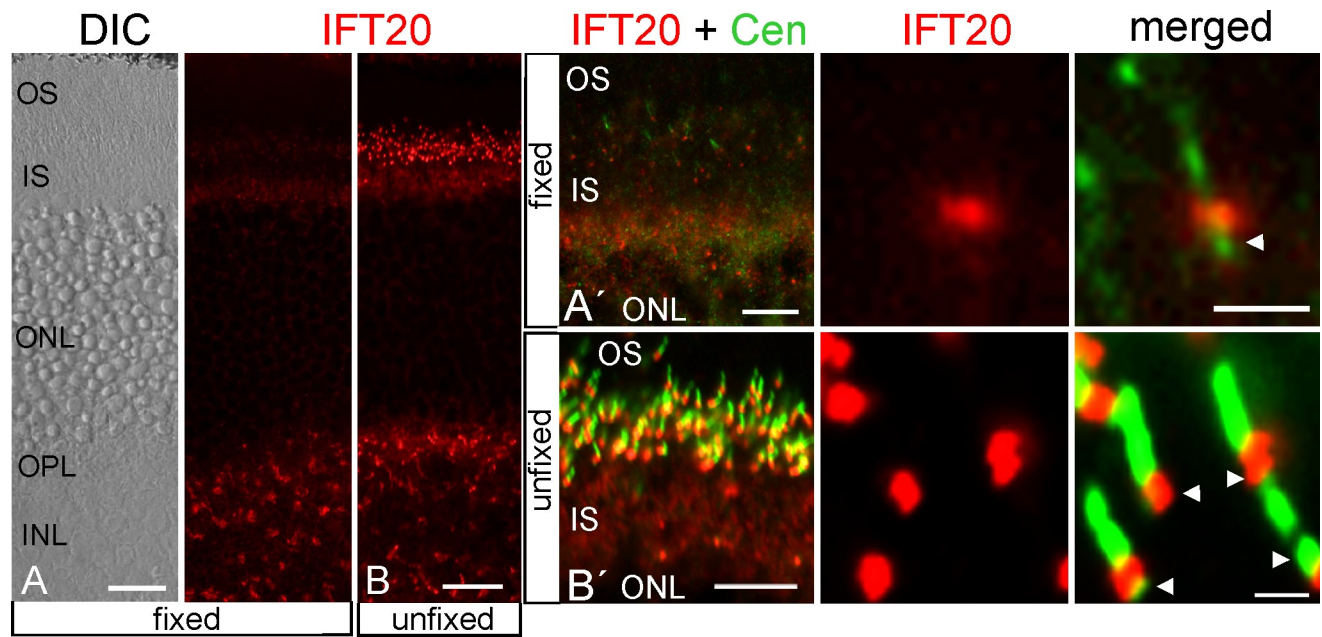
Figure S4. **IFT20 partly colocalizes with centrin in fixed and unfixed mouse retina.** (A–B') Indirect immunofluorescence analysis of methanol-fixed (A and A') and unfixed (B and B') retinal cryosections. (A) Differential interference contrast (DIC) image of fixed longitudinal section. (A' and B') Merged images of immunofluorescence double labeling with antibodies to anti-IFT20 and –centrin-3 (Cen) as marker for the CC with BB and adjacent centriole (arrowheads) in fixed (A') and unfixed (B') cryosections. High magnification images of double immunofluorescences of the ciliary part of photoreceptor cells of IFT20 and centrin-3 are shown. IFT20 partly colocalizes with centrin-3. Bars: (A and B) 10 µm; (A' and B', left) 5 µm; (A' and B', right) 1.25 µm.

2.3 Publication III

Sedmak T and Wolfrum U (2011) Intraflagellar transport proteins in ciliogenesis of photoreceptor cells (submitted)

Intraflagellar transport proteins in ciliogenesis of photoreceptor cells

Sedmak T[1] and Wolfrum U

Department of Cell and Matrix Biology, Institute of Zoology, Johannes Gutenberg University Mainz, Germany

Corresponding author: Uwe Wolfrum, Department of Cell and Matrix Biology, Institute of Zoology, Johannes Gutenberg University Mainz, D-55099 Mainz, Germany. Tel.: +49-6131-39-25148; Fax: +49-6131-39-23815; e-mail: ***wolfrum@uni-mainz.de***
[1] Present address: University of Erlangen-Nuremberg, Department of Biology, Animal Physiology, D-91058 Erlangen, Germany.

Abstract

The assembly and maintenance of cilia depend on intraflagellar transport (IFT) mediated by molecular motors and their interplay with IFT proteins. Here, we analyzed the involvement of IFT proteins in the ciliogenesis of mammalian photoreceptor cilia. Electron microscopy revealed that ciliogenesis in mouse photoreceptor cells follows an intracellular ciliogenesis pathway, divided into six distinct stages. The first stages are characterized by electron dense centriolar satellites and a ciliary vesicle, whereas the formations of the ciliary shaft and the light sensitive outer segment disks are features of the later stages.

IFT proteins were associated with ciliary apparatus during all stages photoreceptor cell development. Our data conclusively provide evidence for the participation of IFT proteins in photoreceptor cell ciliogenesis, including the formation of the ciliary vesicle and the elongation of the primary cilium. In advanced stages of ciliogenesis the ciliary localization of IFT proteins indicate a role in IFT as is seen in mature cilia. A prominent accumulation of IFT proteins in the periciliary cytoplasm at the base of the cilia in these stages most probably resembles a reserve pool of IFT molecules for further delivery into the growing ciliary shaft and their subsequent function in IFT. Nevertheless, the cytoplasmic localization of IFT proteins in the absence of a ciliary shaft in early stages of ciliogenesis indicates roles of IFT proteins beyond their well-established function for IFT in mature cilia and flagella.

Introduction

Cilia are highly conserved thin finger-like organelles emerging from the surface of eukaryotic cells. They are structurally divided into sub-compartments, predominantly into an axoneme and a transition zone, which emerge from the basal body complex. Cilia have multiple functions both in mature and developing organisms, e.g. locomotion or specific sensory function. Disruption of cilia has been associated with numerous ciliopathies – complex syndromes involving cystic kidneys, obesity, mental retardation, deafness, blindness and various developmental malformations (Badano et al., 2006; Baker and Beales, 2009; Gerdes et al., 2009; Goetz and Anderson, 2010).

Cilia are formed by the mother centriole of the centrosome, which matures into the basal body and nucleates the nine microtubule doublets of the axoneme. Sorokin's pioneer studies on ciliogenesis in the 60´s have revealed to two principally different pathways of

ciliogenesis (Sorokin, 1962, 1968), which were recently referred to as the extracellular and intracellular pathways of ciliogenesis (Molla-Herman et al., 2010; Ghossoub et al., 2011). In the extracellular ciliogenesis pathway, the mother centriole directly docks at the plasma membrane from where the ciliary shaft is formed and grows towards the extracellular environment. During, intracellular ciliogenesis, the mother centriole docks to the membrane of an intracellular primary ciliary vesicle, and the cilium is assembled within the ciliary vesicle. After docking and fusion of the elongated intracellular ciliary vesicle with the plasma membrane, the ciliary shaft is released into the extracellular space.

Assembly and maintenance of cilia require intraflagellar transport (IFT), a conserved process mediated by molecular motors and IFT particles (Rosenbaum and Witman, 2002; Pedersen and Rosenbaum, 2008). IFT comprises the bidirectional transport of IFT particles containing ciliary or flagellar cargo along the outer doublet microtubules of the axoneme. IFT particles themselves are composed of individual IFT proteins organized into the two sub-complexes A and B, suggested to participate in anterograde and retrograde IFT, respectively (Cole et al., 1998; Cole 2003; Krock et al., 2009). IFT proteins are conserved among green algae, nematodes and vertebrates. Mutations in genes encoding IFT proteins prevent ciliary assembly in all organisms investigated (Cole et al., 1998; Murcia et al., 2000; Pazour et al., 2002; Tsujikawa and Malicki 2004; Krock and Perkins, 2008; Omori et al., 2008). From these genetic data there is no doubt that IFT is essential for the development of cilia. However, only little substantial data is available on the role of IFT and the specific functions of the individual IFT proteins during ciliogenesis (Pedersen et al., 2008; Sukumaran and Perkins, 2009). This insufficiency is partly due to the deficient knowledge on the specific sub-cellular localization of the IFT components, in particularly individual IFT proteins during ciliogenesis. Here we systematically analyzed the expression and sub-cellular localization of four different IFT-complex B proteins, namely IFT20, IFT52, IFT57, and IFT88 as well as the IFT-complex A protein IFT140 during ciliogenesis in rod photoreceptor cells by a combination of high resolution immunofluorescence and electron microscopy.

We have recently introduced the vertebrate retina and its photoreceptor cells as a useful model system to verify the roles of individual IFT proteins through their sub-cellular localization (Sedmak and Wolfrum, 2010). Photoreceptor cells are highly polarized sensory neurons, organized in morphological and functional distinct cellular compartments. The photosensitive outer segment is a drastically evolutionary modified primary cilium (Besharse and Horst, 1990; Roepman and Wolfrum, 2007; Pazour and Bloodgood, 2008) that contains all components of the visual transduction cascade, which in rod cells are arranged at hundreds of flattened membrane disks separated from the plasma membrane (Sung and Chuang, 2010). The outer segment is linked to the inner segment containing all the organelles necessary for biosynthesis by the connecting cilium, a slightly modified and extended transition zone of a prototypic cilium, (Roepman and Wolfrum, 2007). The axon projects from the photoreceptor cell body to the synaptic terminus connecting the photoreceptor cells with the secondary retinal neurons (tom Dieck and Brandstätter, 2006).

During development of the vertebrate retina, photoreceptor cells mature from precursors present in the outer neuroblastic layer (Livesey and Cepko, 2001). In rodents, the rod photoreceptor differentiation starts postnatally and ciliogenesis of fully mature outer segments lasts over two weeks (LaVail, 1973). The ciliogenesis of rod cells is not completely synchronized throughout development (Tokuyasu and Yamada, 1959; Greiner et al., 1981; Nir et al., 1984; Chaitin, 1992; Sung and Chuang, 2010) and therefore different stages of developing photoreceptor cilia can be analyzed in parallel, offering a useful system to study primary cilia's assembly. However, there are controversial data on the ciliogenesis pathway of photoreceptor cells in the literature. Although recent reviews indicated that mammalian photoreceptor cilia develop via an extracellular pathway (Sung and Chuang, 2010, Ghossoub et al., 2011) an electron microscopy analysis has implicate the intracellular pathway (Greiner

et al., 1981). This evident discrepancy has prompted us to investigate ciliogenesis in photoreceptor cells in a more detailed reanalysis.

In the present study we demonstrate that ciliogenesis in photoreceptor cells occurs via the intracellular pathway. Furthermore, dissection into various developmental stages has allowed us to analyze the spatial distribution of individual IFT proteins at the diverse stages of ciliogenesis. We show that IFT proteins are present at all stages of the intracellular ciliogenesis of photoreceptor cells. These results provide evidence for a role of IFT proteins in ciliogenesis even before the IFT motility system starts to transport cargo along the axonemal microtubules, indicating an IFT protein function independent from IFT.

Results
Ultrastructural analysis of the ciliogenesis in differentiating photoreceptor cells
The ciliogenesis in photoreceptor cells was analyzed in retinas of mice at postnatal day 0 (PN0), PN3, and PN7 by conventional transmission electron microscopy (Fig. 1). The photoreceptor cells differentiate in the apical part of the neuroblastic layer of the developing mouse retina. Ciliogenesis in the differentiating photoreceptor cells is not synchronized (Fig. 1H,I). For the nomenclature of the different stages of ciliogenesis in photoreceptor cells we followed Pedersen and colleagues (2008) who proposed four stages for primary cilia and added two photoreceptor specific stages, S5 and S6, characteristic for the outer segment formation. In retinas of PN0 and PN3 mice we observed photoreceptor cells in stages S1-S4 (Fig. 1H), whereas in PN7 stages S3-S6 of ciliogenesis were predominant (Fig. 1I).

In stage S1 of the photoreceptor cell ciliogenesis, an intracellular primary ciliary vesicle appears at the distal end of the mother centriole. During S1 the mother centriole matures into the basal body and two sets of accessory structures, the distal and sub-distal appendages, appear at the distal part of the basal body (Fig. 2). The distal appendages project to the membrane of the primary vesicle whereas the sub-distal appendages protrude from the basal body into the pericentriolar cytoplasm. These appendages are absent from the daughter and the adjacent centriole.

In stages S1-S3 of the differentiating photoreceptor cells, we observed electron dense spherical granules, the centriolar satellites in the cytoplasm of the periciliary region of the evolving photoreceptor cilium (Fig. 2A,H). The number of centriolar satellites gradually decreases from S1-S3 until they disappear in S4. They are non-membranous cytoplasmic granules which are thought to be involved in the transport of ciliary and centriolar proteins, e.g. centrin, pericentrin and ninein, to the basal body (Kubo et al 1999; Laoukili et al., 2000; Dammermann and Merdes, 2002; Hames et al., 2005).

In stage S2 the ciliary bud emerges from the distal basal body, elongates and forms the ciliary shaft, which projects into the growing ciliary vesicle (Fig. 2). The primary ciliary vesicle expands by the fusion of post-Golgi vesicles to form the so-called ciliary vesicle. At this stage a small ciliary pocket appears at the base of the ciliary shaft (Fig. 2B,E). Periodic bead-like densities which are characteristic for the plasma membrane of the transition zone (Gilula and Satir, 1972; Besharse and Horst, 1990) become apparent in the proximal cilium in stage S2 (Fig. 2B,C). As the cilia continue to mature the transition zone extends to form the connecting cilium of the mature photoreceptor cell (Figs. 1E-G,I, 2C,F). The ciliary vesicle fuses with the plasma membrane and from stage S3 on the cilium is exposed at the surface of the photoreceptor cell (Figs. 1C,G; 2C,F). In conclusion, the early stages of ciliogenesis (S1-S3) in photoreceptor cells exhibit the characteristic hallmarks of an intracellular ciliogenesis pathway (Molla-Herman et al., 2010; Ghossoub et al., 2011).

In stage S4 the distal part of the evolving cilium begins to swell and internal membrane vesicles or tubules appear. These membrane structures fuse to form the disk membranes of the rod outer segment in stage S5 (Fig. 1E). From stage S6 on stacks of outer segment disks can be identified which still lack the characteristic organization of the mature

outer segments (Fig. 1F,G). It is notable that during ciliogenesis the polarity of the photoreceptor cilia differs and evolving cilia can point with their tips either to the outer limiting membrane or to the retinal pigment epithelium (Fig. 1H).

Expression of individual IFT proteins in the developing mouse retina
Indirect immunofluorescence analyses of developing mouse retinas at PN0, -3, -7 revealed that the IFT proteins IFT20, IFT52, IFT57, IFT88 and IFT140 are expressed during all developmental stages of the retina (Fig. 3; Supplemental Fig. S1). The staining patterns of all anti-IFT antibodies applied in the present study were very similar. As example we show anti-IFT57 labeling of retinal cryosections in figure 3. In PN0 and PN3 mouse retinas IFT proteins were concentrated in the apical region of the neuroblastic layer proximal to the retinal pigment epithelium (Fig. 3A-C). Weaker immunofluorescence was observed in the cytoplasm of the cells of the entire neuroblastic layer. At PN7 the characteristic neuronal layers of the vertebrate retina became apparent and the IFT distribution was similar to IFT staining in mature retinas (Figs. 3D,E; Supplemental Fig. S1C; Sedmak and Wolfrum, 2010).

IFT proteins are associated with evolving ciliary structures in developing photoreceptor cells at all stages
To elucidate the sub-cellular localization of individual IFT proteins in the differentiating cilium of photoreceptor cells cryosections of postnatal retinas (PN0, -3, -7 and mature PN21) were analyzed by double labeling with antibodies against IFT proteins and against centrin, a marker for the connecting cilium, the basal body and the associated centriole (Trojan et al., 2008). This co-labeling allowed us to determine the spatial localization of IFT proteins in the photoreceptor ciliary apparatus by immunofluorescence microscopy (Fig. 4, Supplemental Fig. S2). High resolution immunofluorescence analyses of double labeled specimens revealed that, in the early stages S1-S4 of photoreceptor cell ciliogenesis, IFT proteins were partly co-localized with centrin, indicating IFT localization in the mother centriole or basal body, as well as with the elongating ciliary bud and the adjacent daughter centriole (Fig. 4, Supplemental Fig. S2). Subsequently, during the differentiating stages S5 and S6 the sub-ciliary distribution pattern of the IFT proteins resembled the localization recently described for the mature photoreceptor cell (Fig. 4, Supplemental Fig. S2; Sedmak and Wolfrum, 2010). IFT52, IFT57, IFT88, and IFT140 were most concentrated at the border of the anti-centrin positive connecting cilium at the base of the outer segment. These molecules were also detectable along the shaft and in the proximal part of the connecting cilium. In contrast to the other IFT proteins analyzed, IFT20 was only detected in the basal part of the connecting cilium and at the distal region of the adjacent centriole.

To elucidate the sub-cellular localization of IFT molecules during rod photoreceptor ciliogenesis in more detail, immunoelectron microscopy was performed using antibodies against IFT proteins in PN0, -3 and -7 mouse retinas. During the early ciliogenesis stages S1-S2, all investigated IFT proteins were associated with the daughter centriole and the mother centriole or with the basal body (S2) (Fig. 5). At the basal body they were present in the distal and sub-distal centriolar appendages (Fig. 6A-D). In stages S2-S3 the IFT proteins were additionally found in the cytoplasm of the differentiating photoreceptor cells, at the centriolar satellites (Figs. 6, 7, 8) and associated with non-ciliary vesicular structures, putative post-Golgi vesicles (Fig. 7). In the periciliary cytoplasm these vesicles were present close to the mother centriole/basal body and with the exception of IFT88 in the vicinity of the ciliary vesicle or at the vesicle membrane, possibly frozen in the fusion process (Fig. 7A,A`). IFT20 was also found at membrane stacks of the Golgi apparatus in differentiating photoreceptor inner segments, which was confirmed by double immunofluorescence labeling using the Golgi resident marker anti-GM130 (Supplemental Fig. S3).

In addition to their basal body localization, we detected IFT52, IFT57, IFT88 and IFT140 in the evolving ciliary shaft for the first time (in stage S3). In the subsequent stages of ciliogenesis these IFT proteins were found in the proximal and distal cilium, characteristic for stage S4, and the connecting cilium, from stage S5 on (Figs. 4, 7, 9; Supplemental Fig. S2). Immunoelectron microscopy analyses of stages S5 and S6 of photoreceptor ciliogenesis revealed the highest concentration of IFT52, IFT57, IFT88 and IFT140 at the base of the outer segment (Fig. 9). In addition, immunolabeling for IFT88 and IFT140 was detected in the axoneme which projects into the evolving outer segment in stage S6 of photoreceptor ciliogenesis (Fig. 9D-G).

In contrast to other IFT proteins, IFT20 was absent from the ciliary shaft and the connecting cilium in stages S4 and S5, respectively (Figs. 4, 8, 10; Supplemental Fig. S2) which resembles the mature situation (Fig. 10H; Sedmak and Wolfrum 2010). However, we detected IFT20 during the transition of stages S4 to S5/S6 at the base of the evolving rod outer segments (Fig. 10; Supplemental Fig. S3). Nevertheless, we were not able to find IFT20 in connecting cilia and outer segments of mature photoreceptor cells confirming our previous data (Fig. 10H) (Sedmak and Wolfrum, 2010).

Supplementary data
Supplemental Fig. S1 presents the expression of IFT proteins in the developing mouse retina using immunofluorescence analyses. Supplemental Fig. S2 demonstrates the spatial distribution of IFT52 and IFT140 proteins during ciliogenesis of retinal photoreceptor cells. Supplemental Fig. S3 shows sub-cellular localization of IFT20 at the Golgi apparatus and in the cilium of differentiating mouse photoreceptor cell. Supplementary data associated with this article can be found, in the online version.

Discussion
Photoreceptor cilia development follows an intracellular ciliogenesis pathway
In this study we have reinvestigated the ciliogenesis pathway in rod photoreceptor cells for clarification of controversial data previously reported (Sung and Chuang, 2010; Ghossoub et al., 2011). Our results revealed that the photoreceptor ciliogenesis in mammalian retinas follows the intracellular ciliogenesis pathway previously hypothesized by Greiner et al., (1981). This intracellular ciliogenesis pathway is characteristic for fibroblasts and RPE1 cells, but also for neurons (Molla-Herman et al., 2010). Moreover, our analyses revealed that photoreceptor ciliogenesis can in principle be divided into the same stages previously described for cell types with intracellular ciliogenesis (Sorokin, 1962; Pedersen et al., 2008). During the early stages of ciliogenesis, the mother centriole matures into the basal body in the cytoplasm of the differentiating photoreceptor cell, docking with its appendages to the membrane of the intracellular primary ciliary vesicle. The close relation of cytoplasmic vesicles, most probably post-Golgi vesicles, to the ciliary vesicle (e.g. Fig. 2; Fig. 7) indicates that the ciliary vesicle is fed by post-Golgi vesicles which confirm Sorokin´s findings in fibroblasts and smooth muscle cells (Sorokin, 1962). In contrast, we did not find any indications for an endocytotic origin of the ciliary vesicle as previously suggested (Molla-Herman et al., 2010; Rattner et al., 2010; Kim et al., 2010).

IFT molecules are involved in late stages of ciliogenesis
Our results demonstrate that IFT proteins are expressed during all stages of ciliogenesis in photoreceptor cells and are found within the differentiating photoreceptor ciliary shaft as soon as it appears. In the evolving ciliary shaft, the IFT proteins most probably participate in IFT processes. This indicates that IFT is required for the elongation of the differentiating cilium and assembly of the ciliary shaft and axoneme, confirming previous data (reviewed in Rosenbaum and Witman, 2002; Pedersen and Rosenbaum, 2008).

Interestingly, IFT20 appeared in the transition from stage S4 to S5 of rod photoreceptor ciliogenesis in the evolving ciliary shaft and in its distal swelling containing membrane vesicles of the premature outer segment. This is in contrast to our previous observations in mature photoreceptor cells in which IFT20 was absent from the connecting cilium and the axoneme (Sedmak and Wolfrum, 2010). Nevertheless, the association of IFT20 with membrane vesicles in the premature outer segment is consistent with the IFT20 localization at Golgi membranes and post-Golgi transport vesicles as shown previously (Folitt et al., 2006, 2008; Sedmak et al., 2009; Sedmak and Wolfrum, 2010). We therefore speculate that IFT20 may play a role in the delivery of vesicles to differentiating membrane disks in the premature photoreceptor outer segment. In later stages of ciliogenesis, when the outer segment matures, membrane vesicles and IFT20 disappear from the outer segment base. A crucial role of IFT20 has been recently described for the formation of photoreceptor outer segments in knock out (Keady et al., 2011), which is in line the present results on IFT20 in photoreceptor ciliogenesis.

In addition to their location in the ciliary shaft all analyzed IFT proteins were found at the ciliary base during later stages of photoreceptor ciliogenesis. There, the IFT proteins were present at the basal body, which is consistent with the observations for the ciliary region of the mature photoreceptor cell (Sedmak and Wolfrum, 2010). This pool of IFT proteins was previously judged to be involved in the assembly of IFT particles and the sorting of cargo for the delivery into the cilium (reviewed by Pedersen and Rosenbaum, 2008; Insinna and Besharse, 2008; Insinna et al., 2008, 2009; Pigino et al., 2009). Furthermore, in stages S3 to S6, IFT20 and IFT52 were located in the apical periciliary extension of the differentiating inner segment. In mature photoreceptor cells this apical region was recently identified as a periciliary target area for post-Golgi transport vesicles containing cargo with a ciliary destination (Liu et al., 2007; Maerker et al., 2008; Sedmak and Wolfrum, 2010; Yang et al., 2010).

IFT proteins in early stages of intracellular ciliogenesis
We show for the first time that the analyzed IFT proteins are expressed as early as PN0 in the apical part of the neuroblastic layer of the developing murine retina which is in agreement with the localization of IFT52 and IFT88 in the developing zebra fish retina (Sukumaran and Perkins, 2009). Our correlated light and electron microscopy analyses demonstrated that in the absence of any ciliary shaft the IFT proteins are found at the daughter and mother centriole. At these early stages IFT proteins were also associated with the primary ciliary vesicle, centriolar satellites and post-Golgi vesicles in the cytoplasm of the neuroblasts of the developing retina.

As in mature primary cilia and photoreceptors, the prominent accumulation of IFT proteins in the periciliary cytoplasm at the base of the cilia most probably resembles a pool of IFT molecules which is stored for subsequent assembly of IFT complexes and IFT across the growing ciliary shaft in the later stages of ciliogenesis. However, since ciliary shaft does not exist in these differentiating stages, motile processes related to IFT are not occurring. Therefore, the cytoplasmic localization of IFT proteins in these early stages indicates roles of IFT proteins beyond their well-established function for IFT in mature cilia and flagella. Interestingly, the IFT proteins were found in the cytoplasm in close proximity to centriolar satellites and post-Golgi vesicles, structures which are commonly thought to be involved in the delivery of ciliary components to the base of the cilium (Sorokin, 1962; Kubo et al., 1999; Laoukili et al., 2000; Kubo and Tsukita, 2003; Moser et al., 2009). The present association of IFT proteins with post-Golgi transport vesicles during ciliogenesis agrees with data we have recently have reported for IFT proteins in defined periciliary target domains for cytoplasmic transport in mature photoreceptor cells (Sedmak and Wolfrum, 2010; Baldari and Rosenbaum, 2010). During early ciliogenesis IFT proteins may participate in conducting post-Golgi

vesicles to the membrane of the ciliary vesicle for vesicle extension and for the delivery of ciliary membrane cargo to the elongating ciliary bud and shaft. These findings support the hypothesis that IFT proteins are evolutionary related to proteins involved in exocytosis processes, in which post-Golgi vesicles fuse with the plasma membrane previously suggested by Jekely and Arendt (2006).

In previous studies several molecular compounds of centrosomes and basal bodies, e.g. the pericentriolar material-1 (PCM-1) protein, the Bardet-Biedl syndrome protein 4 (BBS4), centrins, pericentrin and the centrosomal protein CEP290 were found to be associated with the centriolar satellites (Kubo et al., 1999; Laoukili et al., 2000; Dammermann and Merdes, 2002; Kubo and Tsukita, 2003; Kim et al., 2004; Nachury et al., 2007; Kim et al., 2008). In these studies the localization of these centrosomal proteins at the centriolar satellites were interpreted as possible roles of these proteins in the transport of non-membrane associated ciliary cargo (e.g. α/β tubulin dimers) to the basal body. Accordingly, we suggest a participation of IFT proteins at the centriolar satellites in cargo transport to the ciliary base. Our results provide evidence for a role of IFT proteins in intracellular transport and cargo targeting even before the IFT system starts to work, delivering cargo within the ciliary shaft. Therefore the present observations confirm data on roles of IFT proteins in non-ciliated systems recently shown in the immune synapse (Finetti et al., 2009) and in dendritic processes of non-ciliated neurons in the mature retina (Sedmak and Wolfrum, 2010).

Our analyses of early ciliogenesis stages showed that the transition zone defines the boundary between the plasma membrane and the ciliary membrane already in the early stages of ciliogenesis. Although there is evidence that the doublet microtubules in the transition zone form independently from IFT (Rohtagi and Snell, 2010) we detected IFT proteins as soon as the transition zone appeared even before the ciliary shaft extended. This observation rises the possibility that IFT proteins play in concert with characteristic transition zone molecules like the recently identified microtubule-membrane linker CEP290 (Craige et al., 2010) in the "quality control" function of the transition zone for ciliary cargo delivery.

Conclusions

In conclusion, this study demonstrates that ciliogenesis in photoreceptor cells follows the intracellular ciliogenesis pathway, which can be divided into six distinct stages (S1 to S6). The first stages (S1-S3) are characterized by electron dense centriolar satellites and a ciliary vesicle, whereas the formation of the ciliary shaft and the light sensitive outer segment disks are features of the three later stages. We provide evidence for the participation of IFT proteins already in early photoreceptor ciliogenesis before the differentiating cilium emerges into the extracellular environment. IFT proteins localized in the periciliary cytoplasm at the base of the cilia may provide a pool of IFT molecules stored for the later delivery into the growing ciliary axoneme for IFT. However, the cytoplasmic localization of IFT proteins in the absence of a ciliary shaft in early stages of ciliogenesis indicates roles of IFT proteins beyond their well-established function for IFT in cilia and flagella.

Material and methods

Animals

All experiments conformed to the guidelines provided by the Association for Research in Vision and Ophthalmology (ARVO) regarding the care and use of animals in research. C57BL/6J mice were maintained on a 12 h light-dark cycle, with food and water *ad libitum*.

Antibodies and fluorescent dyes

Affinity purified antibodies against individual IFT proteins (IFT20, IFT52, IFT57, IFT88 and IFT140) raised in rabbit were previously characterized (Pazour et al., 2002; Follit et al., 2006; Sedmak and Wolfrum, 2010). Monoclonal antibodies to centrin were used as a molecular marker for the ciliary apparatus of photoreceptors (Trojan et al., 2008). Secondary antibodies conjugated to Alexa 488 or Alexa 568 (Invitrogen, Karlsruhe, Germany) and biotinylated

secondary antibodies (Vector Laboratories, Burlingame, USA) were used. Nuclear DNA was stained by 1µg/µl of DAPI (Sigma-Aldrich, Deisenhofen, Germany).

Immunofluorescence microscopy

Postnatal mouse eyes (PN 0, 3, 7 days) were enucleated and cryofixed in melting isopentane enclosed by liquid nitrogen and sectioned with a cryostat as previously described (Wolfrum et al., 1991). Cryosections were placed on poly-L-lysine-precoated coverslips, incubated with 0.01% Tween-20 in PBS, and washed with PBS. Next, the cryosections were incubated with blocking solution (0.5% cold-water fish gelatine, 0.1% ovalbumin in PBS) for 1 h and with primary antibodies, diluted in blocking solution at 4°C, overnight. PBS washed cryosections were incubated with Alexa conjugated secondary antibodies in PBS with DAPI. Cryosections were mounted in Mowiol 4.88 (Hoechst, Frankfurt, Germany), analyzed with a Leica DM 6000 B microscope (Leica, Wetzlar, Germany) through a 63x NA1.32 HCX Plan-Apochromat and a 100x NA 1.4 Plan-Apochromat oil objective lens. Acquired images were processed with Adobe Photoshop CS (Adobe Systems, San Jose, USA).

Conventional electron microscopy

For the ultrastructural analysis of the developing retina, enucleated eyes were fixed in 2.5% glutaraldehyde in 0.1 M cacodylate buffer containing 0.1 M sucrose for 1.5 h at 4°C. After 30 min of this fixation the cornea and lens were removed to obtain an eye cup, which was further fixed for another 1 h. After this fixation step eye cups were washed with 0.1 M cacodylate buffer containing 0.1 M sucrose for 30 min. Subsequently, eyecups were fixed with 2% osmium tetroxide (OsO_4) in 0.1 M cacodylate buffer containing 0.1 M sucrose for 1 h, at RT. After this second fixation step specimens were dehydrated in ethanol (30-100%) and embedded in Renlam® M-1 resin (SERVA Electrophoresis, Heidelberg, Germany).

Immunoelectron microscopy – pre-embedding labeling

For immunoelectron microscopy a previously described protocol of pre-embedding labeling was applied (Maerker et al., 2008; Sedmak et al., 2009). In short, during pre-fixation of isolated mouse eyes in 4% paraformaldehyde in Soerensen buffer (0.1 M $Na_2HPO_4\cdot2H_2O$, 0.1 M KH_2PO_4, pH 7.4) eyes were perforated with a needle and lenses with corneas were removed. Washed retinas were dissected and infiltrated with 10% and 20% sucrose in Soerensen buffer, followed by 30% sucrose overnight. After 4 cycles of freezing in liquid nitrogen and thawing at 37°C retinas were washed in PBS and embedded in buffered 2% Agar (Sigma-Aldrich). Agar blocks were sectioned in 50 µm sections with a vibratome (Leica VT 1000 S). Vibratome sections were blocked in 10% normal goat serum, 1% bovine serum albumin in PBS and incubated with primary antibodies against IFT proteins for 4 days at 4°C. PBS washed sections were incubated with the appropriate biotinylated secondary antibodies, which were visualized by a Vectastain ABC-Kit (Vector Laboratories). To maintain the staining, retina sections were fixed in 2.5% glutaraldehyde in 0.1 M cacodylate buffer (pH 7.4). Further, diaminobenzidine precipitates were silver enhanced and post-fixed in 0.5% OsO_4 in 0.1 M cacodylate buffer on ice. Dehydrated specimens were flat-mounted between ACLAR®-films (Ted Pella Inc., Redding, USA) in Renlam® M-1 resin.

Ultrathin sectioning and transmission electron microscopy

Ultrathin sections were made using an ultramicrotome Reichert Ultracut S (Leica), collected on Formvar-coated copper grids and counterstained with heavy metal staining (2% uranyl acetate in 50% ethanol; 2% aqueous lead citrate). Ultrathin sections were analyzed in a Tecnai 12 BioTwin transmission electron microscope (FEI, Eindhoven, The Netherlands). Images were obtained with a CCD camera (SIS MegaView3, Surface Imaging Systems, Herzogenrath, Germany) and processed with Adobe Photoshop CS (Adobe Systems).

Author contribution

Tina Sedmak performed all experiments, wrote the first draft of the manuscript and contributed to the design of the experiments. Uwe Wolfrum mainly conceived the project. Both authors contributed to the final manuscript.

References

Badano, J.L., Mitsuma, N., Beales, P.L., and Katsanis, N. (2006) The ciliopathies: an emerging class of human genetic disorders. Annu. Rev. Genomics Hum. Genet. **7**, 125-148

Baker, K. and Beales, P.L. (2009) Making sense of cilia in disease: the human ciliopathies. Am. J. Med. Genet. C. Semin. Med. Genet. **151C**, 281-295

Baldari, C.T. and Rosenbaum, J. (2010) Intraflagellar transport: it's not just for cilia anymore. Curr. Opin. Cell Biol. **22**, 75-80

Besharse, J.C. and Horst, C.J. (1990) The photoreceptor connecting cilium - a model for the transition zone. In Ciliary and flagellar membranes (Bloodgood, R.A. eds.), pp. 389-417, Plenum, New York.

Chaitin, M.H. (1992) Double immunogold localization of opsin and actin in the cilium of developing mouse photoreceptors. Exp. Eye Res. **54**, 261-267

Craige, B., Tsao, C.C., Diener, D.R., Hou, Y., Lechtreck, K.F., Rosenbaum, J.L., and Witman, G.B. (2010) CEP290 tethers flagellar transition zone microtubules to the membrane and regulates flagellar protein content. J. Cell Biol. **190**, 927-940

Cole, D.G., Diener, D.R., Himelblau, A.L., Beech, P.L., Fuster, J.C., and Rosenbaum, J.L. (1998) Chlamydomonas kinesin-II-dependent intraflagellar transport (IFT): IFT particles contain proteins required for ciliary assembly in Caenorhabditis elegans sensory neurons. J. Cell Biol. **141**, 993-1008

Cole, D.G. (2003) The intraflagellar transport machinery of Chlamydomonas reinhardtii. Traffic. **4**, 435-442

Dammermann, A. and Merdes, A. (2002) Assembly of centrosomal proteins and microtubule organization depends on PCM-1. J. Cell Biol. **159**, 255-266

Finetti, F., Paccani, S.R., Riparbelli, M.G., Giacomello, E., Perinetti, G., Pazour, G.J., Rosenbaum, J.L., and Baldari, C.T. (2009) Intraflagellar transport is required for polarized recycling of the TCR/CD3 complex to the immune synapse. Nat. Cell Biol. **11**, 1332-1339

Follit, J.A., Tuft, R.A., Fogarty, K.E., and Pazour, G.J. (2006) The intraflagellar transport protein IFT20 is associated with the Golgi complex and is required for cilia assembly. Mol. Biol. Cell **17**, 3781-3792

Follit, J.A., San Agustin, J.T., Xu, F., Jonassen, J.A., Samtani, R., Lo, C.W., and Pazour, G.J. (2008) The Golgin GMAP210/TRIP11 anchors IFT20 to the Golgi complex. PLoS. Genet. 4, e1000315. doi:10.1371/journal.pgen.1000315

Gerdes, J.M., Davis, E.E., and Katsanis, N. (2009) The vertebrate primary cilium in development, homeostasis, and disease. Cell **137**, 32-45

Ghossoub, R., Molla-Herman, A., Bastin, P., and Benmerah, A. (2011) The ciliary pocket: a once-forgotten membrane domain at the base of cilia. Biol. Cell **103**, 131-144

Gilula, N.B. and Satir, P. (1972) The ciliary necklace. A ciliary membrane specialization. J. Cell Biol. **53**, 494-509

Goetz, S.C. and Anderson, K.V. (2010) The primary cilium: a signalling centre during vertebrate development. Nat. Rev. Genet. **11**, 331-344

Greiner, J.V., Weidman, T.A., Bodley, H.D., and Greiner, C.A. (1981) Ciliogenesis in photoreceptor cells of the retina. Exp. Eye Res. **33**, 433-446

Hames, R.S., Crookes, R.E., Straatman, K.R., Merdes, A., Hayes, M.J., Faragher, A.J., and Fry, A.M. (2005) Dynamic recruitment of Nek2 kinase to the centrosome involves microtubules, PCM-1, and localized proteasomal degradation. Mol. Biol. Cell **16**, 1711-1724

Insinna, C., Pathak, N., Perkins, B., Drummond, I., and Besharse, J.C. (2008) The homodimeric kinesin, Kif17, is essential for vertebrate photoreceptor sensory outer segment development. Dev. Biol. **316**, 160-170

Insinna, C. and Besharse, J.C. (2008) Intraflagellar transport and the sensory outer segment of vertebrate photoreceptors. Dev. Dyn. **237**, 1982-1992

Insinna, C., Humby, M., Sedmak, T., Wolfrum, U., and Besharse, J.C. (2009) Different roles for KIF17 and kinesin II in photoreceptor development and maintenance. Dev. Dyn. **238**, 2211-2222

Jekely, G. and Arendt, D. (2006) Evolution of intraflagellar transport from coated vesicles and autogenous origin of the eukaryotic cilium. Bioessays **28**, 191-198

Keady, B.T., Le, Y.Z., and Pazour, G.J. (2011) IFT20 is required for opsin trafficking and photoreceptor outer segment development. Mol. Biol. Cell. (Epub ahead of print)

Kim, J.C., Badano, J.L., Sibold, S., Esmail, M.A., Hill, J., Hoskins, B.E., Leitch, C.C., Venner, K., Ansley, S.J., Ross, A.J., Leroux, M.R., Katsanis, N., and Beales, P.L. (2004) The Bardet-Biedl protein BBS4 targets cargo to the pericentriolar region and is required for microtubule anchoring and cell cycle progression. Nat. Genet. **36**, 462-470

Kim, J., Krishnaswami, S.R., and Gleeson, J.G. (2008) CEP290 interacts with the centriolar satellite component PCM-1 and is required for Rab8 localization to the primary cilium. Hum. Mol. Genet. **17**, 3796-3805

Kim, J., Lee, J.E., Heynen-Genel, S., Suyama, E., Ono, K., Lee, K., Ideker, T., za-Blanc, P., and Gleeson, J.G. (2010) Functional genomic screen for modulators of ciliogenesis and cilium length. Nature **464**, 1048-1051

Krock, B.L. and Perkins, B.D. (2008) The intraflagellar transport protein IFT57 is required for cilia maintenance and regulates IFT-particle-kinesin-II dissociation in vertebrate photoreceptors. J. Cell Sci. **121**, 1907-1915

Krock, B.L., Mills-Henry, I., and Perkins, B.D. (2009) Retrograde intraflagellar transport by cytoplasmic dynein-2 is required for outer segment extension in vertebrate photoreceptors but not arrestin translocation. Invest Ophthalmol. Vis. Sci. **50**, 5463-5471

Kubo, A., Sasaki, H., Yuba-Kubo, A., Tsukita, S., and Shiina, N. (1999) Centriolar satellites: molecular characterization, ATP-dependent movement toward centrioles and possible involvement in ciliogenesis. J. Cell Biol. **147**, 969-980

Kubo, A. and Tsukita, S. (2003) Non-membranous granular organelle consisting of PCM-1: subcellular distribution and cell-cycle-dependent assembly/disassembly. J. Cell Sci. **116**, 919-928

Laoukili, J., Perret, E., Middendorp, S., Houcine, O., Guennou, C., Marano, F., Bornens, M., and Tournier, F. (2000) Differential expression and cellular distribution of centrin isoforms during human ciliated cell differentiation in vitro. J. Cell Sci. **113** (Pt 8), 1355-1364

LaVail, M.M. (1973) Kinetics of rod outer segment renewal in the developing mouse retina. J. Cell Biol. **58**, 650-661

Livesey, F.J. and Cepko, C.L. (2001) Vertebrate neural cell-fate determination: lessons from the retina. Nat. Rev. Neurosci. **2**, 109-118

Liu, Q., Tan, G., Levenkova, N., Li, T., Pugh, E.N., Jr., Rux, J.J., Speicher, D.W., and Pierce, E.A. (2007) The proteome of the mouse photoreceptor sensory cilium complex. Mol. Cell Proteomics. **6**, 1299-1317

Maerker, T., van Wijk, E., Overlack, N., Kersten, F.F., McGee, J., Goldmann, T., Sehn, E., Roepman, R., Walsh, E.J., Kremer, H., and Wolfrum, U. (2008) A novel Usher protein network at the periciliary reloading point between molecular transport machineries in vertebrate photoreceptor cells. Hum. Mol. Genet. **17**, 71-86

Molla-Herman, A., Ghossoub, R., Blisnick, T., Meunier, A., Serres, C., Silbermann, F., Emmerson, C., Romeo, K., Bourdoncle, P., Schmitt, A., Saunier, S., Spassky, N., Bastin, P., and Benmerah, A. (2010) The ciliary pocket: an endocytic membrane domain at the base of primary and motile cilia. J. Cell Sci. **123**, 1785-1795

Moser, J.J., Fritzler, M.J., and Rattner, J.B. (2009) Primary ciliogenesis defects are associated with human astrocytoma/glioblastoma cells. BMC. Cancer **9**, 448

Murcia, N.S., Richards, W.G., Yoder, B.K., Mucenski, M.L., Dunlap, J.R., and Woychik, R.P. (2000) The Oak Ridge Polycystic Kidney (orpk) disease gene is required for left-right axis determination. Development **127**, 2347-2355

Nachury, M.V., Loktev, A.V., Zhang, Q., Westlake, C.J., Peranen, J., Merdes, A., Slusarski, D.C., Scheller, R.H., Bazan, J.F., Sheffield, V.C., and Jackson, P.K. (2007) A core complex of BBS proteins cooperates with the GTPase Rab8 to promote ciliary membrane biogenesis. Cell **129**, 1201-1213

Nir, I., Cohen, D., and Papermaster, D.S. (1984). Immunocytochemical localization of opsin in the cell membrane of developing rat retinal photoreceptors. J. Cell Biol. **98**, 1788-1795

Omori, Y., Zhao, C., Saras, A., Mukhopadhyay, S., Kim, W., Furukawa, T., Sengupta, P., Veraksa, A., and Malicki, J. (2008) Elipsa is an early determinant of ciliogenesis that links the IFT particle to membrane-associated small GTPase Rab8. Nat. Cell Biol. **10**, 437-444

Pazour, G.J., Baker, S.A., Deane, J.A., Cole, D.G., Dickert, B.L., Rosenbaum, J.L., Witman, G.B., and Besharse, J.C. (2002) The intraflagellar transport protein, IFT88, is essential for vertebrate photoreceptor assembly and maintenance. J. Cell Biol. **157**, 103-113

Pazour, G.J. and Bloodgood, R.A. (2008) Targeting proteins to the ciliary membrane. Curr. Top. Dev. Biol. **85**, 115-149

Pedersen, L.B. and Rosenbaum, J.L. (2008) Intraflagellar transport (IFT) role in ciliary assembly, resorption and signalling. Curr. Top. Dev. Biol. **85**, 23-61

Pedersen, L.B., Veland, I.R., Schroder, J.M., and Christensen, S.T. (2008) Assembly of primary cilia. Dev. Dyn. **237**, 1993-2006

Pigino, G., Geimer, S., Lanzavecchia, S., Paccagnini, E., Cantele, F., Diener, D.R., Rosenbaum, J.L., and Lupetti, P. (2009) Electron-tomographic analysis of intraflagellar transport particle trains in situ. J. Cell Biol. **187**, 135-148

Rattner, J.B., Sciore, P., Ou, Y., van der Hoorn, F.A., and Lo, I.K. (2010) Primary cilia in fibroblast-like type B synoviocytes lie within a cilium pit: a site of endocytosis. Histol. Histopathol. **25**, 865-875

Roepman, R. and Wolfrum, U. (2007) Protein networks and complexes in photoreceptor cilia. In Subcellular Proteomics - From Cell Deconstruction to System Reconstruction (Faupel, M. and Bertrand, E. eds.), pp. 209-235, Springer, Dordrecht, The Netherlands

Rohatgi, R. and Snell, W.J. (2010) The ciliary membrane. Curr. Opin. Cell Biol. **22**, 541-546

Rosenbaum, J.L. and Witman, G.B. (2002) Intraflagellar transport. Nat. Rev. Mol. Cell Biol. **3**, 813-825

Sedmak, T. and Wolfrum, U. (2010) Intraflagellar transport molecules in ciliary and nonciliary cells of the retina. J. Cell Biol. **189**, 171-186

Sedmak, T., Sehn E., Wolfrum U. (2009) Immunoelectron microscopy of vesicle transport to the primary cilium of photoreceptor cells. In Methods in Cell Biology: Primary cilia (Vol. 94) (Sloboda, R.D. ed.), pp. 259-272, Academic Press, Elsivier Inc.

Sung, C.H. and Chuang, J.Z. (2010) The cell biology of vision. J. Cell Biol. **190**, 953-963

Sorokin, S. (1962) Centrioles and the formation of rudimentary cilia by fibroblasts and smooth muscle cells. J. Cell Biol. **15**, 363-377

Sorokin, S.P. (1968) Reconstructions of centriole formation and ciliogenesis in mammalian lungs. J. Cell Sci. **3**, 207-230

Sukumaran, S. and Perkins, B.D. (2009) Early defects in photoreceptor outer segment morphogenesis in zebrafish ift57, ift88 and ift172 Intraflagellar Transport mutants. Vision Res. **49**, 479-489

tom Dick, S. and Brandstatter, J.H. (2006) Ribbon synapses of the retina. Cell Tissue Res. **326**, 339-346

Trojan, P., Krauss, N., Choe, H.W., Giessl, A., Pulvermuller, A., and Wolfrum, U. (2008) Centrins in retinal photoreceptor cells: Regulators in the connecting cilium. Prog. Retin. Eye Res. **27**, 237-259

Tokuyasu, K. and Yamada, E. (1959) The fine structure of the retina studied with the electron microscope. IV. Morphogenesis of outer segments of retinal rods. J. Biophys. Biochem. Cytol. **6**, 225-230

Tsujikawa, M. and Malicki, J. (2004) Intraflagellar transport genes are essential for differentiation and survival of vertebrate sensory neurons. Neuron **42**, 703-716

Wolfrum, U. (1991) Tropomyosin is co-localized with the actin filaments of the scolopale in insect sensilla. Cell Tissue Res. **265**, 11-17

Yang, J., Liu, X., Zhao, Y., Adamian, M., Pawlyk, B., Sun, X., McMillan, D.R., Liberman, M.C., and Li, T. (2010) Ablation of whirlin long isoform disrupts the USH2 protein complex and causes vision and hearing loss. PLoS. Genet. 6, e1000955

Figure legends
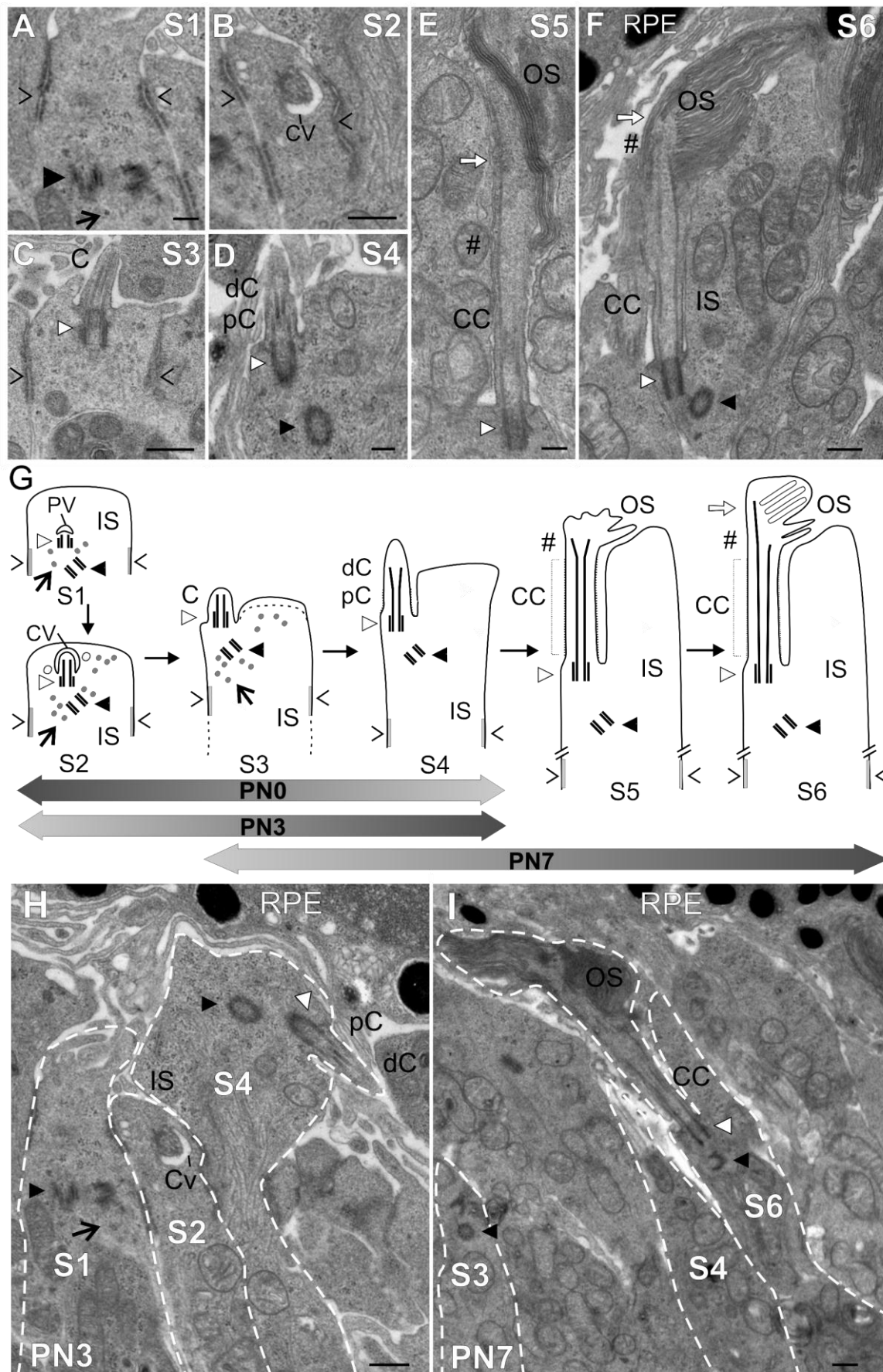
Fig. 1: Different stages of photoreceptor cell ciliogenesis. (A–F) Electron micrographs of different stages of photoreceptor cell ciliogenesis in postnatal day 0 (PN 0), PN3, PN7 mouse retinas schematically illustrated in **(G)**. S1: the mother centriole (*white arrow head*), the daughter centriole (*black arrow head*) and electron dense centriolar satellites (*black arrow*) are present in the cytoplasm of differentiating photoreceptors. The distal end of mother centriole is enclosed by the primary vesicle (PV). S2: ciliary bud elongates to the ciliary shaft and mother centriole matures to the basal body. S3: the flattened PV is enlarged by repeated fusion of post-Golgi vesicles forming the ciliary vesicle (CV). CV fuses with the plasma membrane of the inner segment (IS), and the newly assembling cilium (C) appears on the cell surface. S4: the elongating cilium is divided into the proximal (pC), characterized by periodic bead-like densities in the plasma membrane distal cilium (dC) which are absent in the distal cilium (dC). S5: pC becomes the connecting cilium (CC), the dC forms the outer segment (OS). S6: axoneme (*white arrowhead*) prolongs into the OS in which first stacks of membrane disks appear. Grey circles indicated by *black arrow* represent electron dense granules of centriolar satellites. In S3 the *dotted line* indicates elongation and morphological remodeling of apical IS during development. "> <" indicate adherent junctions at the outer limiting membrane. **(H, I)** Electron micrographs demonstrating the non-synchronized photoreceptor cell ciliogenesis in PN3, PN7 mouse retinas indicated by *arrowbars* in **G**. Defined stages of ciliogenesis are encircled by *dashed lines*. RPE, retinal pigment epithelium.
Scale bars: (A, B, D, E, H) 200 nm; (C, F, I) 400 nm.
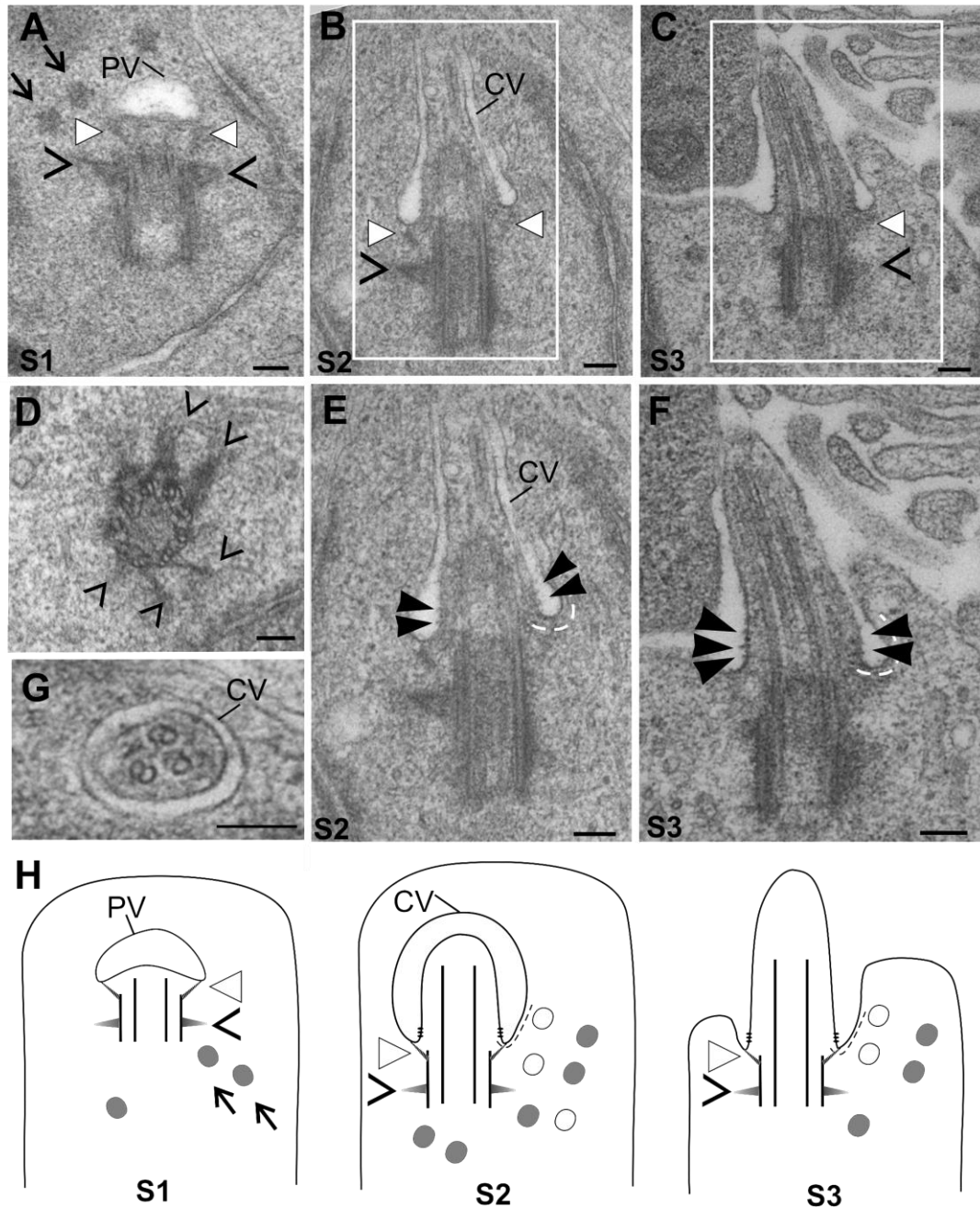
Fig. 2: Structural features of early photoreceptor cell ciliogenesis. (A-G) Electron micrograph of the differentiating centriolar appendages and satellites schematically illustrated in (**H**). (**E, F**) Higher magnification of (**B, C**): periodic bead-like densities of the plasma membrane (*black arrow heads*) characteristic for the transition zone appear at the proximal cilium and ciliary pocket (*dashed line*) in S2 and S3. In S1-S2 distal (*white arrowhead*) and sub-distal (*black open arrow head*) accessory appendages are present before the cilium appears at the cell surface in S3. Centriolar satellites (*arrow*) are organized near the basal body (*white arrowhead*). (**D**) Cross-section through the basal body and sub-distal appendages (*black open arrow head*). (**G**) Cross-section through the axoneme of elongating ciliary shaft enclosed by the membrane of ciliary vesicle (CV). PV, primary ciliary vesicle; *arrow*, centriolar satellites. Scale bars: 100 nm.
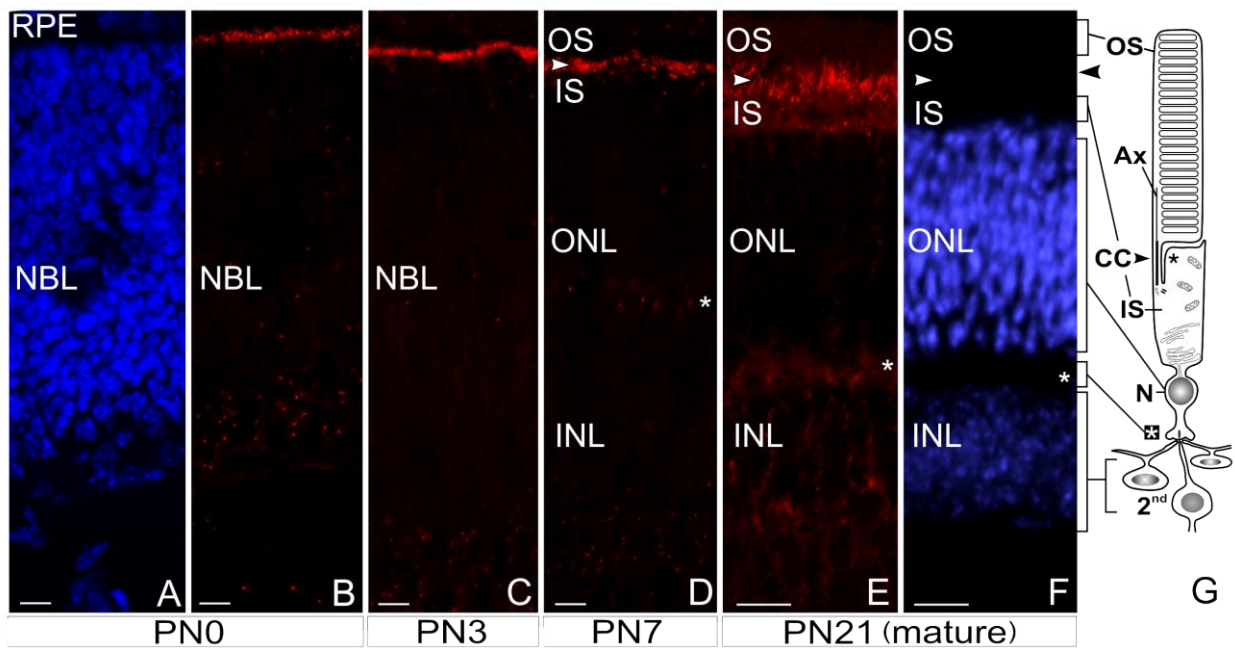
Fig. 3: IFT57 expression in the developing mouse retina. (A, F) DAPI staining of the nuclear DNA in PN0 and PN21 mouse retina, respectively. **(B-E)** Indirect immunofluorescence of antibodies against IFT57 at PN0, PN3, PN7 and PN21 (mature) retinas. At PN0 and PN3 IFT57 is detected as a dotted pattern in the apical region of the neuroblastic layer (NBL). At PN7 and PN21 retinas IFT57 is localized in the region between the photoreceptor cell outer segment (OS) and the inner segment (IS), where the connecting cilium (C, *arrowhead*) is present. In addition scattered dots are stained in the proximal region of the NBL in PN0 and PN3 retinas and in the outer plexiform layer (OPL, *white asterisk*) of PN7 and mature retinas, where the synapse between the photoreceptor cells and secondary neurons (2nd) are present. **(G)** Schema of a rod photoreceptor cell and its connection to 2nd. RPE, retinal pigment epithelium; *black asterisk,* apical IS; N, photoreceptor nuclei in the outer nuclear layer (ONL). Scale bars: 10 μm.
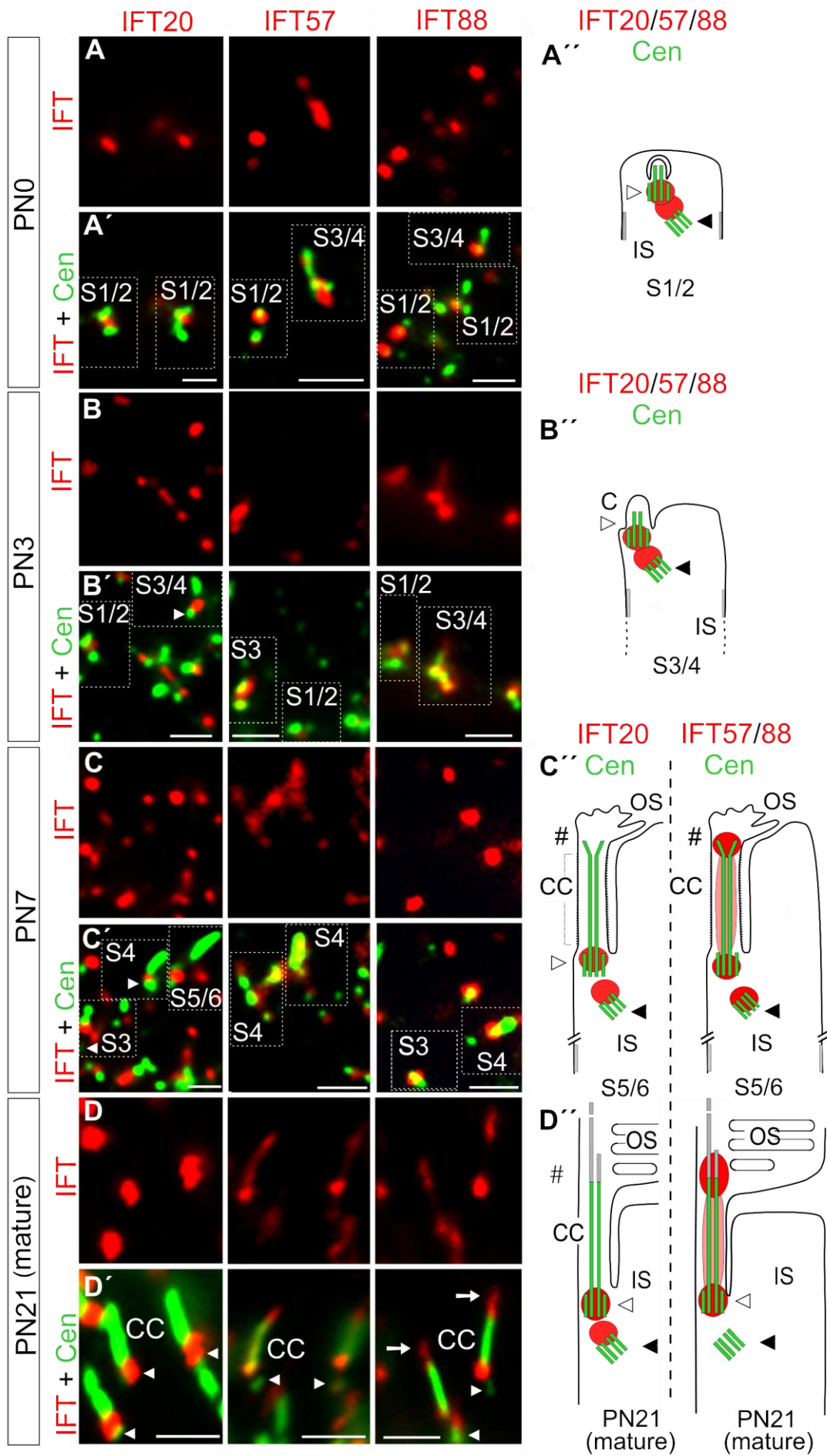
Fig. 4: Localization of IFT20, IFT57 and IFT88 during ciliogenesis in retinal photoreceptor cells. (A-D) Images of indirect immunofluorescence labeling with antibodies to IFT proteins (red) in cryosections through developing PN0, PN3, PN7 and mature (PN21) mouse retinas. **(A´-D´)** Merged images of double immunofluorescence of anti-IFT (red) and anti-centrin antibodies. Cen is applied as a marker for the connecting cilia, the basal body and the adjacent centriole (*white arrow head*). (A´´-D´´) of ciliary localization of IFT proteins (red) in relation to Cen (green) during ciliogenesis. The photoreceptor cell ciliogenesis is not synchronized. Different stages of ciliogenesis (S1-S6) are present in parallel in PN0, PN3 and PN7 mouse retinas. In stages S1 to S4 of ciliogenesis double labeling reveals identical staining pattern of all IFT proteins partially co-localizing with Cen at the basal body and adjacent centriole. In S5, S6 (S5/6) and in the mature cilium IFT proteins are differentially located: All three IFT proteins associate with the basal body at the base of the connecting cilium (CC). IFT20 is additionally found at the adjacent centriole (*arrowhead*), but is not detectable in the CC. The labeling of IFT88 extends into the axoneme (*white arrow*). Scale bars: (A´-C´) 0.125 µm; (D´) 0.5 µm.
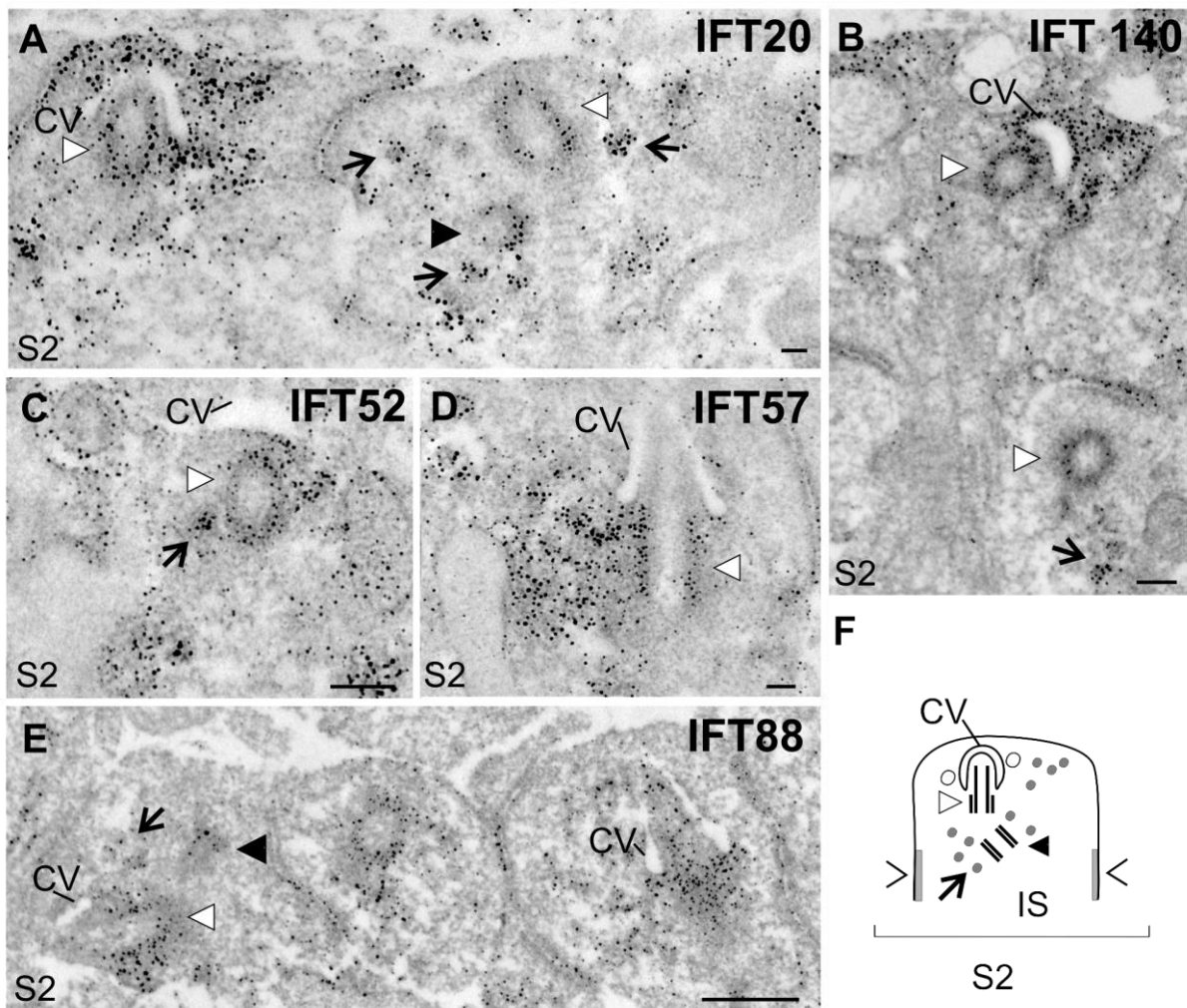
Fig. 5: IFT proteins associated with ciliary structures and in the cytoplasm at stage S2 of photoreceptor cell ciliogenesis. (A-E) Electron micrographs of anti-IFT20, IFT52, IFT57, IFT88 and IFT140 immunolabeling showing parts of differentiating mouse photoreceptor cells. In stage S2 of ciliogenesis, IFT20, IFT52, IFT57, IFT88, IFT140 are localized at the mother centrioles (*white arrow head*) of forming photoreceptor cilia and in the cytoplasm, where they are associated with centriolar satellites (electron dense granules; *black arrow* and *grey circles* in schema F). **(A, B)** In addition to their localization at the mother centriole IFT20 and IFT140 are concentrated around the ciliary vesicle (CV) and in the inner segment (IS) cytoplasm. **(F)** Schema of a photoreceptor cell in stage S2 of ciliogenesis. Scale bars: (A, B, D) 100 nm; (C) 200 nm; (E) 400 nm.
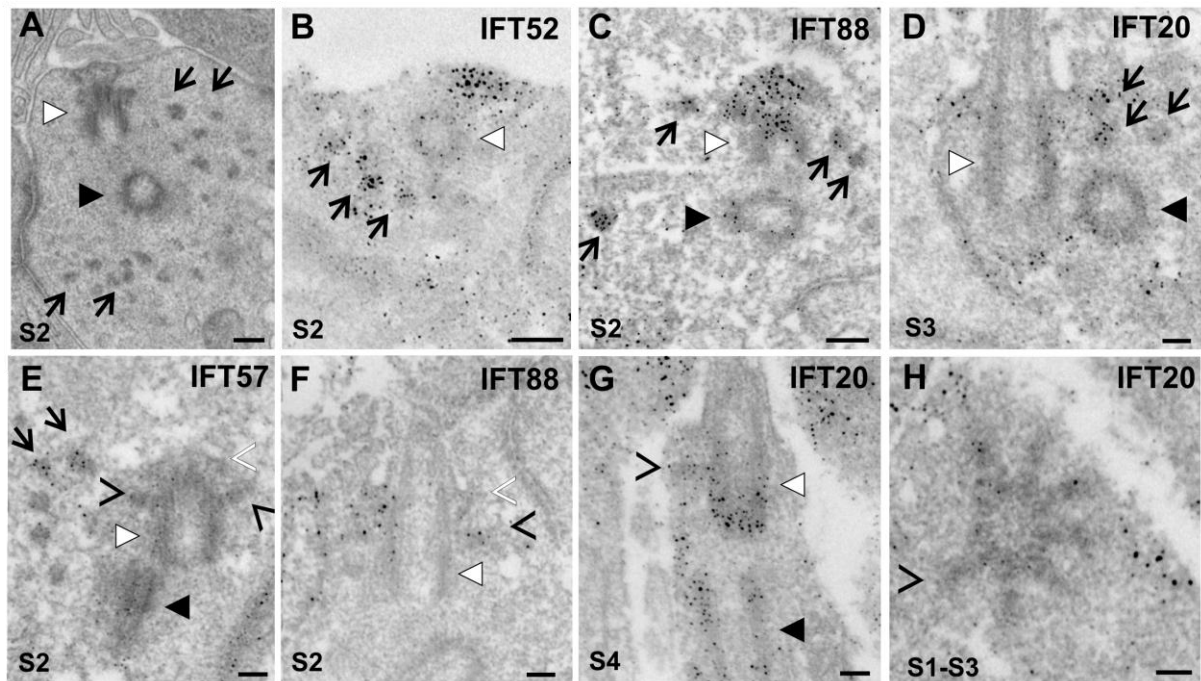
Fig. 6: Association of IFT proteins with centriolar satellites and appendages during early ciliogenesis. (A, E) Conventional electron micrograph of the basal body region during early ciliogenesis in stage S2. **(B-C, E, F, H)** Immunoelectron labeling of IFT20, IFT52, IFT57, and IFT88 of early stages of photoreceptor ciliogenesis. **(D-H)** In stage S2 centriolar satellites (*black arrows*) accumulate around the basal body (*white arrow head*) and the adjacent centriole (*black arrow head*), but in S3 **(D)** the number of centriolar satellites is reduced; and they move more apically, to the apical inner segment (*asterisk*). IFT20, IFT57, and IFT88 proteins are localized at the distal- and sub-distal appendages. Scale bars: (A-C) 200 nm; (D-H) 100 nm.
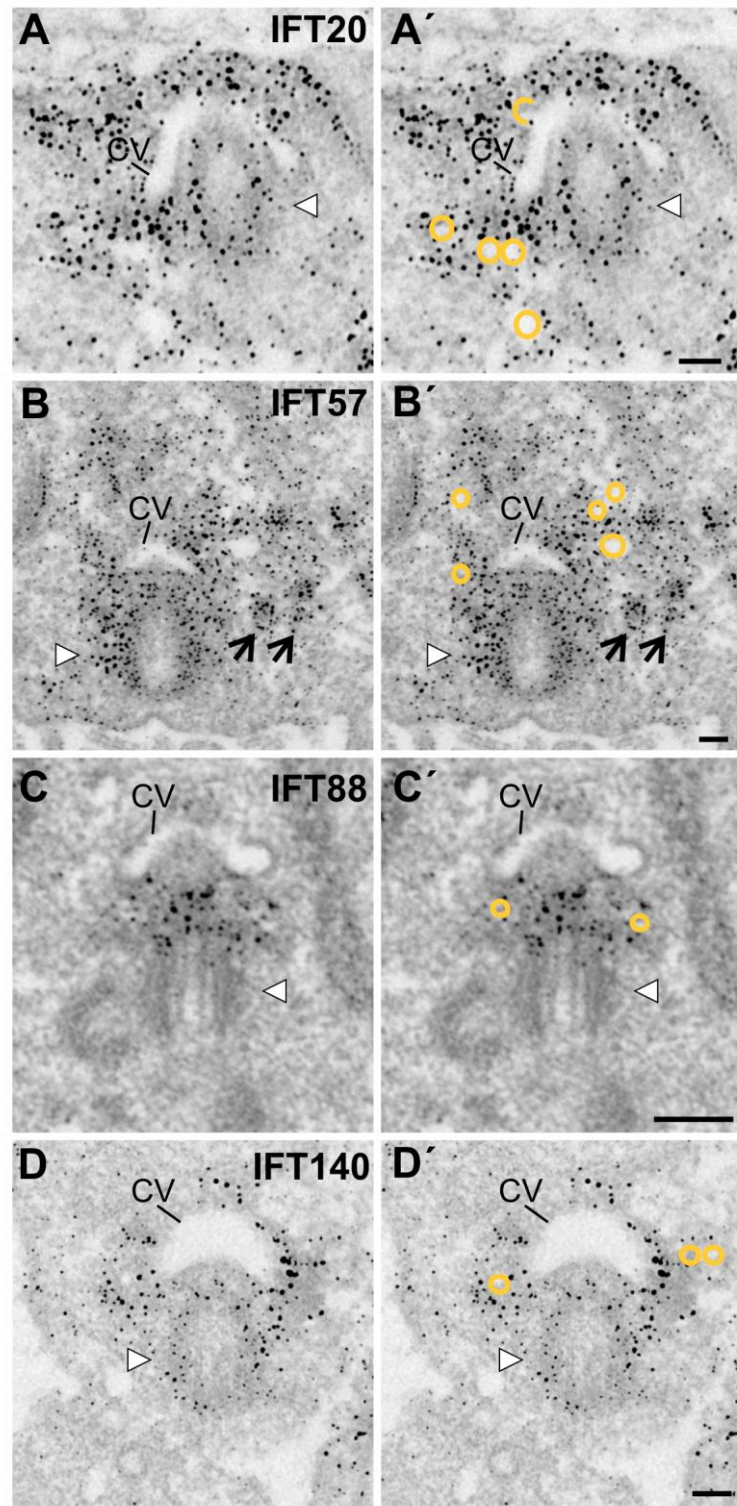
Fig. 7: Association of IFT proteins with the ciliary vesicle and post-Golgi vesicles in early ciliogenesis stages of mouse photoreceptor cells. (A-D) Immunoelectron microscopic labeling of IFT proteins at the ciliary vesicle (CV), the basal body (*white arrow head*) and post-Golgi vesicles indicated by *orange circles* in **A´-D´**. IFT 57 is additionally detected in centriolar satellites (*black arrows*). Scale bars: (A´, B´, D´) 100 nm; (C´) 200 nm.
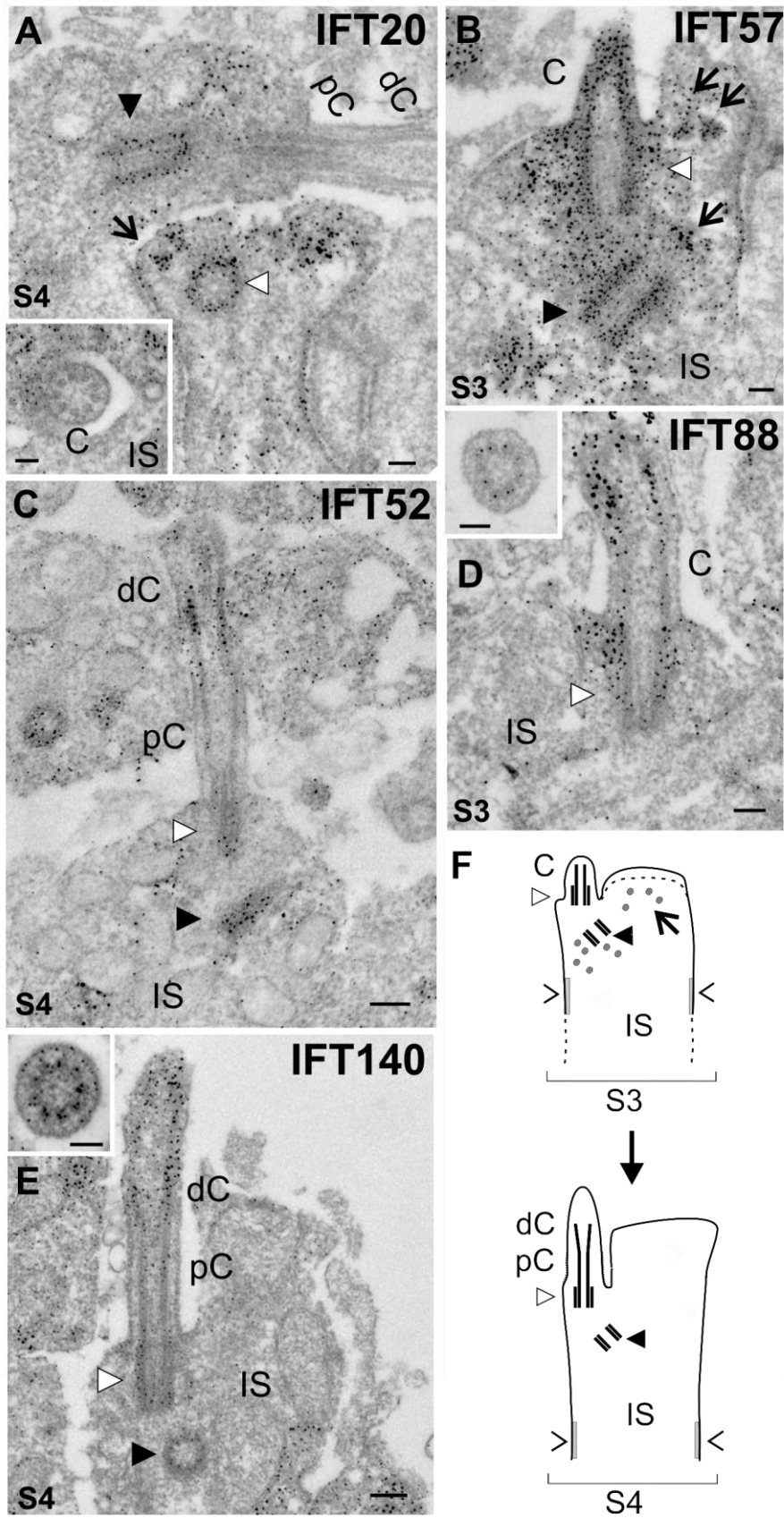
Fig. 8: Immunoelectron microscopic localization of IFT proteins in stage S3 and S4 of photoreceptor cell ciliogenesis. (A-E) Immunoelectron labeling of IFT20, IFT52, IFT57, IFT88 and IFT140 in longitudinal and ciliary cross sections of differentiating mouse photoreceptor cells. **(F)** Schema of stages S3 and S4 of photoreceptor cell ciliogenesis. In S3 the photoreceptor inner segment (IS) extends and its protrusion, the apical IS, grows (*dotted line*), in S4 the elongating cilium (C) can be divided into in a proximal (pC) and a distal cilium (dC) portion. **(A-E)** Antibodies to all IFT proteins are detected the basal body (*white arrow head*) and the adjacent centriole (*black arrow head*). IFT20, IFT52 and IFT57 are labeled in the apical inner segment (IS) .IFT20 and IFT57 are detected at centriolar satellites (*black arrow* and *grey circles* in E). In contrast to IFT20 all other IFT proteins are found in C. IFT52 and IFT57 are also associated with the cytoplasm in the periphery of the basal body. IFT88 and IFT140 are additionally detected in the elongating ciliary shaft of the dC. Scale bars: (A, B, D and insets) 100 nm; (C, F) 200 nm.
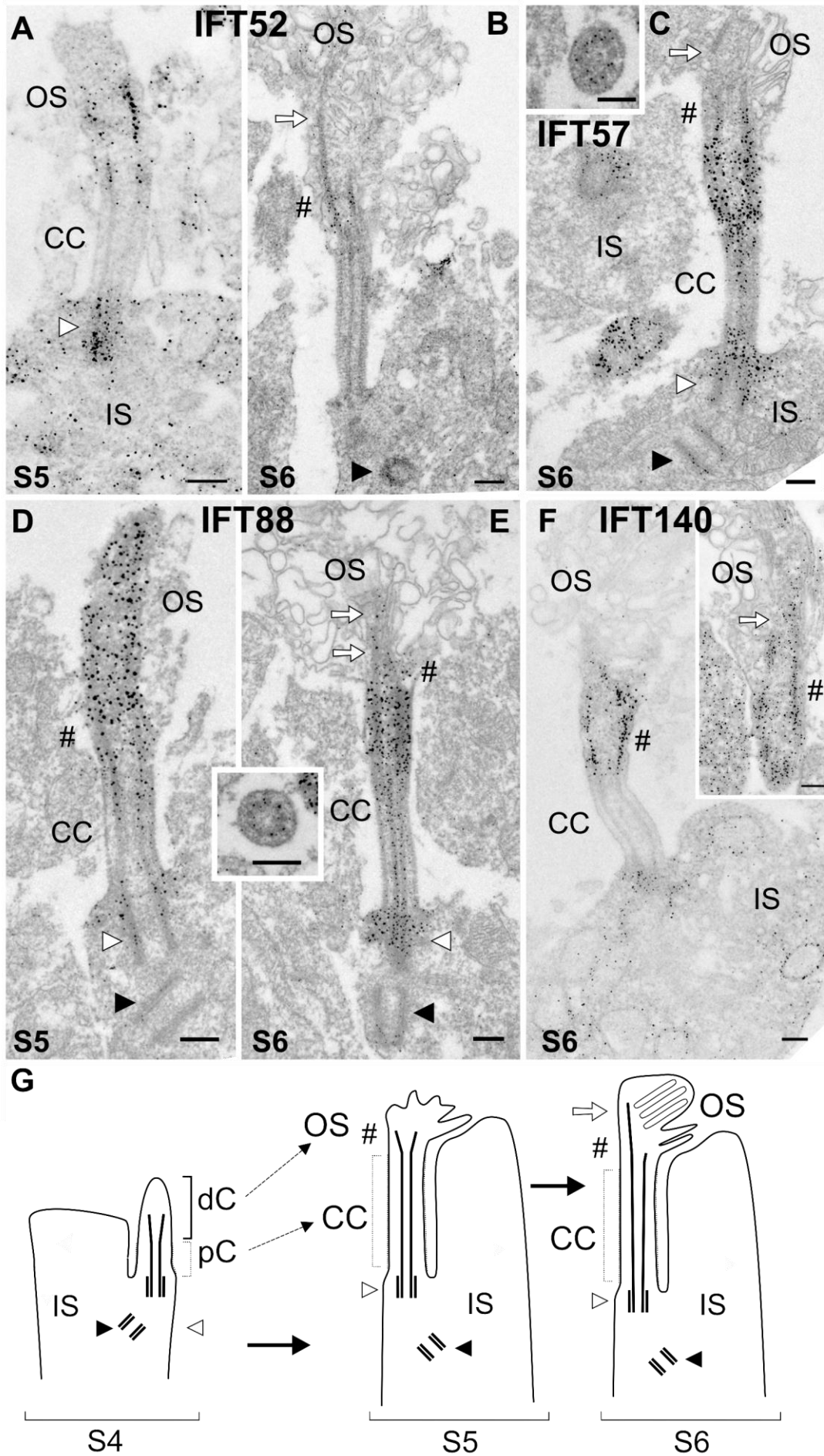
Fig. 9: Localization of IFT proteins in the basal part of the outer segment and at the basal body during late ciliogenesis of photoreceptor cells. (A-F) Immunoelectron microscopy of IFT52 **(A, B)**, IFT57 (**C**), IFT88 (**D**) and IFT140 (**F**) in differentiating photoreceptor cells. **(A-F)** In S5 and S6 IFT52 is associated with the basal body (*white arrow head*) and the distal part of the connecting cilium and present in the base (#) of the outer segment (OS). IFT57, IFT88 and IFT140 are located at the adjacent centriole (*black arrow head*), at the basal body (*white arrow head*), in the CC (cross-section) and at the OS base (#). IFT57 is not detected in the axoneme (*white arrow*). IFT88 and IFT140 labeling are present in the OS base (#) and extend further into the axoneme (*white arrows*). **(G)** Schema of ciliogenesis in stages S4-S6 of differentiating mouse photoreceptor cells. In stage S5 the proximal cilium (pC) becomes the connecting cilium (CC) and the distal cilium (dC) forms the outer segment (OS). Scale bars: 200 nm.
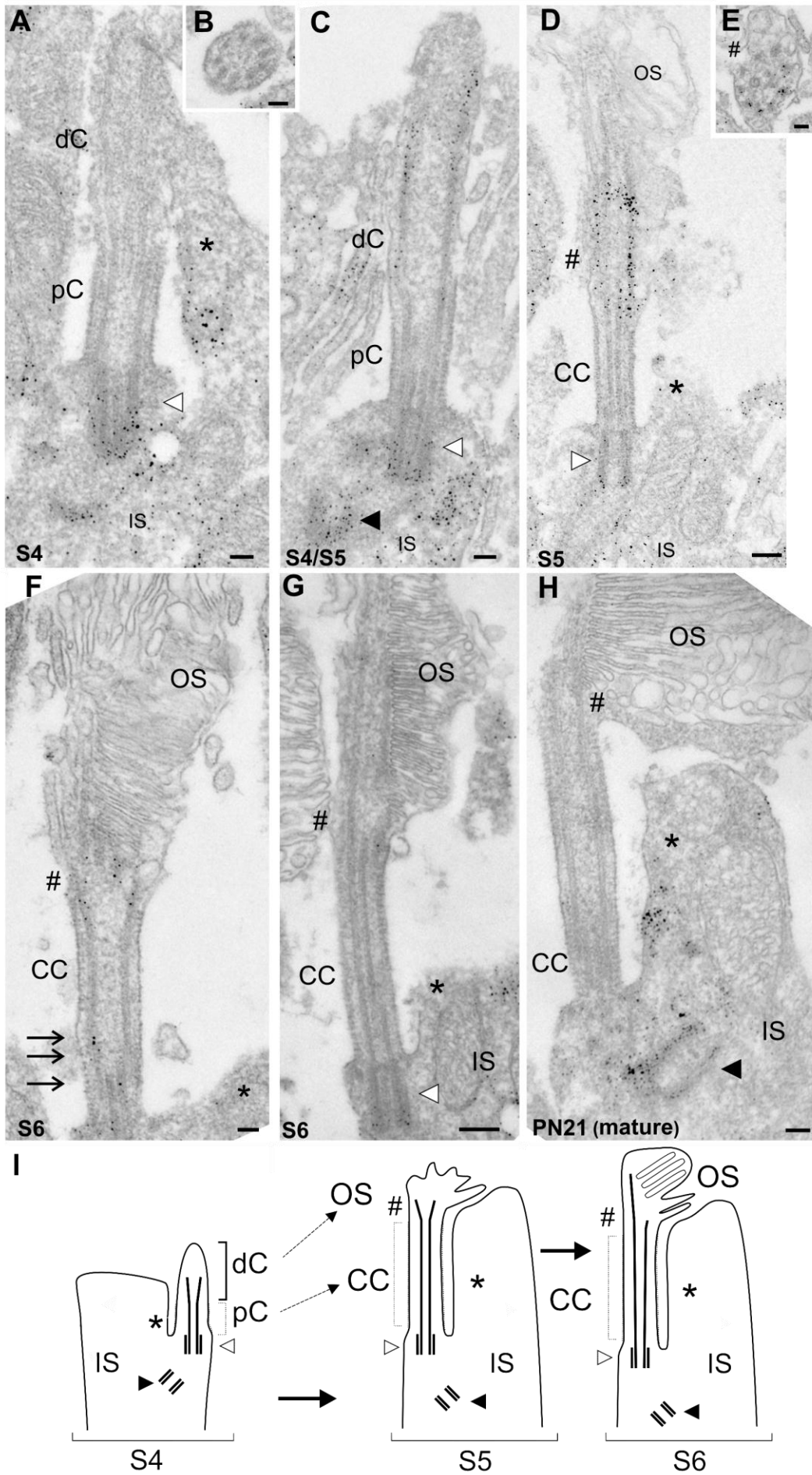
Fig. 10: Differential localization of IFT20 in the outgrowing cilium. (A-H) Immunoelectron localization of IFT20 in longitudinal and cross sections (**B, E**) through differencing mouse photoreceptor cells. (**I**) Schema of ciliogenesis in stages S4-S6 of differentiating mouse photoreceptor cells. In S4 IFT20 is restricted to the basal body (*white arrow head*), the adjacent centriole (*black arrow head*) and the apical inner segment (IS) (*asterisk*). It is absent from the proximal (pC) and distal cilium (dC). (**C**) Between stage S4 and S5 IFT20 is concentrated at the basal body (*white arrow head*) and the adjacent centriole (*black arrow head*) and in the elongating cilium IFT20 is detected at the dC. (**D, E**) In S5 IFT20 is detected at the BB and at the basal outer segment (OS) (#), but in the axoneme (*white arrow*). (**F, G**) During S6 the OS formation proceeds andIFT20 is sporadically detected in the connecting cilium (CC) (indicated by *arrows* in F) and the base of OS (#). In mature photoreceptors IFT20 is concentrated in the apical IS (*asterisk*) and adjacent centriole, but absent from the CC. Scale bars: (A-C, E, F) 100 nm; (D, G, H) 200 nm.
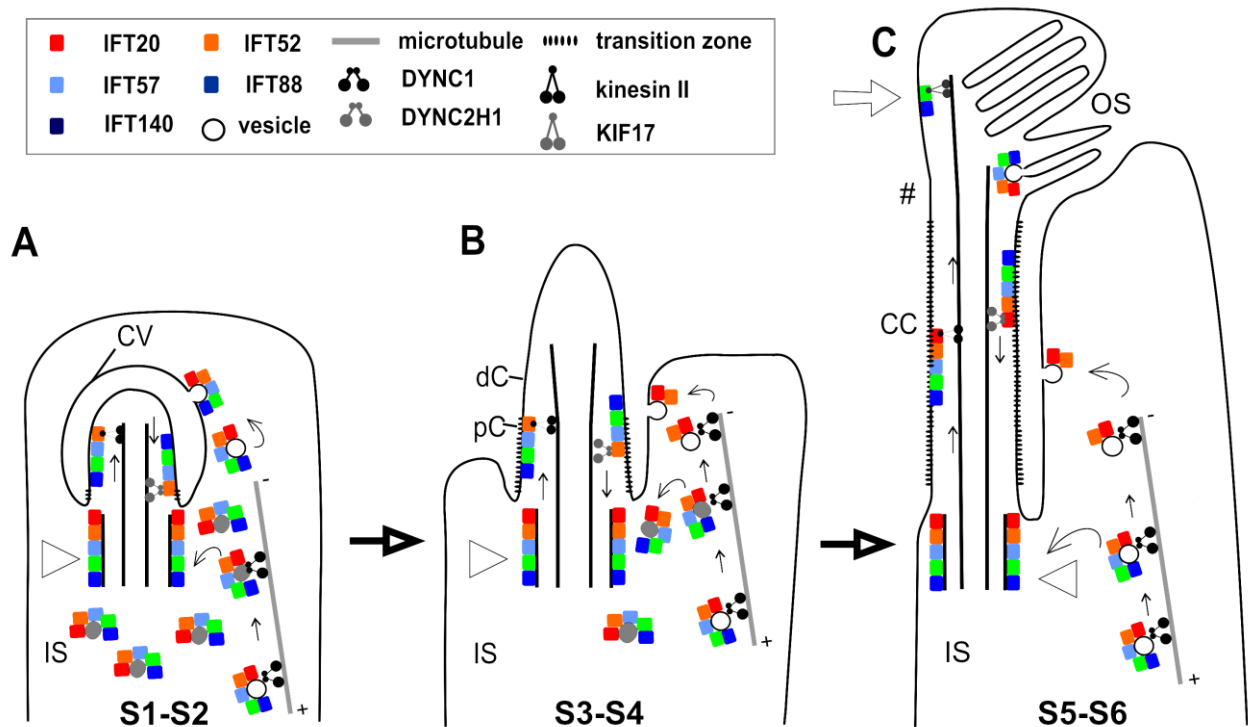
Fig. 11: Models of processes associated with IFT proteins during ciliogenesis in photoreceptor cells. The stages of ciliogenesis are characterized by different processes: **(A)** formation and expansion in S1-S2; **(B)** fusion of the ciliary vesicle with the apical plasma membrane (not shown), elongation of the ciliary bud and first IFT in the proximal cilium (pC) to the distal cilium (dC) in S3-S4; **(C)** outer segment (OS) formation and IFT through the connecting cilium and along axonemal microtubules (*white arrow*) in S5-S6. Present results further support the well-established participation of IFT proteins at the IFT processes in stages S3 to S6 of photoreceptor ciliogenesis. At the OS base (#), the majority of IFT proteins may dissociate from the cargo which is incorporated into OS disk membranes and used for the formation of photo-transductive OS disk membranes in stage S5 and S6. The temporary presence of IFT20 at the OS base (#) during the first stages of OS differentiation suggests that IFT20 may play a role at the initiation of the OS morphogenesis. Further apical in the OS, IFT particles containing IFT88 and IFT140 may participate at the transport processes along axonemal microtubules. However, during all stages the five investigated IFT proteins are associated with the mother centriole/basal body (*white arrow head*), centriolar satellites (*grey circles*) and vesicles in the cytoplasm of the differentiating inner segment (IS) alluding to functions of IFT proteins different from IFT. Conclusively, associations indicate putative participation of IFT proteins at the transport of centriolar satellites (*grey circles*) containing non-membranous ciliary components and post-Golgi vesicles to the basal body (S1-S6). In S1-S2 the special distribution of IFT proteins at the ciliary vesicle and the cytoplasmic vesicles suggests a possible role of IFT proteins in ciliary vesicle formation and extension.

Supplemental material

Intraflagellar transport proteins in ciliogenesis of photoreceptor cells

Sedmak T [1] and Wolfrum U

Department of Cell and Matrix Biology, Institute of Zoology, Johannes Gutenberg University Mainz, Germany
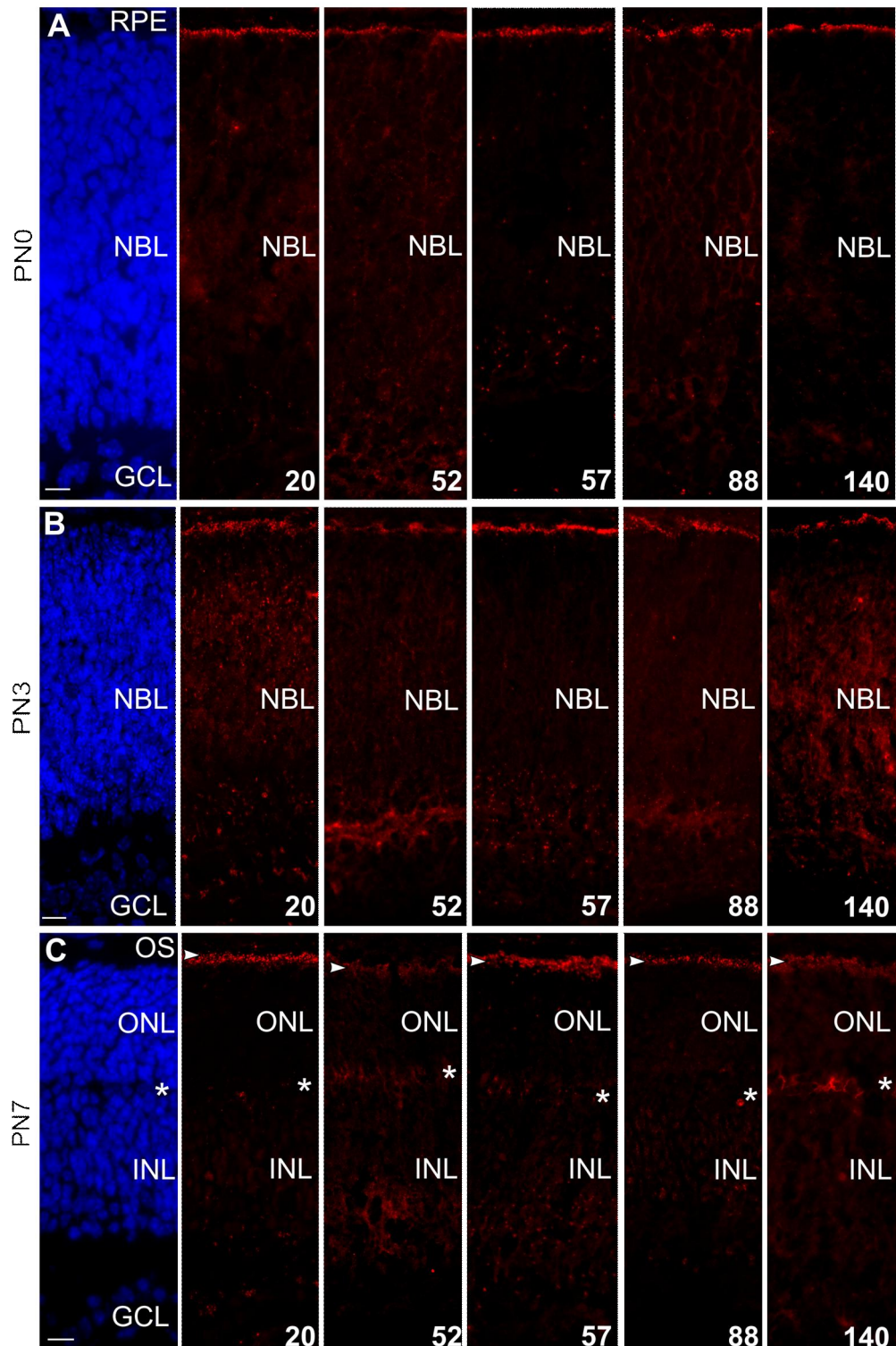
Fig. S1: Expression of IFT proteins in the developing mouse retina. (A-C) DAPI staining of nuclear DNA (left panel) and indirect immunofluorescence labeling of IFT20, IFT52, IFT57, IFT88 and IFT140 in cryosections through the developing retina of PN0, PN3, and PN7 mice. At PN0 and PN3 IFT proteins are mainly detected in the apical region of the neuroblastic layer (NBL). At PN7 IFT proteins are concentrated in the ciliary region (*arrowhead*) of photoreceptor cells. *White asterisk* indicates outer plexiform layer; inner nuclear layer, INL; OS, outer segment; RPE, retinal pigment epithelium; GCL, ganglion cell layer. Scale bars: 10 µm.

IFT52	IFT140	IFT52/140 Cen

PN0

A — IFT

A′ — IFT + Cen
S1/2 S1/2 S1/2 S3/4

A″
IS
S1/2

PN3

B — IFT

B′ — IFT + Cen
S1/2 S3/4 S1/2

B″
C
IS
S3/4

PN7

C — IFT

C′ — IFT + Cen
S3 S5/6 S3 S5/6

C″
OS
#
CC
IS
S5/6

PN21 (mature)

D — IFT

D′ — IFT + Cen
CC CC

D″
OS
IS
PN21
(mature)
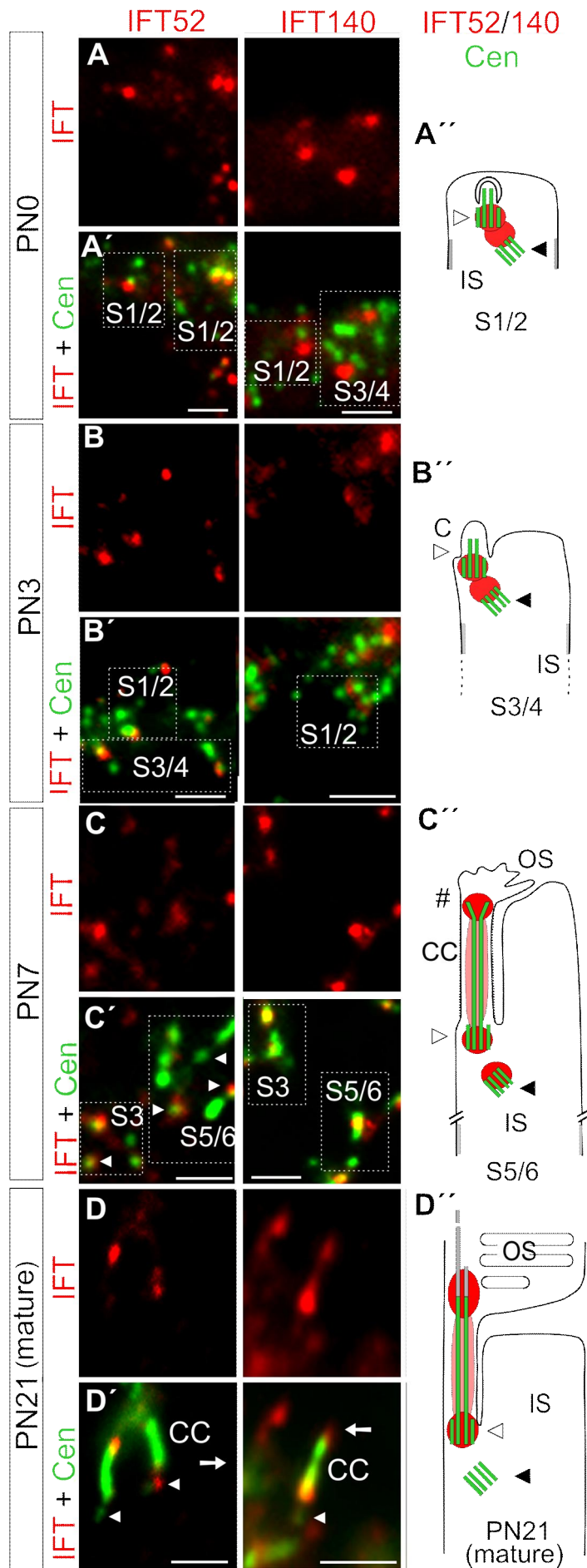
Fig. S2: Localization of IFT52 and IFT140 proteins during ciliogenesis in retinal photoreceptor cells. (A-D) Images of indirect immunofluorescence labeling with antibodies to IFT proteins (red) in cryosections through developing PN0, PN3, PN7 and mature (PN21) mouse retinas. **(A´-D´)** Merged images of double immunofluorescence of anti-IFT (red) and anti-centrin (Cen; green) antibodies. Cen is applied as a marker for connecting cilia, the basal body and adjacent centriole (*white arrow head*). (A´´-D´´) Schema of ciliary localization of IFT proteins (red) in relation to Cen (green) during ciliogenesis. Double immunofluorescence IFT proteins partially co-localize with Cen. IFT52 is detected at the centriole (*arrowhead*) and at the basal and apical part of the connecting cilium (CC). IFT140 labeling is concentrated at the basal and apical part of the CC and extends apically into the axoneme (*white arrow*). Scale bars: (A´-C´) 0.125 µm; (D´) 0.5 µm.
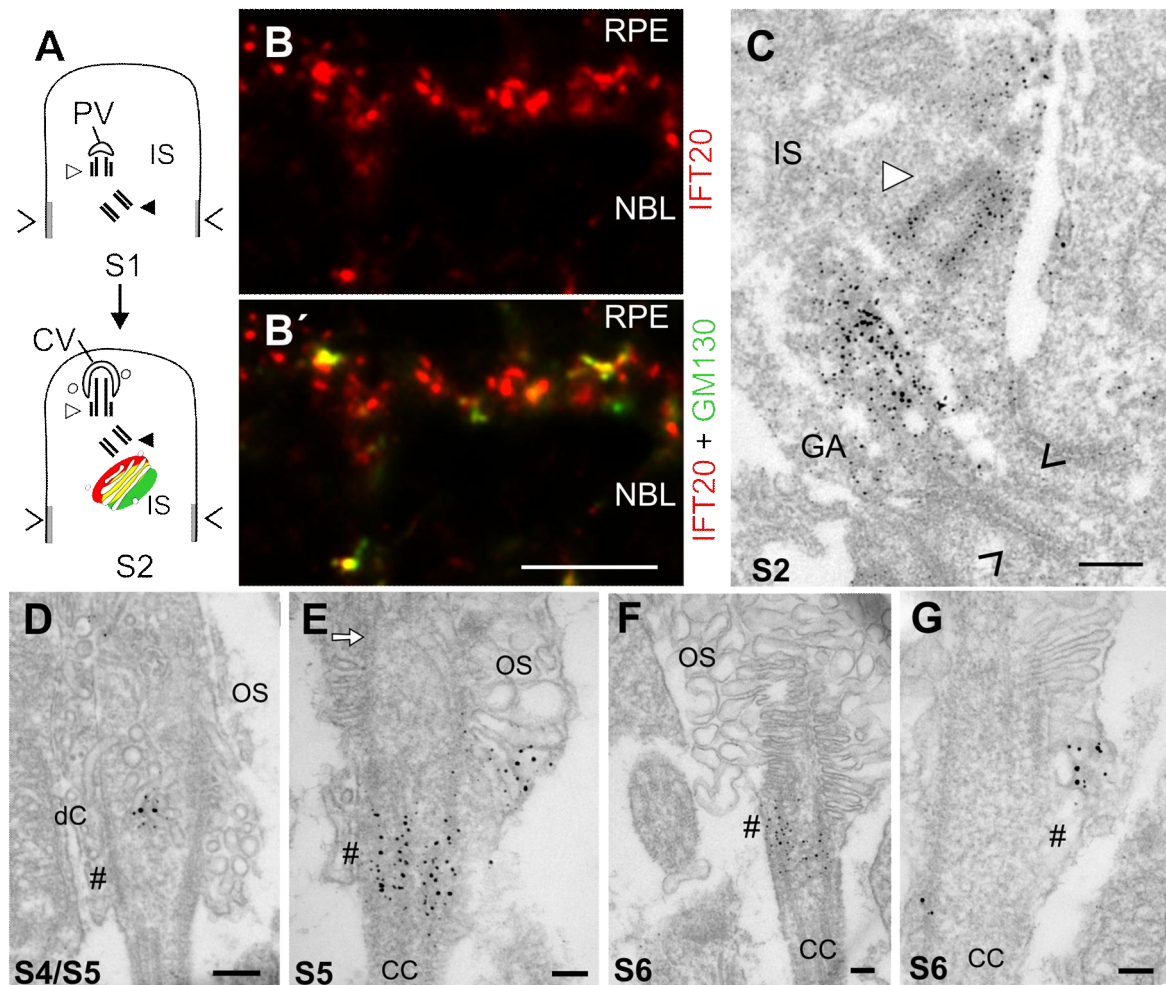
Fig. S3: Subcellular localization of IFT20 at the Golgi apparatus and in the cilium of the differentiating mouse photoreceptor cells. **(A-C)** Indirect immunofluorescence (B) by antibodies to IFT20 (red) and the Golgi matrix protein 130 (GM130; green) (merged in B´) and immunoelectron microscopic (C) labeling of IFT20 at with the Golgi apparatus (GA) illustrated in schematic representation (A). Double labeling of IFT20 and GM130 indicates partial co-localization in the apical part of the neuroblastic layer (NBL). Basal body is indicated by *white arrowhead* and adherent junctions by "> <". **(D-G)** Immunoelectron microscopic localization of IFT20 during late stages of photoreceptor cell ciliogenesis. In S4/S5 IFT20 is detected by a few particles in the distal connecting cilium (dC), whereas in S5 and S6 intense IFT20 labeling is observed at the base of the outer segment (#, OS). In S6 IFT20 is detected by a few particles in the connecting cilium (CC). In all stages IFT20 is absent from the axoneme (*white arrow*). RPE, retinal pigment epithelium. Scale bars: (B, B´) 5 µm; (C, D) 200 nm; (E-G) 100 nm.
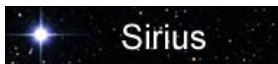
Sirius Biology of the Cell

Your submission is complete

Thank you for submitting to *Biology of the Cell*! You will be receiving an email soon to confirm this submission, and further instructions will be sent to you as needed.

We have received the following files:

Sedmak and Wolfrum_ IFTs in PRC ciliogenesis 17-03-11 Final.pdf
Sedmak and Wolfrum_ IFTs in PRC ciliogenesis 17-03-11 Supplemental material.pdf

Note: if any files are missing please contact the Editorial Office (editorial@biolcell.org).

Options:

- Submission home

- My submissions

3. Summarized results

In the present thesis the subcellular localization of individual IFT proteins was elucidated applying correlative microscopic techniques: indirect immunofluorescence, conventional electron microscopy and immunoelectron microscopy.

3.1 Immunoelectron microscopy of transport vesicles to the primary cilium of photoreceptor cells

For analyses of ciliary cargo vesicles and the distribution of ciliary molecules in subciliary compartments, as an alternative technique to conventional post-embedding, a modified protocol for pre-embedding labeling has been established in this study. The improved protocol is described in detail (Publication I) and represents the basis for the Publications II and III. An important advantage of this method is the mild pre-fixation which enables better preservation of the antigenicity of ciliary antigens and thereby increases the staining intensity (Fig. 3). Its application enabled us to decipher the differential localization of individual IFT proteins in vertebrate photoreceptor cilia. This method also conserves the membrane vesicles and therewith makes it possible to visualize vesicular structures associated with IFT proteins. These results do not only confirm the central function of IFT molecules in ciliary transport, but also strengthen their role in transport processes in the cytoplasm. Furthermore, we gathered evidence for different alternative transport routes of cargo vesicles directed to different target membranes.
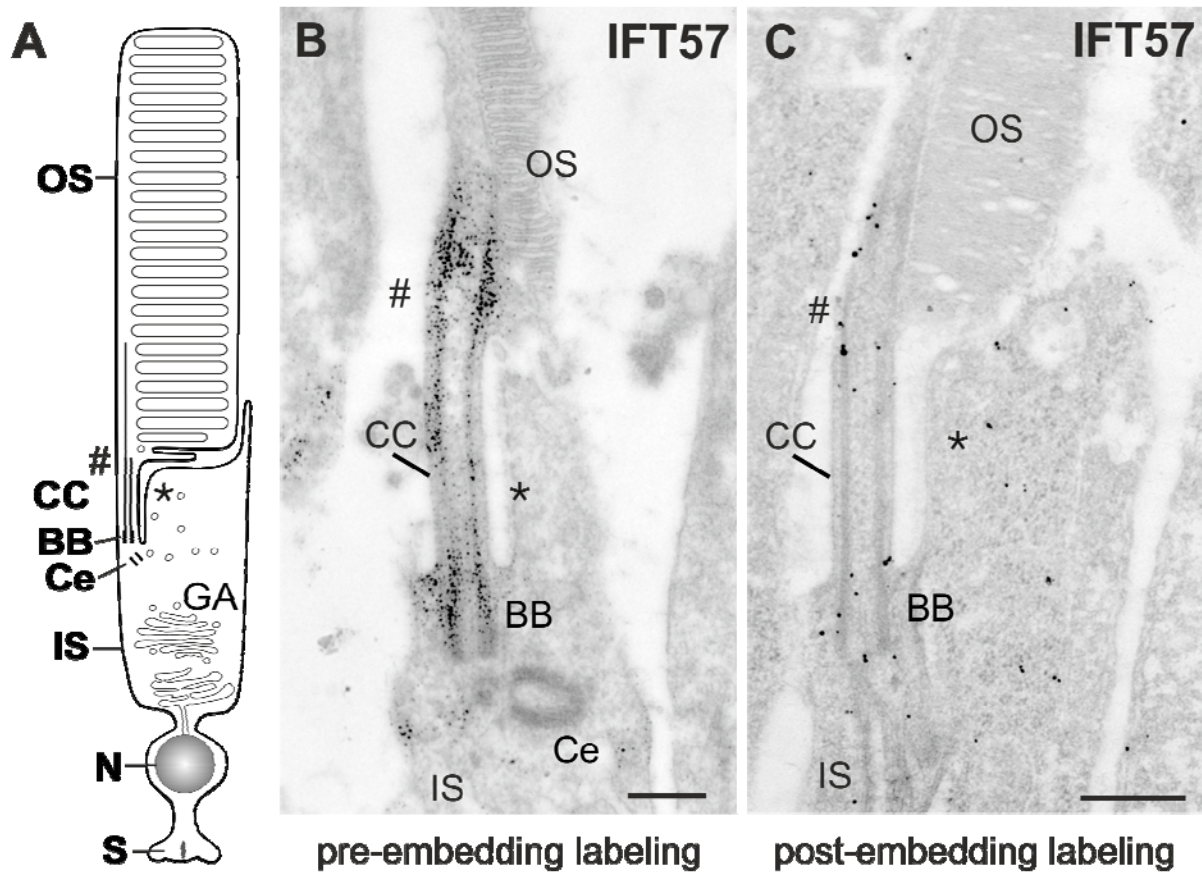
Fig. 3: Comparison of pre-embedding and post-embedding labeling for immunoelectron analyses of IFT57. **(A)** A scheme of the photoreceptor cell. The light sensitive outer segment (OS) is linked by the connecting cilium with a biosynthetically active inner segment (IS). In the IS, proteins are synthetized by Golgi apparatus (GA). Ce, adjacent centriole; N, photoreceptor cell nucleus; S, synapse of photoreceptor cell. **(B)** Immunoelectron microscopy micrograph (pre-embedding labeling) of IFT57 in mouse retina. IFT57 is concentrated at the basal body (BB), at the base (#) of the OS and in the CC. **(C)** Immunoelectron microscopy micrograph of post-embedding labeling on ultrathin sections of the mouse retina using antibodies against IFT57. IFT57 is detected in the BB, CC and at the base of the OS (#). Furthermore, labeling of IFT57 is also present in the apical IS (*asterisk*). Compared to the pre-embedding, **(B)** the IFT57 labeling is in post-embedding is less specific **(C)**. Scale bars: 400 nm.

3.2 Differential ciliary and non-ciliary localization of individual IFT proteins in the mature retina

Knowledge of expression profiles of proteins and their subcellular localization provide important insights into their possible function. We have demonstrated the specificity of the individual IFT antibodies with Western blot analyses, recognizing single bands of predicted sizes in protein extracts of mouse retina and testis (Publication II, Fig. S1). Next we used double immunofluorescence analyses of IFT proteins and centrin, a marker for the connecting cilium with the basal body and adjacent centriole (Trojan et al., 2008) to validate the ciliary localization of individual IFT proteins. This double immunofluorescence analyses demonstrate the differential localization of IFT proteins (Publication II, Fig. 2). IFT52, IFT57, IFT88 and IFT140 were present at the basal body, at the apical part of the connecting cilium and in the cilium itself. IFT88 and IFT140 were also detected in the axoneme, which was confirmed by the partial colocalization with the axonemal protein retinitis pigmentosa1-RP1 (Publication II, Fig. S2). Surprisingly, IFT20 labeling was restricted only to the adjacent centriole and basal body and absent from the connecting cilium and from the outer segment (Publication II, Fig. 2).

The high-resolution immunofluorescence data was confirmed with the results of pre-embedding immunoelectron microscopy (Publication I, II, III). All analyzed IFT proteins were associated with vesicular structures (Publication I, Fig. 4; Publication II, Fig. 3-6). Additionally, IFT20 and IFT52 were detected in the apical inner segment, where the cargo handover between the inner segment transport indicated by cytoplasmic dynein (Tai et al., 1999) to the ciliary transport carrier occurs (Publication II, Fig. 5 and 6).

To further characterize the non-ciliary locality we performed double immunofluorescence microscopy for IFT20 and the Golgi resident protein GM130 (Marzelova et al., 2009). These results revealed partial colocalization of both proteins in the inner segment of photoreceptor cells and, in the cell bodies of horizontal and bipolar cells in the inner nuclear layer. The immunoelectron microscopic analysis confirmed IFT20 at the Golgi apparatus, and also at post-Golgi vesicles (Publication II, Fig. 7). To further specify non-ciliary localization of IFT20, IFT52 and IFT57 in the outer plexiform layer, double immunofluorescence was performed with antibodies against these IFT proteins and RIBEYE, a marker for ribbon synapses (tom Dieck et al., 2005; Publication II, Fig. 8). Pre-embedding immunoelectron microscopy demonstrated that IFT20, IFT52, IFT57 were located in the terminals of horizontal and/or bipolar cells and also in the dendritic tips (Publication II, Fig. 8 and 9).

In conclusion, these data provide evidence for the differential composition of IFT system in cells with and without primary cilia and thereby propose new functions for IFT beyond its well-established role in cilia.

3.3 Intraflagellar transport proteins in the ciliogenesis of photoreceptor cells

Since no details about the ciliogenesis of photoreceptor cells have been described to date, we have analyzed the formation of photoreceptor cells cilia during retinogenesis. For the first time we have described the location of IFT proteins during the ciliogenesis of photoreceptor cells (Publication III).

The electron microscopic analysis revealed that the ciliogenesis in mouse photoreceptor cells follows an intra-cellular pathway and is divided into six distinct stages (S1-S6) (Publication III, Fig. 1). The first stages (S1-S2) are characterized by electron dense centriolar satellites and a ciliary vesicle (Publication III, Fig. 2), while the formation of the ciliary shaft and of the light sensitive outer segment disks are features of later stages (S5-S6) (Publication III, Fig. 1). IFT proteins were expressed during photoreceptor cells differentiation as early as PN0 (Publication III, Fig. 3 and Suppl. Fig. 1). Ac partial co-localization of IFT proteins and the ciliary marker centrin demonstrated that IFT proteins were associated with the ciliary apparatus in all defined stages of ciliogenesis (Publication III, Fig. 4 and Suppl. Fig. 2). High-resolution microscopy analysis revealed the localization of IFT proteins at to the centriole and basal body as well as in the cytoplasm of photoreceptor cells associated with centriolar satellites, appendages, post-Golgi vesicles and also at the surface of the ciliary vesicle (Publication III, Figs. 5, 6, 7). Later in ciliogenesis (S4-S6), with the exception of IFT20 the localization pattern of IFT52, IFT57, IFT88 and IFT140 corresponded in principle to their distribution in the mature photoreceptor cilium (Publication III, Figs. 8, 9, 10).

Our data provide evidence for the participation of IFT proteins in photoreceptor ciliogenesis, both in the formation of the ciliary vesicle and in the elongation of the primary cilium. Furthermore, we demonstrate that the structures characteristic for the mature primary cilium are already formed in early ciliogenesis (S1-S2). The cytoplasmic localization of IFT proteins indicates roles of IFT proteins beyond their well-established function for IFT in mature cilia and flagella.

4. General discussion

Although IFT is currently the focus of intense research, the temporal spatial distribution of individual IFT proteins in the vertebrate retina remains elusive. This detailed study at the subcellular location of ciliary proteins using pre-embedding immunoelectron microscopy allows a more accurate speculation at their possible roles for cellular function and provide insights into the role of ciliary proteins in the broader context linked to ciliary disorders – i.e. ciliopathies. The primary aim of this thesis was to elucidate the precise spatial subcellular localization of individual IFT proteins in mature und developing retinal cells.

The present doctoral thesis presents an improved pre-embedding labeling method for electron microscopy with sensitivity high enough to detect ciliary proteins and IFT proteins associated with subcellular vesicles (Publication I, II, III). With this pre-embedding method of immunoelectron microscopy we were able to elucidate the differential ciliary localizations of individual IFT proteins in the mature retina (Publication II). Furthermore, with the help of electron microscopy we were able to differentiate six different stages (S1-S6) of photoreceptors ciliogenesis in the developing retina and were able to show that ciliogenesis of photoreceptor cells follow the intracellular pathway. Additionally, we show the presence of individual IFT proteins in all stages of photoreceptor cells ciliogenesis.

4.1 Differential ciliary localization of individual IFT proteins in the developing and mature vertebrate retina

During ciliogenesis of photoreceptor cells the localization of IFT proteins in stages S1-S3 corresponds to the labeling of IFT proteins in the mature cilium: all analyzed IFT proteins are associated with the basal body and centriole. In addition, IFT52, IFT57, IFT88 and IFT140 are present in the differentiating cilium, whereas IFT20 is not detected (Publication III; Fig. 3 and Suppl. Fig. S2). Interestingly, using immunoelectron pre-embedding analyses IFT20 is detected at the base of the forming outer segment in S5/S6 of differentiating photoreceptor cilia (Publication III, Fig. 9), converse to with the mature connecting cilium and outer segment, where no IFT20 is detected (Publication II, Fig. 6; Publication III, Fig. 10). These results confirm the proposed differences in the composition of IFT particle complex (Lucker et al., 2005). The absence of IFT20 from the complex B in photoreceptor cells is also supported by Baker et al. (2003), but in disagreement with Follit et al. (2006, 2008, 2009). Nevertheless, with the differential localization of IFT20 in the differentiating photoreceptor cilium we provide further evidence that IFT20 is not a component of IFT core complex B in photoreceptor cilia. However, in S4/S5 of photoreceptor ciliogenesis IFT20 it is found at the

base of differentiating outer segment, this suggests an additional function of IFT20 in promoting a mediator role between the Golgi system and the cargo delivery to target membranes. Recently, Keady et al. (2011) propose that IFT20 is required for the formation of photoreceptor outer segments and that the deletion of this gene in mature cells leads to opsin accumulation in the cell body (Keady et al., 2011).

In the photoreceptor axoneme, which extends from the connecting cilium and projects deep into the outer segment (Liu et al., 2004; Insinna and Besharse, 2008), only IFT88 and IFT140 are detected (Publication II). This suggests that only a subset of IFT proteins participates in IFT processes associated with the transport of cargo that is not incorporated into the nascent disks at the outer segment base and translocates along the microtubules of the axoneme deep into the outer segment. The axonemal location and function of IFT88 is important for correct differentiation of the connecting cilium. Mice carrying the hypomorphic mutation in IFT88 fail to develop photoreceptor outer segments, supporting a role of IFT88 in the ciliogenesis (Tg737orpk; Pazour et al., 2002a; Baker et al., 2004). The work of Insinna and coworkers (2009*) elucidates the presence of KIF17 at the axoneme and describes molecular interaction between IFT88 and KIF17 in agreement with our descriptive results on the location of IFT88 in the photoreceptors outer segment.

In conclusion, based on these data of the differential ciliary localization of IFT proteins we propose a model of IFT in the photoreceptor cells (Publication II, Fig. 10A) and suggest that the differential distribution of IFT protein subsets may depend on the sequential assembly of IFT particles for the delivery into the cilium.

4.2 Non-ciliary localization of individual IFT proteins in the developing and mature vertebrate retina

In addition to the ciliary localization of individual IFT proteins, IFT proteins have been detected in the non-ciliary compartments of retinal cells (Publication II and III). In the cytoplasm of the developing and mature photoreceptor cells all analyzed IFT proteins are associated with vesicles (Publication II, III). Golgi derived vesicles were identified, to associate with IFT20 in the differentiating and mature photoreceptor cell inner segment and in secondary retinal neurons of the mature retina (Publication II, Fig 6; Publication III, Suppl. Fig. S2). During ciliogenesis IFT associated vesicles dock and fuse with the membrane of the periciliary ridge region of the apical inner segment, engulfing the elongating ciliary shaft (Publication III, Fig. 7). These findings support the hypothesis that IFT proteins are evolutionary related to proteins involved in exocytosis processes, in which post-Golgi vesicles fuse with the plasma membrane previously suggested by Jekely and Arendt (2006). On the

other hand these vesicles appear not to originate from Golgi apparatus, but from endosomes (Rattner et al., 2010).

In the dendritic processes of secondary neurons of vertebrate retina IFT20, IFT52, and IFT57 are present in non-ciliary cell compartments, which confirm data of Finetti et al. (2009) describing IFT proteins at the immune synapse. However, the composition of IFT protein complex differs from the one we have recently described for the secondary retinal neurons (Publication II). These discrepancies suggest that IFT protein complexes are modularly composed and that their defined arrangement may be cell specific and/or dependent on a particular role of the IFT protein complex in intracellular membrane trafficking to selective target membranes. At the dendritic tip, IFT particles dissociate from their cargo, which is incorporated into the post-synaptic membrane. In the vertebrate retina, KIF17 was identified as part of a protein complex containing IFT20 and IFT57, which is essential for photoreceptor outer segment development (Insinna and Besharse, 2008; Insinna et al., 2009*). Our present data indicate that the dendritic processes of secondary retinal neurons contain a non-ciliary IFT protein complex that includes IFT20, IFT52, and IFT57 and KIF17 but neither IFT88, IFT140 nor the heterotrimeric kinesin-II (Publication II, Fig. 10B).

In the cytoplasm of differentiating photoreceptor cells in stages S1-S3 of ciliogenesis IFT proteins are associated with centriolar satellites (Publication III, Figs. 1, 2, 6). In previous studies several molecular components of centrosomes and basal bodies, e.g. the pericentriolar material-1 (PCM-1) protein, the Bardet-Biedl syndrome protein 4 (BBS4), centrins, pericentrin and the centrosomal protein CEP290 were identified to be associated with the centriolar satellites (Kubo et al., 1999; Laoukili et al., 2000; Dammermann and Merdes, 2002; Kubo and Tsukita, 2003; Kim et al., 2004; Nachury et al., 2007; Kim et al., 2008). In these studies the association of these centrosomal proteins with centriolar satellites is connected with roles in the transport of non-membrane associated ciliary cargo (e.g. α/β tubulin dimers) to the basal body. Therefore, we assume the participation of IFT proteins at the centriolar satellites in cargo transport to the ciliary base.

Taken together, the location of IFT proteins at all these proposed non-ciliary compartments of the cell reveal that IFT molecules are involved in different transport processes in addition to their involvement in the ciliary IFT machinery.

4.3 Prospects

In future studies it will be interesting to identify new interaction partners of IFT proteins via protein-protein interaction assays as e.g. Yeast-two-hybrid, tandem affinity purification (TAP), immunoprecipitation and/or GST-pulldown experiments. An important focus will be on the function of non-ciliary IFT proteins. As one possible experimental approach is e.g. biochemical fractionation of synaptic compartments can be applied. Since in higher eukaryotes IFT-complex A and IFT-complex B seem not to be the functional complex composition, it is important to elucidate the molecular composition of IFT subcomplexs. Furthermore, the identification of the cargo molecules for the ciliary transport is of great importance focusing on the transport; transport across the connecting cilium, transport to the outer segment and also in the axoneme of the outer segment. More insights into the role of IFT molecules can be gained by down regulation using siRNA. Subretinal injections of adeno-associated viruses into the eye can be used to transduce the photoreceptor cells with the IFT specific siRNA and therewith down-regulate the IFT genes of interest. Subsequently, with immunofluorescence and immunoelectron microscopy analyses, changes in the morphology of transduced cells in the comparison to non-transduction cells can be analyzed. Additionally, the mislocalization of IFT cargo proteins like opsin can be analyzed. With this approach, we could analyze functional changes associated with IFT knock-down. To observe IFT in the *in vivo* system, the living retina transfected with fluorocrome-tagged IFT proteins and/or candidates of IFT cargo can be analyzed using multiphoton-microscopy.

5.   Summary

Intraflagellar transport (IFT) is required for the assembly and maintenance of cilia. In this study we analyzed the subcellular localization of IFT proteins in retinal cells by correlative high-resolution immunofluorescence and immunoelectron microscopy. The rod photoreceptor cell was used as a model system to analyze protein distribution in cilia. To date the expression of IFT proteins has been described in the ciliary region without deciphering the precise spatial and temporal subcellular localization of IFT proteins, which was the focus of my work.

The establishment of the pre-embedding immunoelectron method was an important first step for the present doctoral thesis. Results of this work reveal the differential localization of IFT20, IFT52, IFT57, IFT88, IFT140 in sub-ciliary compartments and also their presence in non-ciliary compartments of retinal photoreceptor cells. Furthermore, the localization of IFT20, IFT52 and IFT57 in dendritic processes of non-ciliated neurons indicates that IFT protein complexes also operate in non-ciliated cells and may participate in intracellular vesicle trafficking in eukaryotic cells in general.

In addition, we have investigated the involvement of IFT proteins in the ciliogenesis of vertebrate photoreceptor cilia. Electron microscopy analyses revealed six morphologically distinct stages. The first stages are characterized by electron dense centriolar satellites and a ciliary vesicle, while the formation of a ciliary shaft and of the light sensitive outer segment disks are features of the later stages. IFT proteins were expressed during all stages of photoreceptor cell development and found to be associated with the ciliary apparatus. In addition to the centriole and basal body IFT proteins are present in the photoreceptor cytoplasm, associated with centriolar satellites, post-Golgi vesicles and with the ciliary vesicle. Therewith the data provide an evidence for the involvement of IFT proteins during ciliogenesis, including the formation of the ciliary vesicle and the elongation of the primary cilium of photoreceptor cells. Moreover, the cytoplasmic localization of IFT proteins in the absence of a ciliary shaft in early stages of ciliogenesis indicates roles of IFT proteins beyond their well-established function for IFT in mature cilia and flagella.

6. List of references

Bae YK, Qin H, Knobel KM, Hu J, Rosenbaum JL, Barr MM (2006) General and cell-type specific mechanisms target TRPP2/PKD-2 to cilia. Development 133: 3859-3870

Baker SA, Freeman K, Luby-Phelps K, Pazour GJ, Besharse JC (2003) IFT20 links kinesin II with a mammalian intraflagellar transport complex that is conserved in motile flagella and sensory cilia. J.Biol.Chem. 278: 34211-34218

Baker, Pazour GJ, Witman GB, Besharse JC (2004) Microtubule motor transport and IFT. In: Williams DS (ed) Recent Advances in Human Biololgy: Cell Biology and Disease of the Outer Retina: Problems of Protein Trafficking. Edition. World Scientific, Singapore, pp 109-139

Baldari CT, Rosenbaum J (2010) Intraflagellar transport: it's not just for cilia anymore. Curr.Opin.Cell Biol. 22: 75-80

Besharse, Horst CJ (1990) The photoreceptor connecting cilium - a model for the transition zone. In: Bloodgood RA (ed) Ciliary and flagellar membranes. Plenum, New York, pp 389-417

Bhowmick R, Li M, Sun J, Baker SA, Insinna C, Besharse JC (2009) Photoreceptor IFT complexes containing chaperones, guanylyl cyclase 1 and rhodopsin. Traffic. 10: 648-663

Chaitin MH (1992) Double immunogold localization of opsin and actin in the cilium of developing mouse photoreceptors. Exp.Eye Res. 54: 261-267

Cole DG, Diener DR, Himelblau AL, Beech PL, Fuster JC, Rosenbaum JL (1998) Chlamydomonas kinesin-II-dependent intraflagellar transport (IFT): IFT particles contain proteins required for ciliary assembly in Caenorhabditis elegans sensory neurons. J.Cell Biol. 141: 993-1008

Cole DG (2003) The intraflagellar transport machinery of Chlamydomonas reinhardtii. Traffic. 4: 435-442

Dammermann A, Merdes A (2002) Assembly of centrosomal proteins and microtubule organization depends on PCM-1. J.Cell Biol. 159: 255-266

Deretic D (2006) A role for rhodopsin in a signal transduction cascade that regulates membrane trafficking and photoreceptor polarity. Vision Res. 46: 4427-4433

Evans JE, Snow JJ, Gunnarson AL, Ou G, Stahlberg H, McDonald KL, Scholey JM (2006) Functional modulation of IFT kinesins extends the sensory repertoire of ciliated neurons in Caenorhabditis elegans. J.Cell Biol. 172: 663-669

Finetti F, Paccani SR, Riparbelli MG, Giacomello E, Perinetti G, Pazour GJ, Rosenbaum JL, Baldari CT (2009) Intraflagellar transport is required for polarized recycling of the TCR/CD3 complex to the immune synapse. Nat.Cell Biol. 11: 1332-1339

Fliegauf M, Benzing T, Omran H (2007) When cilia go bad: cilia defects and ciliopathies. Nat.Rev.Mol.Cell Biol. 8: 880-893

Follit JA, Tuft RA, Fogarty KE, Pazour GJ (2006) The intraflagellar transport protein IFT20 is associated with the Golgi complex and is required for cilia assembly. Mol.Biol.Cell 17: 3781-3792

Follit JA, San Agustin JT, Xu F, Jonassen JA, Samtani R, Lo CW, Pazour GJ (2008) The Golgin GMAP210/TRIP11 anchors IFT20 to the Golgi complex. PLoS.Genet. 4: e1000315. doi:10.1371/journal.pgen.1000315

Follit JA, Xu F, Keady BT, Pazour GJ (2009) Characterization of mouse IFT complex B. Cell Motil.Cytoskeleton 66: 457-468

Greiner JV, Weidman TA, Bodley HD, Greiner CA (1981) Ciliogenesis in photoreceptor cells of the retina. Exp.Eye Res. 33: 433-446

Ghossoub R, Molla-Herman A, Bastin P, Benmerah A (2011) The ciliary pocket: a once-forgotten membrane domain at the base of cilia. Biol.Cell 103: 131-144

Hoffmeister H, Babinger K, Gurster S, Cedzich A, Meese C, Schadendorf K, Osten L, de VU, Rascle A, Witzgall R (2011) Polycystin-2 takes different routes to the somatic and ciliary plasma membrane. J.Cell Biol. 192: 631-645

Insinna C, Besharse JC (2008) Intraflagellar transport and the sensory outer segment of vertebrate photoreceptors. Dev.Dyn. 237: 1982-1992

Insinna C, Humby M, Sedmak T, Wolfrum U, Besharse JC (2009) Different roles for KIF17 and kinesin II in photoreceptor development and maintenance. Dev.Dyn. 238: 2211-2222

Jekely G, Arendt D (2006) Evolution of intraflagellar transport from coated vesicles and autogenous origin of the eukaryotic cilium. Bioessays 28: 191-198

Jenkins PM, Hurd TW, Zhang L, McEwen DP, Brown RL, Margolis B, Verhey KJ, Martens JR (2006) Ciliary targeting of olfactory CNG channels requires the CNGB1b subunit and the kinesin-2 motor protein, KIF17. Curr.Biol. 16: 1211-1216

Jurczyk A, Gromley A, Redick S, Agustin JS, Witman G, Pazour GJ, Peters DJ, Doxsey S (2004) Pericentrin forms a complex with intraflagellar transport proteins and polycystin-2 and is required for primary cilia assembly. J.Cell Biol. 166: 637-643

Kayadjanian N, Lee HS, Pina-Crespo J, Heinemann SF (2007) Localization of glutamate receptors to distal dendrites depends on subunit composition and the kinesin motor protein KIF17. Mol.Cell Neurosci. 34: 219-230

Keady BT, Le YZ, Pazour GJ (2011) IFT20 Is Required for Opsin Trafficking and Photoreceptor Outer Segment Development. Mol.Biol.Cell (Epub ahead of print)

Kim JC, Badano JL, Sibold S, Esmail MA, Hill J, Hoskins BE, Leitch CC, Venner K, Ansley SJ, Ross AJ, Leroux MR, Katsanis N, Beales PL (2004) The Bardet-Biedl protein BBS4 targets cargo to the pericentriolar region and is required for microtubule anchoring and cell cycle progression. Nat.Genet. 36: 462-470

Kim J, Krishnaswami SR, Gleeson JG (2008) CEP290 interacts with the centriolar satellite component PCM-1 and is required for Rab8 localization to the primary cilium. Hum.Mol.Genet. 17: 3796-3805

Kozminski KG, Johnson KA, Forscher P, Rosenbaum JL (1993) A motility in the eukaryotic flagellum unrelated to flagellar beating. Proc.Natl.Acad.Sci.U.S.A 90: 5519-5523

Krock BL, Perkins BD (2008) The intraflagellar transport protein IFT57 is required for cilia maintenance and regulates IFT-particle-kinesin-II dissociation in vertebrate photoreceptors. J.Cell Sci. 121: 1907-1915

Krock BL, Mills-Henry I, Perkins BD (2009) Retrograde intraflagellar transport by cytoplasmic dynein-2 is required for outer segment extension in vertebrate photoreceptors but not arrestin translocation. Invest Ophthalmol.Vis.Sci. 50: 5463-5471

Kubo A, Sasaki H, Yuba-Kubo A, Tsukita S, Shiina N (1999) Centriolar satellites: molecular characterization, ATP-dependent movement toward centrioles and possible involvement in ciliogenesis. J.Cell Biol. 147: 969-980

Kubo A, Tsukita S (2003) Non-membranous granular organelle consisting of PCM-1: subcellular distribution and cell-cycle-dependent assembly/disassembly. J.Cell Sci. 116: 919-928

Laoukili J, Perret E, Middendorp S, Houcine O, Guennou C, Marano F, Bornens M, Tournier F (2000) Differential expression and cellular distribution of centrin isoforms during human ciliated cell differentiation in vitro. J.Cell Sci. 113 (Pt 8): 1355-1364

Liu Q, Zuo J, Pierce EA (2004) The retinitis pigmentosa 1 protein is a photoreceptor microtubule-associated protein. J.Neurosci. 24: 6427-6436

Liu X, Udovichenko IP, Brown SD, Steel KP, Williams DS (1999) Myosin VIIa participates in opsin transport through the photoreceptor cilium. J.Neurosci. 19: 6267-6274

Lucker BF, Behal RH, Qin H, Siron LC, Taggart WD, Rosenbaum JL, Cole DG (2005) Characterization of the intraflagellar transport complex B core: direct interaction of the IFT81 and IFT74/72 subunits. J.Biol.Chem. 280: 27688-27696

Maerker T, van Wijk E, Overlack N, Kersten FF, McGee J, Goldmann T, Sehn E, Roepman R, Walsh EJ, Kremer H, Wolfrum U (2008) A novel Usher protein network at the periciliary reloading point between molecular transport machineries in vertebrate photoreceptor cells. Hum.Mol.Genet. 17: 71-86

Marszalek JR, Goldstein LSB (2000) Understanding the functions of kinesin-II. Biochimica Et Biophysica Acta Molecular Cell Research 1496: 142-150

Mazelova J, Astuto-Gribble L, Inoue H, Tam BM, Schonteich E, Prekeris R, Moritz OL, Randazzo PA, Deretic D (2009) Ciliary targeting motif VxPx directs assembly of a trafficking module through Arf4. EMBO J. 28: 183-192

Molla-Herman A, Ghossoub R, Blisnick T, Meunier A, Serres C, Silbermann F, Emmerson C, Romeo K, Bourdoncle P, Schmitt A, Saunier S, Spassky N, Bastin P, Benmerah A (2010) The ciliary pocket: an endocytic membrane domain at the base of primary and motile cilia. J.Cell Sci. 123: 1785-1795

Murcia NS, Richards WG, Yoder BK, Mucenski ML, Dunlap JR, Woychik RP (2000) The Oak Ridge Polycystic Kidney (orpk) disease gene is required for left-right axis determination. Development 127: 2347-2355

Nachury MV, Loktev AV, Zhang Q, Westlake CJ, Peranen J, Merdes A, Slusarski DC, Scheller RH, Bazan JF, Sheffield VC, Jackson PK (2007) A core complex of BBS proteins cooperates with the GTPase Rab8 to promote ciliary membrane biogenesis. Cell 129: 1201-1213

Nir I, Cohen D, Papermaster DS (1984) Immunocytochemical localization of opsin in the cell membrane of developing rat retinal photoreceptors. J.Cell Biol. 98: 1788-1795

Omori Y, Zhao C, Saras A, Mukhopadhyay S, Kim W, Furukawa T, Sengupta P, Veraksa A, Malicki J (2008) Elipsa is an early determinant of ciliogenesis that links the IFT particle to membrane-associated small GTPase Rab8. Nat.Cell Biol. 10: 437-444

Papermaster DS (2002) The birth and death of photoreceptors: the Friedenwald Lecture. Invest Ophthalmol.Vis.Sci. 43: 1300-1309

Pazour GJ, Wilkerson CG, Witman GB (1998) A dynein light chain is essential for the retrograde particle movement of intraflagellar transport (IFT). J.Cell Biol. 141: 979-992

Pazour GJ, Dickert BL, Witman GB (1999) The DHC1b (DHC2) isoform of cytoplasmic dynein is required for flagellar assembly. J.Cell Biol. 144: 473-481

Pazour GJ, Dickert BL, Vucica Y, Seeley ES, Rosenbaum JL, Witman GB, Cole DG (2000) Chlamydomonas IFT88 and its mouse homologue, polycystic kidney disease gene tg737, are required for assembly of cilia and flagella. J.Cell Biol. 151: 709-718

Pazour GJ, Baker SA, Deane JA, Cole DG, Dickert BL, Rosenbaum JL, Witman GB, Besharse JC (2002a) The intraflagellar transport protein, IFT88, is essential for vertebrate photoreceptor assembly and maintenance. J.Cell Biol. 157: 103-113

Pazour GJ, San Agustin JT, Follit JA, Rosenbaum JL, Witman GB (2002b) Polycystin-2 localizes to kidney cilia and the ciliary level is elevated in orpk mice with polycystic kidney disease. Curr.Biol. 12: R378-R380

Pedersen LB, Veland IR, Schroder JM, Christensen ST (2008) Assembly of primary cilia. Dev.Dyn. 237: 1993-2006

Pedersen LB, Rosenbaum JL (2008) Intraflagellar transport (IFT) role in ciliary assembly, resorption and signalling. Curr.Top.Dev.Biol. 85: 23-61

Qin H, Burnette DT, Bae YK, Forscher P, Barr MM, Rosenbaum JL (2005) Intraflagellar transport is required for the vectorial movement of TRPV channels in the ciliary membrane. Curr.Biol. 15: 1695-1699

Qin P, Pourcho RG (2001) Immunocytochemical localization of kainate-selective glutamate receptor subunits GluR5, GluR6, and GluR7 in the cat retina. Brain Res. 890: 211-221

Rattner JB, Sciore P, Ou Y, van der Hoorn FA, Lo IK (2010) Primary cilia in fibroblast-like type B synoviocytes lie within a cilium pit: a site of endocytosis. Histol.Histopathol. 25: 865-875

Roepman, Wolfrum U (2007) Protein networks and complexes in photoreceptor cilia. In: Faupel M, Bertrand E (eds) Subcellular Proteomics - From Cell Deconstruction to System

Reconstruction, Subcellular Biochemistry. Edition. Springer, Dordrecht, The Netherlands, pp 209-235

Rosenbaum JL, Witman GB (2002) Intraflagellar transport. Nat.Rev.Mol.Cell Biol. 3: 813-825

Sedmak T, Sehn E, Wolfrum U (2009) Immunoelectron microscopy of vesicle transport to the primary cilium of photoreceptor cells. In: R.D.Sloboda (ed) Primary cilia. Methods in Cell Biology. Academic Press Elsivier Inc, pp 259-272

Sedmak T, Wolfrum U (2010) Intraflagellar transport molecules in ciliary and nonciliary cells of the retina. J.Cell Biol. 189: 171-186

Sedmak T, Wolfrum U (2011) Intraflagellar transport proteins in ciliogenesis of photoreceptor cells. submitted

Signor D, Wedaman KP, Orozco JT, Dwyer ND, Bargmann CI, Rose LS, Scholey JM (1999) Role of a class DHC1b dynein in retrograde transport of IFT motors and IFT raft particles along cilia, but not dendrites, in chemosensory neurons of living Caenorhabditis elegans. J.Cell Biol. 147: 519-530

Sorokin S (1962) Centrioles and the formation of rudimentary cilia by fibroblasts and smooth muscle cells. J.Cell Biol. 15: 363-377

Sorokin SP (1968) Reconstructions of centriole formation and ciliogenesis in mammalian lungs. J.Cell Sci. 3: 207-230

Sung CH, Tai AW (2000) Rhodopsin trafficking and its role in retinal dystrophies. Int.Rev.Cytol. 195: 215-267

Sung CH, Chuang JZ (2010) The cell biology of vision. J.Cell Biol. 190: 953-963

Swaroop A, Kim D, Forrest D (2010) Transcriptional regulation of photoreceptor development and homeostasis in the mammalian retina. Nat.Rev.Neurosci. 11: 563-576

Tai AW, Chuang JZ, Bode C, Wolfrum U, Sung CH (1999) Rhodopsin's carboxy-terminal cytoplasmic tail acts as a membrane receptor for cytoplasmic dynein by binding to the dynein light chain Tctex-1. Cell 97: 877-887

Tokuyasu K, Yamada E (1959) The fine structure of the retina studied with the electron microscope. IV. Morphogenesis of outer segments of retinal rods. J.Biophys.Biochem.Cytol. 6: 225-230

tom Dieck S., Altrock WD, Kessels MM, Qualmann B, Regus H, Brauner D, Fejtova A, Bracko O, Gundelfinger ED, Brandstatter JH (2005) Molecular dissection of the photoreceptor ribbon synapse: physical interaction of Bassoon and RIBEYE is essential for the assembly of the ribbon complex. J.Cell Biol. 168: 825-836

Trojan P, Krauss N, Choe HW, Giessl A, Pulvermuller A, Wolfrum U (2008) Centrins in retinal photoreceptor cells: Regulators in the connecting cilium. Prog.Retin.Eye Res. 27: 237-259

Tsujikawa M, Malicki J (2004) Intraflagellar transport genes are essential for differentiation and survival of vertebrate sensory neurons. Neuron 42: 703-716

Wässle H (2004) Parallel processing in the mammalian retina. Nat.Rev.Neurosci. 5: 747-757

Wolfrum U, Schmitt A (2000) Rhodopsin transport in the membrane of the connecting cilium of mammalian photoreceptor cells. Cell Motil.Cytoskeleton 46: 95-107

Young RW (1976) Visual cells and the concept of renewal. Invest.Ophthalmol.Visual Sci. 15: 700-725

7. Appendix

7.1 Abbreviations

Abbreviations listed in alphabetical order.

Ax   axoneme

BB   basal body

CC   connecting cilium

DYNC2H1   cytoplasmic dynein 2 heavy chain 1

IFT   intraflagellar transport

LCA   Leber congenital amaurosis

TZ   transition zone

7.2 Contribution to the publications of the present thesis

In this chapter, the detailed contributions of the experimental work and results of following publications: Sedmak et al., 2009 published in *Methods in Cell Biology*; Sedmak and Wolfrum, 2010 in *Journal of Cell Biology*; Sedmak and Wolfrum submitted manuscript (Publications I-III), are listed. Additional publications, which were published during my doctoral thesis, are marked in the text with asterisk (*).

The project and experimental design of all three publications (Publication I, II, III) were (in 80%) planned by my supervisor prof. Dr. Uwe Wolfrum. The experiments and analyses (indirect double immunofluorescence analyses, conventional electron microscopy and immunoelectron microscopy; pre-embedding labeling) were exclusively preformed (100%) by me. Elisabeth Sehn prepared the ultra-thin sections for all analyses at the transmission electron microscope. Western blot analyses of mouse retina and testis extracts were performed by Ulrike Maas and Dr. Martin Latz, respectively. I designed all the figures and prepared all schemes in Publications I, II, III. Additionally, I wrote the first drafts of each of three manuscripts, which were subsequently corrected and edited by my supervisor.

In the paper den Hollander et al., 2007* published in *Nature Genetics*, I performed the pre-embedding labeling experiment (Fig. 3G, H). During my doctoral thesis I collaborated with the Institute for Virology (Mainz), and I analyzed the cytomegalovirus by using conventional and immunoelectron microscopy (post-embedding labeling), resulting in publications Becke et al., 2010a* (Fig. 4A, B) and Becke et al., 2010b* (Fig. 1B). In the work of Insinna et al., 2009* I performed the pre-embedding labeling experiments (Figs. 1A-C and Fig. 1D-E). In Charakova et al., 2011* (E pub) published in *Human Molecular Genetics*, I performed the indirect immunofluorescence analysis of mouse retina using molecular markers s RP-1, γ-tubulin, MAP2 and centrin in order to determine the precise subcellular localization of TOPORS at the ciliary region of photoreceptor cells (Fig. 2B-E; Fig. Suppl. 2A-D). Jaillard et al.*, (submitted) is a work of intensive cooperation with the INSERM-Institute of Vision in Paris. In this lab in Paris I conducted all steps of the fixation procedure for the post-embedding method. Their submitted manuscript demonstrates that the loss of rod visual function of the Nxnl2-/- mouse results from a deficit in the transport of opsin. In Mainz the post-embedding experiments were done under the supervision of Gabriele Stern-Schneider. In order to validate a difference in opsin transport in Nxnl2 homozygote retinae, I quantified the immunoelectron microscopic images by counting the opsin particles.

7.3 Published publications and congress contributions

Parts of the listed work were published in a form of paper, poster or oral presentation.

Publications:

<u>Sedmak T</u> and Wolfrum U (2011) Intraflagellar transport protein participation in ciliogenesis of photoreceptor cells (submitted).

Jaillard C, Mouret A, Niepon ML, Lee-Rivera I, Clerin E, Aït-Ali N, Millet-Puel G, **<u>Sedmak T</u>**, Yang Y, Raffelsberger W, Kinzel B, Trembleau A, Poch O, Bennett J, Wolfrum U, Lledo PM, Sahel JA, Leveillard T (2011) The Mouse Nucleoredoxin-like 2 Gene is Involved in the Maintenance of Vision and Olfaction (submitted).

Chakarova CF, Khanna H, Shah AZ, **<u>Sedmak T</u>**, Murga-Zamalloa C, Papaioannou M, Nagel-Wolfrum K, Lopez I, Munro P, Cheetham M, Koenekoop R, Sanchez R, Matter K, Wolfrum U, Swaroop A, Bhattacharya S (2011) TOPORS, implicated in retinal degeneration, is a cilia-centrosomal protein. **Hum Mol Genet**, 20: 975-987.

Becke S, Fabre-Mersseman V, Aue S, Auerochs S, **<u>Sedmak T</u>**, Wolfrum U, Strand D, Marschall M, Plachter B, Reyda S (2010) Modification of the major tegument protein pp65 of human cytomegalovirus inhibits viral growth and leads to the enhancement of a protein complex with pUL69 and pUL97 in infected cells without impairing pUL97 kinase activity. **J Gen Virol** 91, 2531-2541.

Becke S, Aue S, Thomas D, Schader S, Podlech J, Bopp T, **<u>Sedmak T</u>**, Wolfrum U, Plachter B, Reyda S (2010) Optimized recombinant dense bodies of human cytomegalovirus efficiently prime virus specific lymphocytes and neutralizing antibodies without the addition of adjuvant. **Vaccine** 28, 6191-6198.

<u>Sedmak T</u> and Wolfrum U (2010) Intraflagellar transport molecules in ciliary and nonciliary cells of the retina. **J. Cell Biol.** 189: 171–186.

<u>Sedmak T</u>, Sehn E, Wolfrum U (2009) Immunoelectron microscopy of vesicle transport to the primary cilium of photoreceptor cells. In Primary cilia. **Methods in Cell Biology**, vol. 94, R.D. Sloboda, editor. Academic Press, London. 259–272.

Insinna C, Humby M, **<u>Sedmak T</u>**, Wolfrum U, Besharse JC (2009) Different roles for KIF17 and kinesin II in photoreceptor development and maintenance. **Dev. Dyn.** 238:2211-2222.

den Hollander AI, Koenekoop RK, Mohamed MD, Arts HH, Boldt K, Towns KV, **<u>Sedmak T</u>**, Beer M, Nagel-Wolfrum K, McKibbin M, Dharmaraj S, Lopez I, Ivings L, Williams GA, Springell K, Woods CG, Jafri H, Rashid Y, Strom TM, van der ZB, Gosens I, Kersten FF, van Wijk E, Veltman JA, Zonneveld MN, van Beersum SE, Maumenee IH, Wolfrum U, Cheetham ME, Ueffing M, Cremers FP, Inglehearn CF, Roepman R (2007) Mutations in LCA5, encoding the ciliary protein lebercilin, cause Leber congenital amaurosis. **Nat. Genet.** 39: 889-895.

Congress contributions (Abstracts):

Sedmak T, Wolfrum U (2011) Intraflagellar transport proteins in ciliogenesis of photoreceptor cells. 9th Göttingen Meeting of the German Neuroscience Society, T15-10B, Göttingen, Germany.

Sedmak T, Wolfrum U (2010) Ciliary and non-ciliary localization of individual IFT molecules in the retina. FASEB Summer research conference: "The biology of cilia and flagella", Vermont, USA.

Sedmak T, Wolfrum U (2010) Differential ciliary and non-ciliary localization of IFT molecules in the mammalian retina. Pro Retina Research-Colloquium, Retinal Degeneration: 10 years into the new century, where do we go from here? Potsdam, Germany.

Sedmak T, Wolfrum U (2010) Differential expression of IFT molecules in ciliary and non-ciliary cells of the mammalian retina. 33rd Annual Meeting of the German Society for Cell Biology, Regensburg, Germany.

Sedmak T, Sehn E, Wolfrum U (2009) Intraflagellar transport proteins are involved in the ciliogenesis of retinal photoreceptor cells. 9th Annual Meeting of the Interdisciplinary Science Network Molecular and Cellular Neurobiology, Mainz, Germany.

Sedmak T, Latz M, Wolfrum U (2009) Expression and differential subcellular distribution of individual IFT molecules in the developing and mature mouse retina. ARVO/International Society for Ocular Cell Biology, 119/B62, Ericeira, Portugal.

Wolfrum U, Latz M, Pazour GJ, **Sedmak T** (2009) Differential ciliary and non-ciliary localization of IFT molecules in the mammalian retina. ARVO Annual Meeting - Reducing disparities in eye disease and treatment, Fort Lauderdale, USA.

Wolfrum U, **Sedmak T** (2009) Subcellular localizations of intraflagellar transport (IFT) molecules indicate differential ciliary and novel non-ciliary functions in retinal neurons. 8th Göttingen Meeting of the German Neuroscience Society, T21-6C, Göttingen, Germany.

Shah AZ, Khanna H, **Sedmak T**, Nagel-Wolfrum K, Murga-Zamalloa CA, Lopez I, Papaioannou M, Munro P, Cheetham M, Rios RM, Koenekoop R, Beales P, Matter K, Wolfrum U, Swaroop A, Bhattacharya SS, Chakarova C. TOPORS, mutated in retinal degeneration, is a novel centrosomal and ciliary protein (2009). 495/W/Poster Board 153 The American society of human genetics 59th Annual Meeting, Honolulu, Hawaii, USA.

Shah AZ, Chakarova C, Khanna H, **Sedmak T**, Cheetham M, Matter K, Wolfrum U, Koenekoop R, Swaroop A, Bhattacharya SS (2008) Novel ciliary function for TOPORS associated with autosomal dominant retinitis pigmentosa. Association for Research in Vision and Ophthalmology (ARVO) - Annual Meeting, Eyes on innovation, 2418, Fort Lauderdale, USA.

Sedmak T, Latz M, Pazour GJ, Wolfrum U (2008) Oral presentation: Intraflagellar transport (IFT) molecules in the neuronal retina. 2nd Balkan Vision Meeting, Ljubljana, Slovenia.

Sedmak T, Latz M, Wolfrum U (2007) Subcellular localization of IFT molecules in mammalian photoreceptor cells. 7th Annual Meeting of the Interdisciplinary Science Network Molecular and Cellular Neurobiology, Mainz, Germany.

8.   Curriculum Vitae

9.   Eidesstattliche Erklärung

Hiermit erkläre ich an Eides statt, dass ich meine Dissertation selbstständig und nur unter Verwendung der angegebenen Hilfsmittel angefertigt habe. Ich habe keinen anderen Promotionsversuch unternommen.

Mainz, den 18.03.2011

Tina Sedmak